Doklady Physics, Vol. 48, No. 8, 2003, pp. 389–393. Translated from Doklady Akademii Nauk, Vol. 391, No. 4, 2003, pp. 462–466.

PHYSICS

Systematic Distortions of Signal Propagation Times in Random Inhomogeneous Media

O. A. Godin

Presented by Academician L.M. Brekhovskikh April 8, 2003

Received April 8, 2003

Times of signal propagation between given sources and receivers contain valuable information on the properties of the medium. In particular, important methods of investigating the Earth, such as seismic tomography [1], acoustic tomography [2, 3], and thermometry of the ocean [4], are based on precisely measuring signal propagation times. In these and numerous other applications, large-scale inhomogeneities of a medium (and, in the case of investigating the ocean, their variations with time) are of interest. At the same time, an effect of small-scale random inhomogeneities that are not resolved by data inversion represents noise. In order to suppress fluctuations associated with small-scale inhomogeneities, the method of averaging with respect to either the radiation time or positions of corresponding points is employed. Apart from fluctuations, random inhomogeneities generate systematic distortions of the arrival time, i.e., differences between the signal average velocities in deterministic and fluctuating media. These differences were studied by numerical methods for a number of specific cases and turned out to be rather substantial in the acoustical tomography of the ocean [5–7] and seismology [8]. The analytical studies [9–11] are limited to the case of statistically homogeneous media without regular refraction. This excludes application of the results obtained in [9–11] to problems of propagating seismic waves, sound in the ocean, and radio waves in the ionosphere for long distances.

In the present study, we develop a theory that allows us to calculate statistical moments of signal arrival times from known fluctuation moments of a medium that, along with small-scale fluctuations, has a large-scale structure. The wave frequency is assumed to be sufficiently high in order to allow the application of the ray theory to small-scale inhomogeneities. For simplicity, the medium is assumed to be isotropic and free of dispersion.

Let a source and a receiver be located at the points $\mathbf{r}_S = (x_S, 0, z_S)$, $\mathbf{r}_R = (x_R, 0, z_R)$, and the wave velocity $C(\mathbf{r})$ be represented in the form

$$C(\mathbf{r}) = c(x, z) + \varepsilon c_1(\mathbf{r}) + \varepsilon^2 c_2(\mathbf{r}) + \ldots,$$

where $\|c_z\| \gg \|c_x\|$ and the parameter ε ($0 \le \varepsilon \ll 1$) characterizes the smallness of deviations of C from the unperturbed velocity c. Such a choice of the model of the medium is dictated by the three following reasons. First, after averaging over small spatial scales, in geophysical applications, the medium becomes close to a vertically stratified one. Second, propagation times are much more sensitive to horizontal gradients of C in the vertical plane that contains the source and the receiver than along the normal to this plane [12]. Third, numerical realizations of the ray theory in a two-dimensional inhomogeneous medium turn out to be rather efficient and are widely used. Below, we consider as known all quantities related to a ray in an unperturbed medium, including the trajectory $\mathbf{r}_0 = (x, 0, z_0(x))$, the sliding angle χ formed with the plane z = const, and the derivative $p = \left(\frac{\partial z_0}{\partial \chi_S}\right)_x$ with respect to the angle χ_S of the ray exit from the source. All these quantities, including the derivative p used for expressing the field amplitude in the ray [13], are calculated with the help of standard ray-geometry codes adapted to a two-dimensional inhomogeneous medium. We also assume for definiteness that $x_S < x_R$ and $|\chi| < \frac{\pi}{2}$, i.e., the wave propagates towards increasing values of x.

In order to calculate the terms T_j ($j \ge 1$) caused by fluctuations and entering into the expression $T = T_0 + \varepsilon T_1 + \varepsilon^2 T_2 + \ldots$ that describes the signal propagation time along the ray, we employ perturbation theory for an eikonal (PTE) [14]. This theory solves ordinary differential equations for T_j, which follow from the eikonal equation $(\nabla T)^2 = c^{-2}$. The theory leads to the

CIRES, University of Colorado
and NOAA/Environmental Technology Laboratory,
David Skaggs Research Center,
325 Broadway, Boulder, Colorado, CO 80305-3328, USA
e-mail: Oleg.Godin@noaa.gov

1028-3358/03/4808-0389$24.00

following linear (T_1) and quadratic ($T_2 = T_{21} + T_{22} + T_{23}$) corrections:

$$T_\alpha = \int_{x_S}^{x_R} \frac{A_\alpha dx}{\cos\chi}, \quad A_1 = -\frac{c_1}{c^2}, \quad A_{21} = \frac{c_1^2 - cc_2}{c^3}, \tag{1}$$
$$A_{22} = -\frac{c}{2}\left(\frac{\partial T_1}{\partial y}\right)^2, \quad A_{23} = -\frac{c}{2}\left(\cos\chi\frac{\partial T_1}{\partial z} - \sin\chi\frac{\partial T_1}{\partial x}\right)^2.$$

Hereinafter, except as otherwise noted, the integration occurs along the unperturbed ray, i.e., for $y = 0$, $z = z_0(x)$. The contributions of terms T_1 and T_{21} to the arrival time are due to fluctuations of the wave velocity along the unperturbed ray, whereas the contributions of terms T_{22} and T_{23} are due to the variation of the ray trajectory. In this case, T_{22} and T_{23} describe the so-called horizontal refraction effect, i.e., escaping of the ray from the plane xz, and the effect of ray deformation in this plane, respectively. To calculate T_{23}, we apply the method used in [12] for analyzing the horizontal refraction. Thus, we can derive from formula (1) the explicit formulas for quadratic corrections in terms of the fluctuations ∇C:

$$A_{22}(x) = -\frac{c}{2g^2}\left(\int_{x_S}^{x}\frac{\partial c_1}{\partial y}\frac{g\,dx'}{c^2\cos\chi}\right)^2, \quad g(x) = \int_{x_S}^{x}\frac{c\,dx'}{\cos\chi},$$
$$A_{23}(x) = -\frac{c}{2p^2\cos^2\chi}\left(\int_{x_S}^{x} pa\frac{dx'}{c}\right)^2, \tag{2}$$
$$a(x) = \cos\chi\frac{\partial}{\partial z}\left(\frac{c_1}{c}\right) - \sin\chi\frac{\partial}{\partial x}\left(\frac{c_1}{c}\right).$$

It follows from formulas (1) and (2) that, in accordance with the Fermat principle, the corrections to the propagation time, which are associated with small ray deformations, are negative and quadratic with respect to perturbations.

On the caustic, $p = 0$ [13], which results in diverging values of T_{23} if the ray turns out to be tangent to the caustic on the way from the source to the receiver. The divergence testifies to the inapplicability of the PTE in the case of the existence of caustics. To find results that are applicable in the case of long-range propagation, we use the perturbation theory for rays (PTR), in which perturbations of the ray trajectory are expanded in powers of a small parameter:

$$z(x) = z_0(x) + \varepsilon z_1(x) + \varepsilon^2 z_2(x) + \ldots.$$

For a ray connecting the source and the receiver, $z_j(x_{S,R}) = 0$ as $j \geq 1$. In the PTR, the number of contacts of the ray with the caustic is unlimited. However, it is assumed in this case that the receiver does not lie on the caustic of the rays outgoing from the source. Otherwise, the perturbations are singular, and the PTR is inapplicable for the family of the rays forming the caustic.

Now, neglecting the terms $O(\varepsilon^3)$ and allowing for additivity of the contributions of the horizontal refraction and perturbations in the xz plane to the signal propagation time, we may apply the PTR to the two-dimensional inhomogeneous medium. The differential equations of a ray [13, 14] can be represented in the form of a closed nonlinear equation of the second order with respect to $z(x)$:

$$\frac{d^2z}{dx^2} = C^{-1}\left[1 + \left(\frac{dz}{dx}\right)^2\right]\left(\frac{C_x dz}{dx} - C_z\right). \tag{3}$$

From Eq. (3), it follows the equation for trajectory perturbation

$$\frac{d^2z_1}{dx^2} - \frac{B_1 dz_1}{dx} - B_2 z_1 = -a\cos^{-3}\chi, \tag{4}$$

where the coefficients are calculated in the unperturbed ray. Here,

$$B_1 = c^{-1}c_x(1 + 3\tan^2\chi) - 2c^{-1}c_z\tan\chi,$$
$$B_2 = c^{-2}\cos^{-2}\chi[cc_{zz} + c_z^2 + (cc_{xz} - c_xc_z)\tan\chi]. \tag{5}$$

If the unperturbed trajectory depends on a certain parameter b, e.g., on the coordinate of the source or on the ray emission angle, then, for the derivative $f(x) = \left(\frac{\partial z_0}{\partial b}\right)_x$, differentiating Eq. (3) with respect to b yields the equation

$$\frac{d^2f}{dx^2} - \frac{B_1 df}{dx} - B_2 f = 0. \tag{6}$$

One of the solutions to Eq. (6) is the quantity p introduced above. By virtue of the reversibility of rays, which follows from the reciprocity principle (see [13]), the derivative $q(x) = \left(\frac{\partial z_0}{\partial \chi_R}\right)_x$ with respect to the sliding angle χ_R at the point $\mathbf{r}_R$ is also the solution to Eq. (6) for rays outgoing from this point towards decreasing values of x. The solutions $q(x)$ and $p(x)$ are linearly independent. Indeed, $p(x_S) = q(x_R) = 0$ and $p(x_R) \neq 0$, since the receiver does not lie on the caustic. For the Wron-

skian of the two solutions, we obtain from Eqs. (5) and (6)

$$w(x) \equiv p_x q - p q_x = c^{-1}(x_S, 0, z_0(x_S))q(x_S) \times \cos\chi_S c(x, 0, z_0(x))\cos^{-3}\chi(x, 0, z_0(x)). \quad (7)$$

The solutions to inhomogeneous equation (4) can be simply expressed in terms of the solution to the homogeneous equation (6). Taking into account the boundary conditions for the values of z_1 in the source and receiver, we find for the perturbation of the ray trajectory

$$z_1(x) = \int_{x_S}^{x_R} G(x, x')\frac{a\,dx'}{\cos^3\chi}, \quad G(x, x') = \frac{p(x_<)q(x_>)}{w(x')}, \quad (8)$$
$$x_< = \min(x, x'), \quad x_> = \max(x, x').$$

It follows from formulas (7) and (8) that z_1 is certainly limited along the entire ray and has no singularities or caustics. It is worth noting that the choice of linearly independent solutions to Eq. (6), which enter into the Green's function G of Eq. (8), is arbitrary. We use the solutions p and q, since they have a clear physical sense and can be calculated using standard ray codes.

The signal propagation time along a ray having the trajectory $\mathbf{r} = (x, y(x), z(x))$ is

$$T = \int_{x_S}^{x_R} C^{-1}\sqrt{1 + \left(\frac{dy}{dx}\right)^2 + \left(\frac{dz}{dx}\right)^2}\,dx. \quad (9)$$

Here, the integration is performed along this ray. We now expand the trajectory in powers of the perturbation. After a number of transformations based on Eq. (4) and on the identities

$$\int_{x_S}^{x_R}\frac{dx}{c\cos\chi}\left[\mathbf{m}(\mathbf{m}\cdot\nabla)\mathbf{F} - \mathbf{F}\frac{\nabla c}{c}\right] = 0, \quad (10)$$
$$\mathbf{m} = (\cos\chi, 0, \sin\chi),$$

valid for arbitrary smooth vector functions $\mathbf{F}(\mathbf{r})$ such that $\mathbf{F}(\mathbf{r}_S) = \mathbf{F}(\mathbf{r}_R) = 0$, we again arrive at the relationship

$$T = T_0 + \varepsilon T_1 + \varepsilon^2(T_{21} + T_{22} + T_{23}) + O(\varepsilon^3).$$

Here, T_1, T_{21}, and T_{22} are given by the same formulas (1) (for T_α, A_1, and A_{21}) and by formulas (2) (for A_{22}), which we deal with in the case of PTE). For the contribution T_{23} to the signal propagation time perturbation (which corresponds to the ray deformation in the xz plane), we obtain

$$T_{23} = -\frac{1}{2}\int_{x_S}^{x_R} c^{-1}z_1 a\,dx. \quad (11)$$

Thus, the PTR reduces finding fluctuations of signal propagation times in a three-dimensional inhomogeneous medium to calculating integrals along an unperturbed ray. The practical advantage of formulas (1), (2), (8), and (11) compared to the results obtained by other methods (see [3, Appendix 2; 15]) consists in the fact that calculating the integrands does not require solving any supplementary differential equations.

The condition of applicability of the PTR consists in the smallness of the ray deformation z_1 being calculated by formula (8) compared to the characteristic spatial scale of inhomogeneities in the medium along the z coordinate. Furthermore, the maximum distance of the perturbed ray from the xz plane must be small compared to the characteristic spatial scale of inhomogeneities in the medium along the y coordinate. The latter condition has been thoroughly discussed in [12]. We can show that, for rays having no caustics, when both the PTR and the PTE are applicable, formulas (1) and (2) for T_{23} are equivalent to formulas (8) and (11). Therefore, the results of the two different perturbation theories are identical in this case.

We now assume that the quantity C is a random function. We consider that the wave velocity fluctuations arise as a result of small (proportional to ε) fluctuations with a zero average value of medium parameters (e.g., temperature, pressure, or composition). In this case, $\langle c_1\rangle = 0$. The higher terms in the expansion of C in powers of ε are stipulated by the nonlinear dependence of the velocity on parameters of the medium so that, in the general case, $\langle c_2\rangle \neq 0$. We consider the fluctuations to be locally statistically homogeneous and small-scale in the sense that the variation of c can be ignored at distances where strong variations of the correlation function

$$\langle c_1(\mathbf{r}_1)c_1(\mathbf{r}_2)\rangle = K\left(\mathbf{r}_1 - \mathbf{r}_2; \frac{\mathbf{r}_1 + \mathbf{r}_2}{2}\right) \quad (12)$$

with respect to its first argument $\mathbf{r}_1 - \mathbf{r}_2$ take place. Variations in the space of one-point moments such as $\langle c_2\rangle$ and also of the correlation function K with respect to its second argument $\frac{\mathbf{r}_1 + \mathbf{r}_2}{2}$ are assumed to be large-scale. No constraints are imposed on the relative variation of the fluctuation intensity.

The formulas obtained above predict fluctuations of the signal arrival time for each realization of C and make it possible to calculate different statistical

moments of T using the known moments of C. Here, we restrict our consideration to both the average value $\langle T\rangle$ and the dispersion σ_T^2 of the signal propagation time to distances much longer than the fluctuation correlation radius. Under the above assumptions, the signal arrival time perturbations linear in ε and quadratic corrections introduce basic contributions to the dispersion and into the deviation of the arrival time from the unperturbed signal, respectively:

$$\begin{aligned}\sigma_T^2 &= \varepsilon^2\langle T_1^2\rangle[1 + O(\varepsilon)],\\ \langle T\rangle &= T_0 + \varepsilon^2\langle T_{21} + T_{22} + T_{23}\rangle + O(\varepsilon^3).\end{aligned} \tag{13}$$

Thus, we obtain from formulas (1) and (2)

$$\langle T_1^2\rangle = \int_{x_S}^{x_R}\int \frac{K(\mathbf{r}_0(x) - \mathbf{r}_0(x');\ (\mathbf{r}_0(x) + \mathbf{r}_0(x'))/2)\,dx\,dx'}{c^2(\mathbf{r}_0(x))c^2(\mathbf{r}_0(x'))\cos\chi(\mathbf{r}_0(x))\cos\chi(\mathbf{r}_0(x'))}. \tag{14}$$

Passing in (14) to integration over difference and summary coordinates $x - x'$ and $\frac{x + x'}{2}$ and taking into account that the fluctuations in the medium are small-scale, we find in the principal order with respect to ε

$$\begin{aligned}\sigma_T^2 &= 2\varepsilon^2\int_{x_S}^{x_R}\frac{D_1 dx}{c^4\cos\chi},\\ D_1(\chi, \mathbf{r}) &= \frac{1}{\cos\chi}\int_0^{+\infty} K(x, 0, x\tan\chi;\ \mathbf{r})dx\\ &= \int_0^{+\infty} K_I(R;\ \mathbf{r})dR.\end{aligned} \tag{15}$$

When calculating the integral characteristic D_1 for fluctuations in the medium, the integration is performed along a straight line. The last of expressions for D_1 in (15) refers to the special case of isotropic fluctuations in the medium, when $K(\mathbf{R};\ \mathbf{r}) = K_I(|\mathbf{R}|;\ \mathbf{r})$. Below, we need two further integral characteristics of fluctuations

$$\begin{aligned}D_2(\chi, \mathbf{r}) &= \frac{1}{\cos\chi}\int_0^{+\infty} K_{yy}\big|_{y = 0,\, z = x\tan\chi}dx = \int_0^{+\infty}\frac{\partial K_I}{\partial R}\frac{dR}{R},\\ D_3(\chi, \mathbf{r}) &= \frac{1}{\cos\chi}\int_0^{+\infty}(\sin^2\chi K_{xx}\\ &\quad - 2\sin\chi\cos\chi K_{xz} + \cos^2\chi K_{zz})\big|_{y = 0,\, z = x\tan\chi}dx.\end{aligned} \tag{16}$$

In the isotropic case, the terms $D_{1,2,3}$ do not depend on the direction of the tangent to the ray, so that $D_2 = D_3$. In a statistically homogeneous medium, $D_{1,2,3}$ are independent of coordinates.

Formulas (1), (2), (8), and (11) for T_{21}, T_{22}, and T_{23} are averaged similarly to the derivation of formula (15). As a result, we have

$$\begin{aligned}\langle T\rangle - T_0 &= \varepsilon^2\int_{x_S}^{x_R}\frac{dx}{c\cos\chi}\\ &\times\left[\frac{K(0;\ \mathbf{r}_0)}{c^2} - \frac{\langle c_2\rangle}{c} + M_1 + \frac{c^2 pqD_3}{w\cos\chi}\right],\\ M_1(x) &= \frac{c^2}{g^2}\int_{x_S}^{x}\frac{D_2 g^2 dx'}{c^4\cos\chi}.\end{aligned} \tag{17}$$

When the PTE is applicable, the last term in square brackets of (17) can be replaced by

$$M_2(x) = \frac{c^2}{p^2\cos^2\chi}\int_{x_S}^{x}\frac{D_3 p^2\cos\chi dx'}{c^4}. \tag{18}$$

It is worth noting that $M_{1,2} < 0$. Formula (17) describes [with an accuracy to the terms $O(\varepsilon^3)$] the deviation of the average signal propagation time in a random medium from the propagation time in the absence of fluctuations. If we eliminate the term containing $c\langle c_2\rangle$ on the right-hand side of (17), then the expression obtained represents (with the same accuracy) the difference between the average arrival time and the arrival time in the averaged medium. We would like to emphasize that due to random deformations of a ray, the average propagation time differs from the propagation time in an unperturbed and averaged media, even when wave velocity fluctuations vanish along an unperturbed ray. If the fluctuations in the medium are caused by several uncorrelated random processes, then, by virtue of formulas (15)–(18), the contributions of these processes to both the dispersion of arrival times and the deviation of the average arrival time from the unperturbed arrival time are additive.

In the absence of regular refraction (c = const), formulas (15) and (17) are transformed into the results of [9] (in the isotropic case) and of [11] (in the special case of anisotropy considered there). In the general case, formulas (15) and (17) reduce the problem of determining dispersion and the systematic shift (bias) in signal travel time, which are caused by fluctuations in environment parameters, to that of calculating certain definite integrals. Here, we imply integrals of quantities that characterize three-dimensional random inhomogeneities in a two-dimensional inhomogeneous

medium. These integrals are calculated along an unperturbed deterministic eigenray.

ACKNOWLEDGMENTS

This study was supported in part by the ONR, project nos. N00014-01-F-0317 and N00014-02-IP2-0039.

I am grateful to A.G. Voronovich and V.U. Zavorotnyĭ for stimulating discussions of the results obtained.

REFERENCES

1. *Seismic Tomography with Applications in Global Seismology and Exploration Geophysics*, Ed. by G. Nolet (D. Reidel, Dordrecht, 1987).
2. W. Munk, P. Worcester, and C. Wunsch, *Ocean Acoustic Tomography* (Cambridge Univ. Press, Cambridge, 1995).
3. V. V. Goncharov, V. Yu. Zaitsev, V. M. Kurtepov, *et al.*, *Ocean Acoustic Tomography* (Inst. Prikl. Fiz., Ross. Akad. Nauk, Nizhni Novgorod, 1997).
4. P. N. Mikhalevsky, A. N. Gavrilov, and A. B. Baggeroer, IEEE J. Oceanic Eng. **24** (2), 182 (1999).
5. J. A. Mercer and J. R. Booker, J. Geophys. Res. **88** (1), 689 (1983).
6. J. L. Spiesberger, J. Acoust. Soc. Am. **77** (1), 83 (1985).
7. J. A. Colosi, S. M. Flatté, and C. Bracher, J. Acoust. Soc. Am. **96**, 452 (1994).
8. G. Nolet and T.-J. Moser, Geophys. J. Int. **114** (1), 185 (1993).
9. W. Boyse and J. B. Keller, J. Opt. Soc. Am. **12** (2), 380 (1995).
10. Y. Samuelides, J. Acoust. Soc. Am. **104** (5), 2596 (1998).
11. B. Iooss, Ph. Blanc-Benon, and C. Lhuillier, Waves Random Media **10** (3), 381 (2000).
12. O. A. Godin, J. Comput. Acoust. **10** (1), 123 (2002).
13. L. M. Brekhovskihk and O. A. Godin, *Acoustics of Layered Media*, Vol. 2: *Point Sources and Bounded Beams* (Springer-Verlag, Berlin, 1999), Sects. 1.3, 6.1, 7.3.6.
14. Yu. A. Kravtsov and Yu. I. Orlov, *Geometrical Optics of Inhomogeneous Media* (Nauka, Moscow, 1980).
15. R. Snieder and M. Sambridge, Geophys. J. Int. **109** (2), 294 (1992).

Translated by G. Merzon

Doklady Physics, Vol. 48, No. 8, 2003, pp. 394–397. Translated from Doklady Akademii Nauk, Vol. 391, No. 4, 2003, pp. 467–470.

PHYSICS

Atomistic Simulation of the Properties and Phase Transformations of FeO Wustite under High Pressures

I. Yu. Kantor* and Academician V. S. Urusov**

Received April 11, 2003

According to current concepts, $Fe_{1-x}O$ wustite enters into the composition of the Earth's mantle both as one of the components of (Mg, Fe)O magnowustite and, perhaps, as an individual phase. Therefore, knowledge of its properties at high pressures and temperatures is of great importance not only for solving problems of materials science but also for geophysics and geochemistry when interpreting data on the composition and structure of deep geospheres. In addition, the study of interactions between wustite and metallic iron is important for explanation of the formation and composition of the Earth's core, where iron–nickel alloy must contain "light" elements, e.g., oxygen as impurities [1]. For these reasons, wustite is extensively studied both experimentally and theoretically.

Since Fe is a transition element, the properties of wustite result from the magnetic and chemical interactions between unpaired 3*d* electrons in iron atoms. These interactions are responsible for the polymorphic transformations in wustite with increasing pressure, which are absent in compounds such as MgO periclase. Under normal conditions, wustite has the cubic NaCl-type structure (hereafter, the structural type B1). Below the Néel point (198 K), the FeO structure is no longer strictly cubical, because it acquires rhombohedral symmetry that is not associated with the displacements of atoms from the regular sites in the cubic lattice [2]. This symmetry appears due to the ordering of magnetic moments along one of the third-order crystallographic axes. With an increase in pressure, rhombohedral distortion of the cubic structure in wustite is observed. Such a distortion is associated with the extension of a cubic cell along one of the three axes (structural type rB1) [2–4]. The main indicator of the distortion degree of the structure is the rhombohedral angle α, which is equal to 60° in the undistorted cubic structure and less than 60° in the rB1 structure. This transition is attributed neither to the discontinuity in density nor to essential transformations in the structure and belongs to second-order polymorphic transitions. At room temperature, the rhombohedral distortion appears at about 15 GPa [2, 4]. At pressures 100–150 GPa (the available data are widely spread), FeO transforms to a new phase. At present, there is no commonly accepted opinion on the structural type of this phase. The structural type NiAs (B8), anti-NiAs (aB8, where the Fe and O atoms are replaced by the As and Ni atoms, respectively), or even complex polytypes consisting of alternating layers of the B8, aB8, and B1 structures are usually considered [5]. The very recent experimental data indicate in favor of the B8 structure [2]. The summary phase diagram of FeO is available in [3].

Under normal conditions, wustite is not entirely stoichiometric. The iron deficit in it is equal to 0.03–0.10. However, when pressure and temperature increase, the stoichiometry of wustite improves. Therefore, under high pressures, deviation in the FeO composition can be neglected when calculating the FeO properties. In addition, at the Earth's mantle–core interface (in equilibrium with metallic iron), wustite must exist in the strictly stoichiometric form.

In order to simulate the Fe–O system, various methods and approaches are applied. In this study, computer simulation of the structure and properties of wustite are carried out by the atomistic method. In this method, in accordance with the classical crystal-chemistry approach, atoms are characterized by some effective properties (charges, radii, etc.). The interaction between such atoms determines the structural energy E_{str} that is the sum of Coulomb forces and the energy of short-range repulsive and attractive potentials defined in an explicit form. Among available programs, the GULF software package for Linux [6] is the most elaborate for these calculations in terms of both capabilities and operation speed.

The parameters of interatomic interaction potentials were chosen by fitting the calculated crystal properties (elastic constants C_{11}, C_{12}, and C_{44} and the lattice

Moscow State University, Vorob'evy gory, Moscow, 119899 Russia

** e-mail: kesha_kantor@aport.ru*

*** e-mail: urusov@geol.msu.ru*

1028-3358/03/4808-0394$24.00

parameters) to the experimentally determined properties of FeO at 298 K [7] by minimizing the atomization energy [8]

$$E_{at} = E_{str} + E_{tr}, \quad (1)$$

where $E_{tr} = \Delta E(O) + \Delta E(Fe)$ is the energy of the charge transfer from a cation to an anion. To evaluate E_{tr}, the ionization energy was approximated by both the fourth power function [9]

$$\Delta E(O) = 6.62q + 5.76q^2 + 0.92q^3 + 0.32q^4, \quad -2 \le q \le 0$$

and the parabola

$$\Delta E(Fe) = 2.22q + 4.91q^2, \quad 2 \ge q \ge 0.$$

To estimate $\Delta E(Fe^{1+})$, we used the following data about the ionization potentials I^V of valence *sd* states [10]: $I^V(Fe^+) = 7.13$ eV and $\sum I^V(Fe) = 24.09$ eV.

The structural energy of the B1 and rB1 phases was calculated with the pair Buckingham potential V_B for interactions of O ions with each others and with Fe ions, pair Morse potential V_M for partially covalent interaction between Fe and O ions, and three-particle potential V_θ for interaction in O–Fe–O triples of atoms. These potentials have the form

$$V_B = A_{ij}\exp\left(\frac{-r_{ij}}{\rho_{ij}}\right) - \frac{C_{ij}}{r_{ij}^6}, \quad (2)$$

where r_{ij} is the distance between the *i*th and *j*th atoms and the optimum parameters are $A_{O-O} = 22764$ eV, $\rho_{O-O} = 0.149$ Å, $C_{O-O} = 22.88$ eV Å^6, $A_{Fe-O} = 342.98$ eV, $\rho_{Fe-O} = 0.389$ Å, and $C_{Fe-O} = 0$;

$$V_M = D_{ij}\left\{\left(1 - \exp\left(\frac{-a_{ij}}{r_{ij} - r_0}\right)\right)^2 - 1\right\}, \quad (3)$$

where $D_{Fe-O} = 0.097$ eV, $a_{Fe-O} = 0.247$ Å^{-1}, and $r_0 = 2.07$ Å; and

$$V_\theta = (J_{ijk}\exp(L_{ijk}\bar{r}) + M_{ijk})(\theta - \theta_0)^2, \quad (4)$$

where $J_{O-Fe-O} = -16.07 \times 10^5$ eV, $L_{O-Fe-O} = -0.105$ Å^{-1}, $M_{O-Fe-O} = 12.81 \times 10^5$ eV, $\bar{r}$ is the average Fe–O distance in a given triple of atoms, and θ is the O–Fe–O angle ($\theta_0 = 90°$ is the equilibrium angle).

The three-particle potential is applied in form (4) for the first time and enables us both to reproduce the deviation from the Cauchy relation ($C_{12} = C_{44}$) and to take into account the interatomic-distance dependence of the potential in addition to the dependence on the angle between the bonds. This makes it possible to describe both the experimentally observed decrease in C_{44} with increasing pressure and the rhombohedral distortion of the cubic lattice, i.e., the B1–rB1 phase transition.

For the B8 and B1 phases, the minimum in the atomization energy $E_{at}(FeO)$ corresponds to the ion charges $\pm 1.41e_0$ and $\pm 1.80e_0$, respectively. The atomization energy obtained for the B1 phase of FeO is equal to 11.96 eV (its experimental value is 9.67 eV).

In the B8 structure, as well as in the B1 structure, Fe ions have octahedral coordination. However, octahedrons have not only common edges, but also common faces, forming columns along the hexagonal axis. This indicates that the Fe–Fe interactions in the B8 phase are much stronger than those in the B1 phase. In addition, since iron can transit from the high-spin state to the low-spin state at high pressures, the effective charges of ions in the B8 phase are expected to be much smaller than those in the B1 phase. Therefore, in order to describe the B8 phase in FeO, we used another set of interatomic potentials, which were found using the minimum experimental data concerning the B8 phase in FeO. At present, it is only reliably known that, at the point of the B1–B8 transition (~100–120 GPa), volume decreases by about 2% and the $\frac{c}{a}$ ratio for the hexagonal cell is equal to 1.985 [4]. Based on these data, we found the following set of the interatomic potentials for the B8 phase in FeO: (i) Buckingham potentials (2) with the same parameters of the O–O interaction, $A_{Fe-O} = 317.39$ eV, $\rho_{Fe-O} = 0.389$ Å, and $C_{Fe-O} = 0$; (ii) Morse potentials (3) of the partially covalent Fe–O interaction and the Fe–Fe interaction with the parameters $D_{Fe-O} = 0.245$ eV, $a_{Fe-O} = 0.675$ Å, $r_0 = 2.07$ Å, $D_{Fe-Fe} = 1.14$ eV, $a_{Fe-Fe} = 1.11$ Å, and $r_0 = 2.48$ Å.

To compare the enthalpies of the B1 and B8 phases in FeO, a difference of 11.17 eV between the energies of the charge transfer from Fe to O must be subtracted from the structural energy of the B8 phase. The atomization energies of both phases as functions of the effective charges on ions are shown in Fig. 1.

Using the above sets of interatomic potentials, it is possible to calculate the *P–V* diagram for FeO (Fig. 2). To this end, one often uses the Birch–Murnagham equation (it is generally a fourth-order equation) [13]. For most compounds, it is sufficient to apply the third-order equation:

$$P = 3K_0 f_E(1 + 2f_E)^{\frac{5}{2}}\left(1 + \frac{3}{2}(K' - 4)f_E\right), \quad (5)$$

where $f_E = \frac{1}{2}\left[\left(\frac{V_0}{V}\right)^{\frac{2}{3}} - 1\right]$, V_0 is the volume at zero pressure, and V is the volume at pressure P.

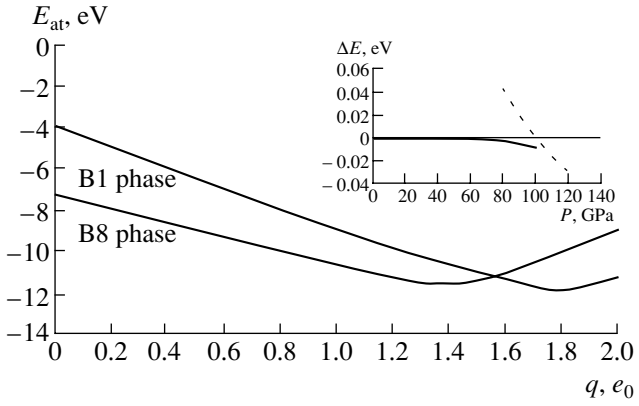

Fig. 1. Atomization energies of the B1 and B8 phases in FeO vs. the effective charge of the ions. The insert shows the energy diagram of the polymorphic transitions in FeO: the difference in enthalpies (solid thick line) between the B1 and rB1 phases and (dashed line) between the rB1 and B8 phases.

If we take $K' = 4$, then Eq. (5) transforms to the second-order equation

$$P = 3K_0 f_E (1 + 2f_E)^{\frac{5}{2}}. \quad (6)$$

The parameters of the equation of state from the known P–V data can be found by the EoSFit program [13]. Some experimental and theoretical parameters of the equation of state of FeO are listed in the table. The recent experiments show [11, 12] that K' is not equal to 4 at normal temperatures; i.e., it is necessary to apply the third-order equation of state (5). This conclusion is corroborated by our calculations. However, the experiment for 1500 K [4] demonstrates that the second-order equation of state (6) quite accurately describes the P–V diagram of the B1 phase for high temperatures.

The calculated pressure dependence of the elastic constants of wustite (Fig. 3) reproduces experimental data well, including the "softening" of C_{44} with an increase in pressure. At a pressure of about 39 GPa, the transition of wustite from the cubic phase to the rhombohedral phase is accompanied by a steplike change in the elastic constants and a continuous change in the volume and bulk modulus $K = \frac{1}{3}(C_{11} + 2C_{12})$. In the static approximation (at $T = 0$), the points of polymorphic transitions are found from the condition that the enthalpies of both phases are equal to each other. The insert in Fig. 1 shows the differences in enthalpies between the B1 and rB1 phases, as well as between the rB1 and B8 phases. It is seen that the slopes of these curves are considerably different, because the B1–rB1 and rB1–B8 transitions are second- and first-order transitions, respectively. In this case, the enthalpy of the rB1 phase is the enthalpy of the relaxed structure with $\alpha \le 60°$ (Fig. 4). Comparing the insert in Fig. 1 with the insert in Fig. 4, one can note the following interesting feature. Although the rhombohedral distortion of the B1 phase starts at a pressure of 39 GPa, the enthalpies of the B1 and rB1 phases virtually coincide with each other up to a pressure of 60 GPa. However, this cannot be treated as the coexistence of the two phases, because almost zero difference between enthalpies is characteristic for second-kind phase transitions.

Thus, the calculations demonstrate that the atomistic computer simulation of crystal properties has rather high prediction ability even in static calculations.

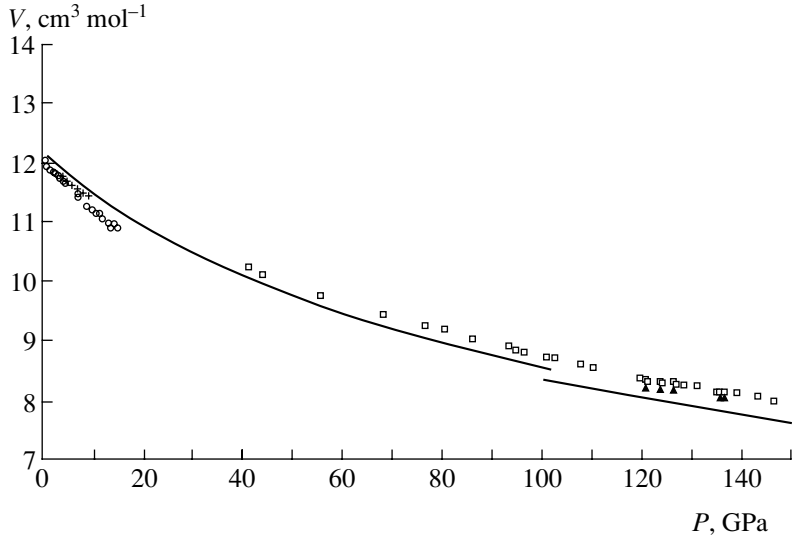

Fig. 2. P–V diagram in FeO. Solid line is our results (the point of discontinuity at 100 GPa corresponds to the polymorphic rB1–B8 transition); crosses and circles are experimental data for $Fe_{0.946}O$ (T = 298 K) [11] and ○, $Fe_{0.94}O$ (T = 300 K) [12], respectively; and squares and triangles are experimental data for the B1 and B8 phases in $Fe_{0.91}O$ (T = 1500 K) [4], respectively.

Calculated and experimental parameters of the Birch–Murnagham equations of state given by Eqs. (5) and (6) for FeO

Parameter	B1 phase					B8 phase, our calculation
	our calculation	$Fe_{0.946}O$, 298 K [11]	$Fe_{0.94}O$, 300 K [12]	$Fe_{0.95}O$, 1500 K [4]	FeO, 0 K (theory) [2]	
V_0, cm^3/mol	12.172	12.03	12.04	12.04	11.99	12.045
K_0	158.92	153.0	125.41	128.39	193	130.84
K'	3.32	5.55	3.32	(4.0)	3.72	(4.0)

Moreover, the use of the methods of molecular dynamics in the future will make it possible to find the complete and rather reliable *P–V–T* state diagram of FeO.

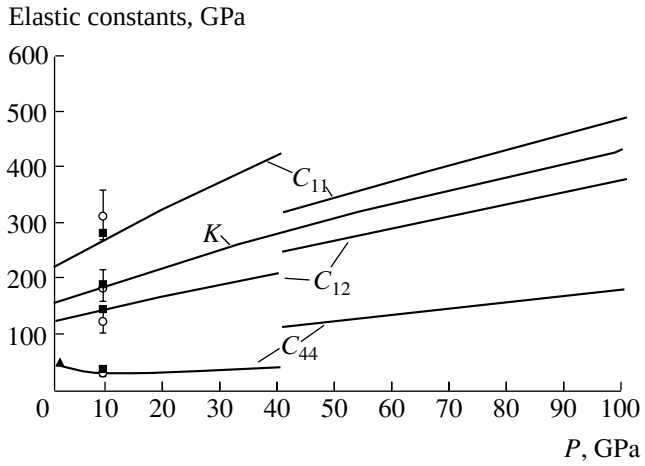

Fig. 3. Pressure dependence of the elastic constants C_{11}, C_{12}, and C_{44} and the bulk modulus K. Discontinuity of the elastic constants at 39 GPa for the continuous variation in the bulk modulus corresponds to the second-order polymorphic B1–rB1 transition. Triangles, circles, and squares are the experimental data under normal conditions [7], X-ray diffraction data [12], and ultrasonic measurements [14], respectively.

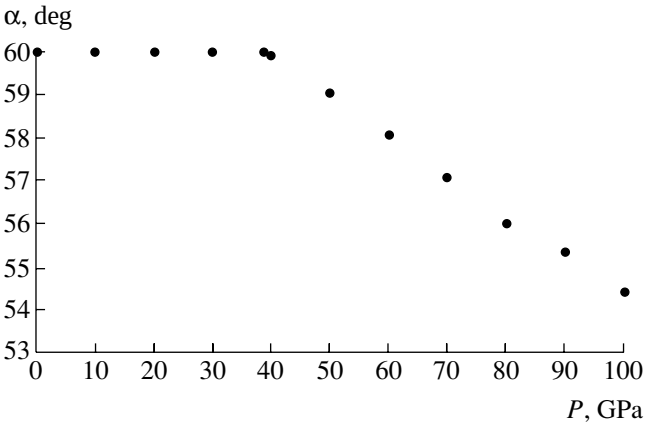

Fig. 4. Pressure dependence of the rhombohedral angle α for the rB1 phase, where α = 60° corresponds to the undistorted cubic structure.

ACKNOWLEDGMENTS

This work was supported by the Russian Foundation for Basic Research (project nos. 00-15-98582 and 02-05-64845). We are grateful to L.S. Dubrovinsky at Bayerisches Forschungsinstitut für experimentelle Geochemie und Geophysik (Bayerisches Geoinstitut), Universität Bayreuth [Bavarian Research Institute of Experimental Geochemistry and Geophysics (Bavarian Geoinsitute), University of Bayreuth] for helpful proposals and discussions.

REFERENCES

1. C. A. McCammon, A. E. Ringwood, and I. Jackson, Geophys. J. R. Astron. Soc. **72**, 577 (1983).
2. S. A. Gramsh, R. E. Cohen, and S. Yu. Savrasov, Am. Mineral. **88**, 257 (2003).
3. Y. Fei and H. Mao, Science **266**, 1668 (1994).
4. N. Sata, G. Shen, M. L. Rivers, *et al.*, Phys. Rev. (2003) (in press).
5. I. I. Mazin, Y. Fei, R. Downs, and R. Cohen, Am. Mineral. **83**, 451 (1998).
6. J. D. Gale, J. Chem. Soc., Faraday Trans. **93**, 629 (1997).
7. *Mineral Physics and Crystallography: a Handbook of Physical Constants*, Ed. by T. J. Ahrens (Am. Geophys. Union, Washington, DC, 1995).
8. V. S. Urusov and L. S. Dubrovinsky, *Computer Simulation of the Structural Properties of Minerals* (Mosk. Gos. Univ., Moscow, 1989).
9. V. S. Urusov and I. Yu. Kantor, Dokl. Akad. Nauk **386**, 614 (2002) [Dokl. Phys. **47**, 717 (2002)].
10. O. P. Charkin, *Stability and Structure of Inorganic Gas Molecules, Radicals, and Ions* (Nauka, Moscow, 1980).
11. S. D. Jacobsen, H. J. Reichmann, H. A. Spetzler, *et al.*, J. Geophys. Res. **107**/**2**, 2037 (2002).
12. A. K. Singh, H. Mao, J. Shu, and R. J. Hemley, Phys. Rev. Lett. **80**, 2157 (1998).
13. R. J. Angel, Rev. Mineral. **41**, 35 (2000).
14. I. Jackson, S. K. Khanna, A. Revcolevschi, and J. Berthon, J. Geophys. Res. **95**, 21671 (1990).

Translated by Yu. Vishnyakov

Doklady Physics, Vol. 48, No. 8, 2003, pp. 398–404. Translated from Doklady Akademii Nauk, Vol. 391, No. 4, 2003, pp. 471–477.

PHYSICS

Possibility of Intensifying Chain Reactions in Combustible Mixtures by Laser Radiation Exciting Electronic States of O_2 Molecules

A. M. Starik* and N. S. Titova

Presented by Academician O.N. Favorskiĭ February 18, 2003

Received March 5, 2003

INTRODUCTION

The application of resonance radiation to intensify combustion processes has been studied for a long time [1–6]. At present, three possible methods of initiating combustion by laser radiation are discussed. First, the local heating of a gas due to radiation absorption by molecules (SF_6, NH_3, etc.) specially introduced into a mixture [1, 2]. Second, the photodissociation of molecules by resonance laser radiation, which leads to the formation of free radicals [4]. Third, the generation of a plasma in the field of a narrow intense laser beam ($\sim 10^{10}$ W cm^{-2}) [5, 6]. However, all these methods have considerable restrictions and low efficiency [5].

In this work, we discuss another method of initiating combustion, which is based on the intensification of chain reactions when exciting electron degrees of freedom of O_2 molecules by laser radiation.

FORMULATION OF THE PROBLEM AND FEATURES OF EXCITATION OF O_2 MOLECULES TO THE $a^1\Delta g$ AND $b^1\Sigma_g^+$ STATES

We consider an H_2/O_2 homogeneous gas mixture subjected to a radiation pulse whose frequency is in resonance with the center of the line of the electronic–vibrational transition in the O_2 molecule

$$m(e', v', j', K') \to n(e'', v'', j'', K''),$$

where $e' = X^3\Sigma_g^-$, $e'' = a^1\Delta_g$ or $b^1\Sigma_g^+$, v' and v'' vibrational quantum numbers, and j' and K' and j'' and K'' are rotational quantum numbers in the ground $X^3\Sigma_g^-$ and excited $a^1\Delta_g$ ($b^1\Sigma_g^+$) states, respectively. The $X^3\Sigma_g^- \longrightarrow a^1\Delta_g(b^1\Sigma_g^+)$ transition is allowed only in the magnetic-dipole approximation. Rotational levels are manifested only beginning with $j'' \geq K'' \geq 2$. Every rotational level in the $X^3\Sigma_g^-$ state with the quantum number K' involves three components with $j' = K' + 1$, K', and $K' - 1$ [7].

We analyze transitions of the ${}^QP(9)$ branch with $v' = v'' = 0$, $j' = 10$, and $j'' = K' = K'' = 9$. In this case, the spectral-line center for the $X^3\Sigma_g^- \longrightarrow a^1\Delta_g$ and $X^3\Sigma_g^- \longrightarrow b^1\Sigma_g^+$ transitions corresponds to the wavelength λ_I = 1268 and 762 nm, respectively. The Einstein coefficients A_{mn} for these transitions are equal to 2.58×10^{-4} and 8.5×10^{-2} s^{-1}, respectively. Variation in the concentration of excited $O_2(a^1\Delta_g)$ and $O_2(b^1\Sigma_g^+)$ molecules is determined by the rate of induced transitions

$$W_I = \frac{\sigma_{mn} I}{h\nu_I}, \text{ where } \sigma_{mn} = \frac{\lambda_{mn}^2}{4\pi b_D} A_{mn} \sqrt{\frac{\ln 2}{\pi}} H(x, a).$$

Here, I and ν_I are the intensity and frequency of acting radiation, respectively; h is Planck's constant; λ_{mn} is the wavelength of the center of the $m \longrightarrow n$ transition line; b_D is the Doppler FWHM; and $H(x, a)$ is the Voight function. In the absence of chemical reactions, the concentration of $O_2(a^1\Delta_g)$ and $O_2(b^1\Sigma_g^+)$ molecules decreases due to electronic translational relaxation

$$O_2(b^1\Sigma_g^+) + M = O_2(a^1\Delta_g) + M$$

and

$$O_2(a^1\Delta_g) + M = O_2(X^3\Sigma_g^-) + M,$$

because the radiative lifetimes of these states are anomalously long. Under the typical experimental conditions (initial temperature T_0 = 300–700 K and $P_0 = 10^3$–10^4 Pa), the time of electronic transitional relaxation of excited O_2 molecules is equal to $\tau_Q \sim 0.1$–3 s, and the induced-transition time is equal to $\tau_I = 10^{-3}$–10^{-5} s for

Baranov Central Institute of Aviation Motors, Aviamotornaya ul. 2, Moscow, 111116 Russia
** e-mail: star@ciam.ru*

1028-3358/03/4808-0398$24.00

$I = 1$–10 kW/cm^2. Thus, high excitation efficiency ($\tau_I \ll \tau_Q$) can be ensured even for low intensities of acting radiation. At the same time, for these I values, we have $\tau_I \gg \tau_R$ and τ_V, where τ_R and τ_V are the characteristic times of rotational and vibrational relaxation, respectively. Therefore, one can think that translational, rotational, and vibrational degrees of freedom are in thermodynamic equilibrium.

Variation of the hydrodynamic parameters in the irradiation zone is determined by the hierarchy of the characteristic times of various macro- and microtransport processes. For a nonreacting inviscid gas, these times are the time τ_a of propagating acoustic perturbations across the interaction region; the times τ_D^i and τ_{Ti} of multicomponent and thermal diffusion of the ith component, respectively; the thermal-conductivity time τ_λ; the induced-transition time τ_I; the relaxation time τ_Q of the excited $O_2(a^1\Delta_g)$ and $O_2(b^1\Sigma_g^+)$ states; the pulse duration τ_P of acting radiation; and the time τ_F of change in the medium state due to the striction force [8]. For a reacting gas, it is necessary to additionally introduce the time τ_{iq}^{ch} of a chemical reaction leading to the appearance (destruction) of the component responsible for the chain mechanism of the reaction. The quantity τ_{iq}^{ch} determines the ignition delay time or induction period τ_{in}.

We consider the ignition of the H_2/O_2 (2/1) mixture in a laser beam with a Gaussian radial distribution of intensity

$$I(r, t) = I_0(t)\exp\left(-\frac{r^2}{R_a^2}\right),$$

where R_a is the characteristic beam radius and $I_0(t) = I_0$ and 0 for $0 < t \le \tau_P$ and $t > \tau_P$, respectively. For $I_0 = 1$–10 kW/cm^2, $R_a = 10$ cm, $P_0 = 10^3$–10^4 Pa, and $T_0 = 300$–700 K, we have $\tau_a = 2 \times 10^{-4}$ s, $\tau_D^i \sim \tau_{Ti} \sim \tau_\lambda = 0.3$–$10$ s, and $\tau_F = 0.5$–10 s. We consider regimes where $\tau_a \ll \tau_P \sim \tau_I \le \tau_{in} \ll \tau_D, \tau_F$. Under these conditions, the absorptivity k_ν of 762-nm radiation varies from 8×10^{-5} to 2×10^{-3} cm^{-1} and therefore $k_\nu^{-1} \gg R_a$. In this case, the approximation of a thin optical layer is applicable, variation in the parameters in the reacting mixture can be considered only across the beam, and macrotransport processes can be disregarded in the $[0, \tau_{in}]$ interval. In this case, the equations describing the state of the medium in the central irradiation zone ($r \ll R_a$) can be represented in the form

$$\frac{\partial N_i}{\partial t} = G_i + q_I^i,$$

$$\rho\frac{\partial E}{\partial t} = k_\nu I - \rho\sum_{i=1}^{3} h_{0i}q_I^i - \rho\sum_{i=1}^{M} h_{0i}G_i,$$

$$G_i = \sum_{q=1}^{M_1} S_{iq}, \quad S_{iq} = (\alpha_{iq}^- - \alpha_{iq}^+)[R_q^+ - R_q^-],$$

$$R_q^{+(-)} = k_{+(-)q}\prod_{j=1}^{n_q^{+(-)}} N_j^{\alpha_{jq}^{+(-)}},$$

$$q_I^i = l_{Ii}W_{Ii}\left(\frac{g_{ni}}{g_{mi}}N_m - N_n\right), \quad k_\nu = \sigma_{mn}\left(\frac{g_n}{g_m}N_m - N_n\right),$$

$$E = \sum_{i=1}^{M} C_{VT}^i T,$$

$$C_{VT}^i = \frac{R}{\mu}\gamma_i\left(\frac{3}{2} + C_R^i + C_V^i\right),$$

$$C_V^i = \sum_{l=1}^{L_i}\left(\frac{\theta_{il}}{T}\right)^2 \frac{\exp\dfrac{\theta_{il}}{T}}{\left[\exp\left(\dfrac{\theta_{il}}{T} - 1\right)\right]^2},$$

$$\mu = \sum_{i=1}^{M}\mu_i\gamma_i, \quad \gamma_i = \frac{N_i}{N}, \quad N = \sum_{i=1}^{M} N_i.$$

Here, ρ and T are the density and temperature of the mixture, respectively; N_i and μ_i are, respectively, the density and molecular mass of molecules (or atoms) of the ith kind [$i = 1$, 2, and 3 correspond to $O_2(X^3\Sigma_g^-)$, $O_2(a^1\Delta_g)$, and $O_2(b^1\Sigma_g^+)$ molecules, respectively, while $i = 4$–11 correspond to the other components of the reacting mixture H_2, H_2O, OH, HO_2, H_2O_2, O_3, O, H]; h_{0i} is the enthalpy of the formation of the ith component; M is the total number of components in the mixture; $C_R^i = 1$ and 1.5 for components involving linear and nonlinear molecules, respectively; θ_{ij} is the characteristic vibrational temperature of the jth mode of the ith component ($j = 1, 2, \ldots, L_i$); M_i is the number of reactions leading to the formation (destruction) of the ith component; α_{iq}^+ and α_{iq}^- are the stoichiometric coefficients of the qth reaction; n_q^+ and n_q^- are the numbers of components involved into the direct and inverse reactions, respectively; k_+ and k_- are the rates of the respective reactions; R is the universal gas constant; l_{Ii} is the number of quanta acquired by the ith component

(i = 1, 2, 3) in induced transitions; N_m and N_n are the densities of O_2 molecules in the lower and upper states involved into the $m \longrightarrow n$ transition, respectively; and g_m and g_n are the degrees of degeneracy of the respective states.

KINETIC MODEL

As is known, to describe the ignition of H_2/O_2 mixtures in a wide range of P_0 and T_0, it is necessary to use a quite complete kinetic scheme, including 29 reversible reactions even in the absence of excited O_2 molecules [9]. The excitation of O_2 molecules to the $a^1\Delta_g$ and $b^1\Sigma_g^+$ states initiates new reactions, the most important of which are presented in Table 1. Below, we will refer to reactions according to their numbering in Table 1.

The rates of reactions involving unexcited O_2 molecules in the reacting H_2/O_2 system are known quite well. At the same time, information for processes involving $O_2(a^1\Delta_g)$ and $O_2(b^1\Sigma_g^+)$ molecules is sparse. Experimental data are available only for certain reactions (nos. 3, 9, 29–33) [10]. Two types can be separated among the processes under consideration: first, endothermic reactions with activation barrier (reactions 1–6, 9–24) and, second, barrierless reactions (nos. 7, 8, 25–28). The rates of reactions of the first type were calculated by using the procedure of decreasing the activation barrier. This procedure is based on the assumption that the potential surfaces u_1 and u_1^e of direct reactions involving unexcited and excited molecules, respectively, are equidistant [11]:

$$u_1(r) = \Delta H + E_a^0 \exp\frac{r}{r_1},$$

$$u_1^e(r) = \Delta H + E_e + E_a^0 \exp\frac{r}{r_1}.$$

Taking into account that the potential-energy surface for the inverse reaction is expressed as

$$u_2(r) = (\Delta H + E_a^0)\exp\left(-\frac{r}{r_2}\right)$$

and using the ordinary relation $r_1 \approx r_2$ [11], one can rep-

Table 1

No.	Reaction	No.	Reaction
1	$O_2(a^1\Delta_g) + M = O + O + M$	17	$H_2O + O_2(a^1\Delta_g) = H_2O_2 + O$
2	$O_2(b^1\Sigma_g^+) + M = O + O + M$	18	$H_2O + O_2(b^1\Sigma_g^+) = H_2O_2 + O$
3	$O_2(a^1\Delta_g) + H = OH + O$	19	$O_3 + M = O + O_2(a^1\Delta_g) + M$
4	$O_2(b^1\Sigma_g^+) + H = OH + O$	20	$O_3 + M = O + O_2(b^1\Sigma_g^+) + M$
5	$H_2 + O_2(a^1\Delta_g) = 2OH$	21	$O_3 + H = OH + O_2(a^1\Delta_g)$
6	$H_2 + O_2(b^1\Sigma_g^+) = 2OH$	22	$O_3 + H = OH + O_2(b^1\Sigma_g^+)$
7	$HO_2 + M = O_2(a^1\Delta_g) + H + M$	23	$O_3 + O = O_2(X^3\Sigma_g^-) + O_2(a^1\Delta_g)$
8	$HO_2 + M = O_2(b^1\Sigma_g^+) + H + M$	24	$O_3 + O = O_2(X^3\Sigma_g^-) + O_2(b^1\Sigma_g^+)$
9	$H_2 + O_2(a^1\Delta_g) = H + HO_2$	25	$O_3 + OH = HO_2 + O_2(a^1\Delta_g)$
10	$H_2 + O_2(b^1\Sigma_g^+) = H + HO_2$	26	$O_3 + OH = HO_2 + O_2(b^1\Sigma_g^+)$
11	$H_2O + O_2(a^1\Delta_g) = OH + HO_2$	27	$O_3 + HO_2 = OH + O_2(X^3\Sigma_g^-) + O_2(a^1\Delta_g)$
12	$H_2O + O_2(b^1\Sigma_g^+) = OH + HO_2$	28	$O_3 + HO_2 = OH + O_2(X^3\Sigma_g^-) + O_2(b^1\Sigma_g^+)$
13	$OH + O_2(a^1\Delta_g) = O + HO_2$	29	$O_3 + O_2(a^1\Delta_g) = 2O_2(X^3\Sigma_g^-) + O$
14	$OH + O_2(b^1\Sigma_g^+) = O + HO_2$	30	$O_3 + O_2(b^1\Sigma_g^+) = 2O_2(X^3\Sigma_g^-) + O$
15	$2HO_2 = H_2O_2 + O_2(a^1\Delta_g)$	31	$2O_2(a^1\Delta_g) = O_2(b^1\Sigma_g^+) + O_2(X^3\Sigma_g^-)$
16	$2HO_2 = H_2O_2 + O_2(b^1\Sigma_g^+)$	32	$O_2(a^1\Delta_g) + M = O_2(X^3\Sigma_g^-) + M$
		33	$O_2(b^1\Sigma_g^+) + M = O_2(a^1\Delta_g) + M$

resent the activation barrier for the reaction involving an excited molecule in the form

$$E_a^e = \frac{1}{2}(\sqrt{(\Delta H + E_e)^2 + 4E_a^0(\Delta H + E_a^0)} - (\Delta H + E_e)).$$

Here, ΔH is the thermal effect of the reaction; E_a^0 is the activation energy of the reaction in the absence of the excitation of reacting molecules; E_e is the energy of an excited molecule; and r_1 and r_2 are the radii of exchange forces for reagents and products, respectively. The rate of such a reaction has the Arrhenius form

$$k_{ex} = AT^n \exp\left(-\frac{E_a^e}{T}\right),$$

where A and n are the parameters of the corresponding dependence for the reaction involving an unexcited molecule.

Similar to [10], the probability of the formation of the O_2 molecule in the $X^3\Sigma_g^-$, $a^1\Delta_g$, and $b^1\Sigma_g^+$ electronic states in reactions of the second type with $E_a^0 \approx 0$ is proportional to the degree of degeneracy of these states, i.e., $g_X = 0.5$, $g_a = 0.33$, and $g_b = 0.17$. The rates of the inverse processes for the two types of reactions under consideration were calculated based on the principle of detailed balance.

IGNITION DYNAMICS FOR A MIXTURE UNDER RADIATION

Combustible mixtures are ignited by chain reactions. For the H_2/O_2 mixture, these are reactions involving O and H atoms and OH radicals. For ignition, the rate of the formation of O, H, and OH must exceed the rate of their destruction in chain-break reactions or the rate of leaving of these components from the reaction zone due to diffusion processes (their characteristic time is determined by the diffusion time H, τ_D^H of light carriers, H atoms, of the chain mechanism). Since $\tau_{in} \sim \tau_{iq}^{ch}$, the ignition condition has the form $\tau_{in} \le \tau_D^H$.

Figure 1 shows $\tau_{in}(T_0)$ and $\tau_D^H(T_0)$ for radiation with the parameters λ_I = 1268 and 762 nm, $\tau_P = 10^{-3}$ s, and various I_0 values. It is seen that 762-nm radiation reduces τ_{in} stronger than 1268-nm radiation does and correspondingly reduces the self-ignition temperature T_{ign}, which can be determined in the first approximation from the relation

$$\tau_{in}(T_{ign}, I_0, P_0) = \tau_D^H(T_{ign}, P_0).$$

For a supplied energy of $E_{in} = I_0\tau_P = 5$ J/cm^2, 762-nm radiation reduces the temperature T_{ign} to 300 K. We

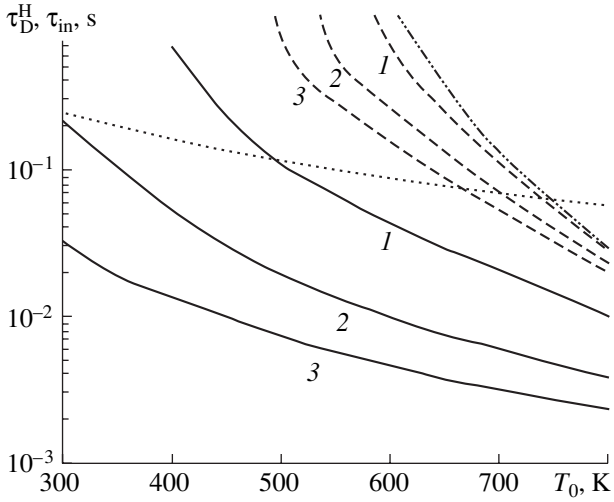

Fig. 1. (Dotted line) $\tau_D^H(T_0)$ and $\tau_{in}(T_0)$ for the $H_2/O_2 = 2/1$ mixture at $P_0 = 10^3$ Pa under (dashed lines) 1268- and (solid lines) 762-nm radiation with I_0 = (*1*) 1, (*2*) 5, and (*3*) 10 kW/cm^2 and $\tau_P = 10^{-3}$ s. The dash–dotted line is $\tau_{in}(T_0)$ for $I_0 = 0$.

emphasize that this E_{in} value corresponds to 0.082-eV energy spent on the excitation of one O_2 molecule to the $b^1\Sigma_g^+$ state. At the same time, the photodissociation of the O_2 molecule from the ground state (this process initiates the chain mechanism of the ignition of the H_2/O_2 mixture due to the formation of O atoms) requires 5.8 eV. Moreover, the recombination of O atoms for low gas temperatures ($T_0 \le 600$ K) proceeds at a very high rate. This additionally reduces the efficiency of the photochemical method of ignition based on the photodissociation of molecules by laser radiation [12].

Figure 2 shows the time variation in the mole fractions γ_i of the components of the reacting H_2/O_2 mixture in the absence of irradiation and under radiation with the parameters λ_I = 1268 and 762 nm, I_0 = 10 kW/cm^2, and $\tau_P = 10^{-3}$ s. As is seen, the $\gamma_i(t)$ behavior, as well as the τ_{in} value, changes when O_2 molecules are excited to the $a^1\Delta_g$ and $b^1\Sigma_g^+$ states. We emphasize that the concentration of both $O_2(b^1\Sigma_g^+)$ and $O_2(a^1\Delta_g)$ molecules increases under 762-nm radiation in the $[0, \tau_{in}]$ interval. This effect is caused by the quenching of the $b^1\Sigma_g^+$ state (reaction no. 33). In this case, the concentration of $O_2(a^1\Delta_g)$ molecules at $t = \tau_P$ is much higher (by a factor of about 40) than that produced by the excitation of O_2 molecules to the $a^1\Delta_g$ state by 1268-nm radiation. This difference is attributed to the fact that the rate of the induced $X^3\Sigma_g^- \longrightarrow b^1\Sigma_g^+$ transi-

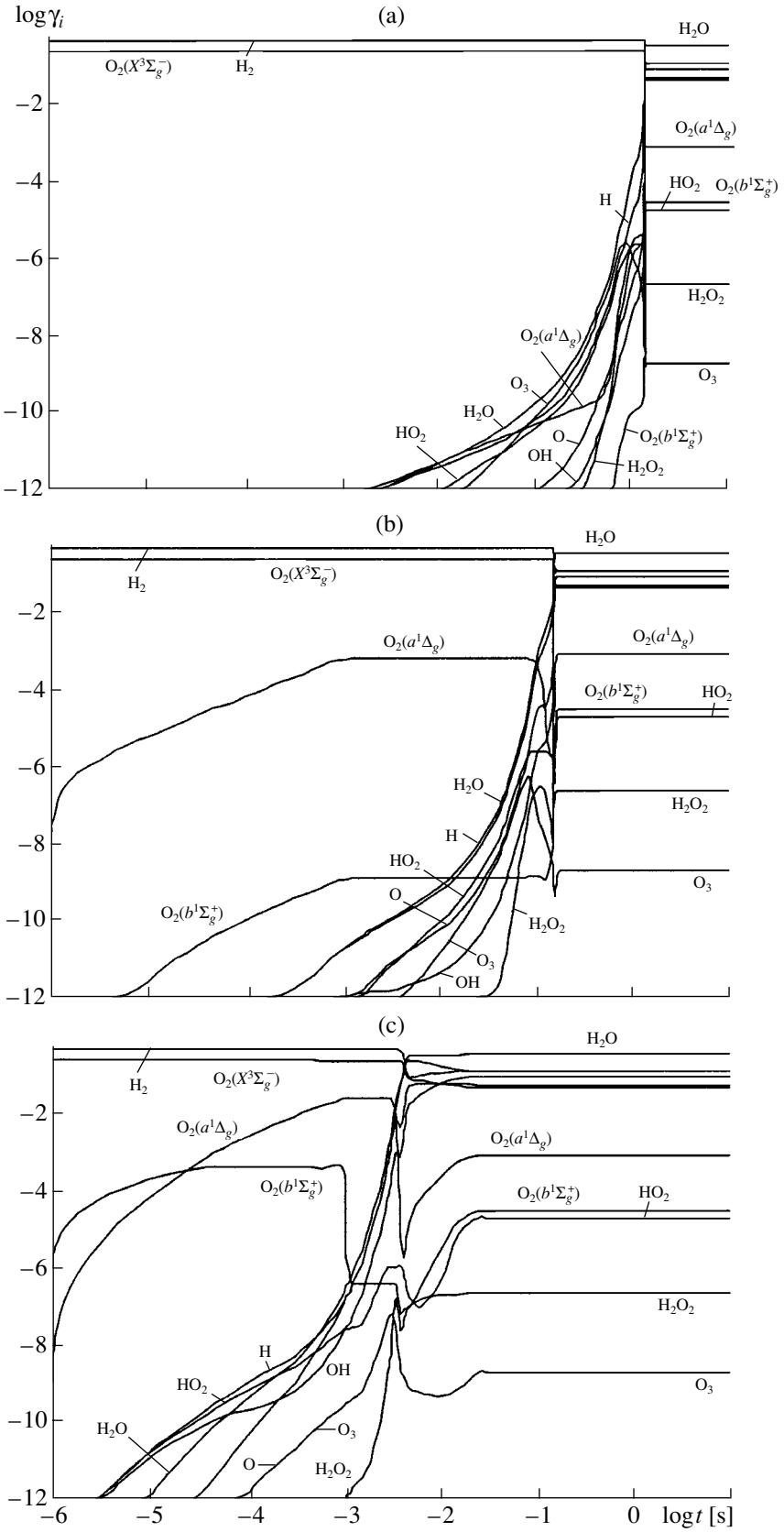

Fig. 2. Time variation in the concentrations of the components of the $H_2/O_2 = 2/1$ mixture for $T_0 = 600$ K and $P_0 = 10^3$ Pa (a) in the absence of irradiation and under (b) 1268- and (c) 762-nm radiation with $I_0 = 10$ kW/cm^2 and $\tau_p = 10^{-3}$ s.

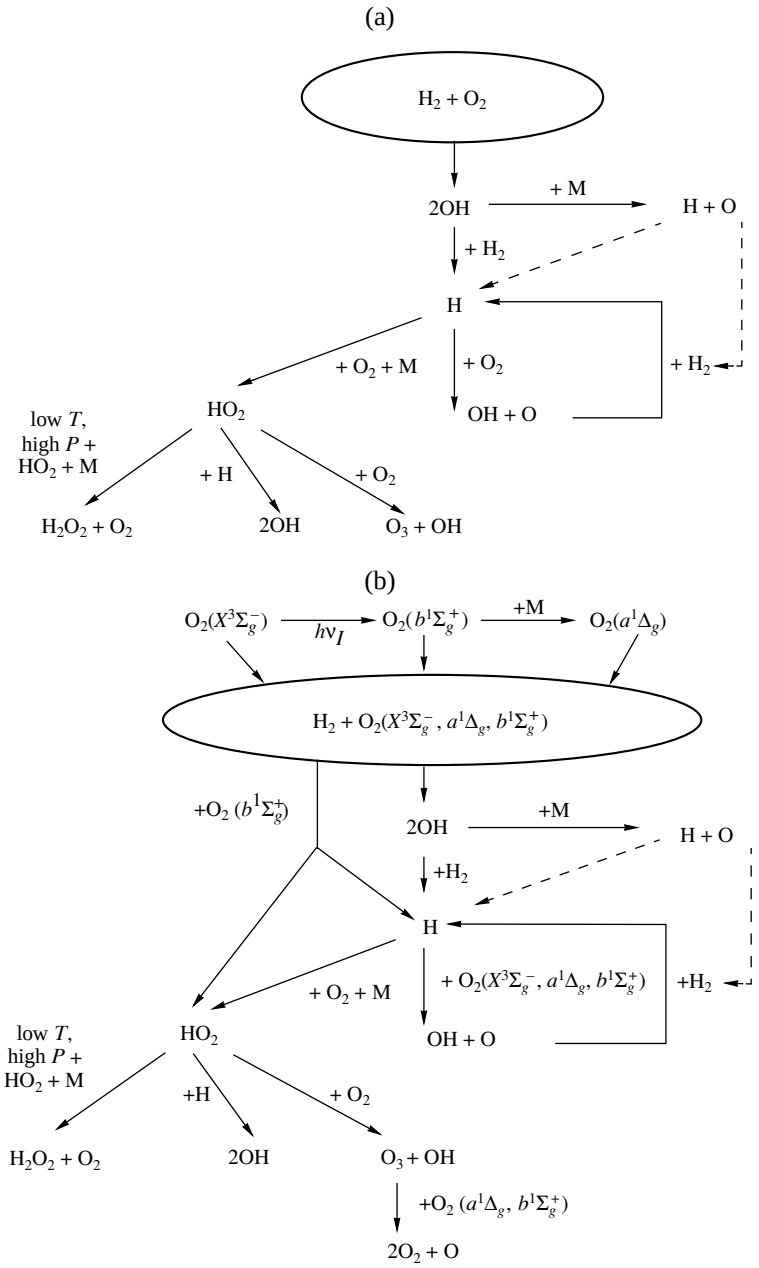

Fig. 3. Processes responsible for the formation of O and H atoms and OH radicals (a) in the absence of irradiation and under (b) 762-nm radiation.

tion is higher than the rate of the $X^3\Sigma_g^- \longrightarrow a^1\Delta_g$ transition by a factor of 75 for the same I_0 value.

Collisional quenching of the $b^1\Sigma_g^+$ state slightly increases T in the $[0, \tau_p]$ interval. In particular, for I_0 = 10 kW/cm^2 and $\tau_p = 10^{-3}$ s, temperature increases from 600 K at $t = 0$ to 688 K at $t = \tau_p$. However, τ_{in} decreases in this case due not to an increase in T but to the appearance of new channels of the formation of O and H atoms and OH radicals. Indeed, an increase in T_0 from 600 to 688 K reduces τ_{in} to 0.14 s. This value is larger than the value of 4.6×10^{-3} s, which is achieved when the radical mechanism, along with thermal one, is taken into account, by a factor of 30. Figure 3 shows the processes responsible for the formation of O and H atoms and OH radicals in the absence of radiation and under 762-nm radiation. In the absence of excited O_2 molecules, the $H_2 + O_2 = 2OH$ reaction is the basic chain-initiation reaction for $T_0 < 1000$ K. The reaction of OH radicals with H_2 molecules yields H atoms, which are involved in the chain-branching reaction $H + O_2 = OH + O$. The $H_2 + O = OH + H$ process is the second reaction of chain propagation.

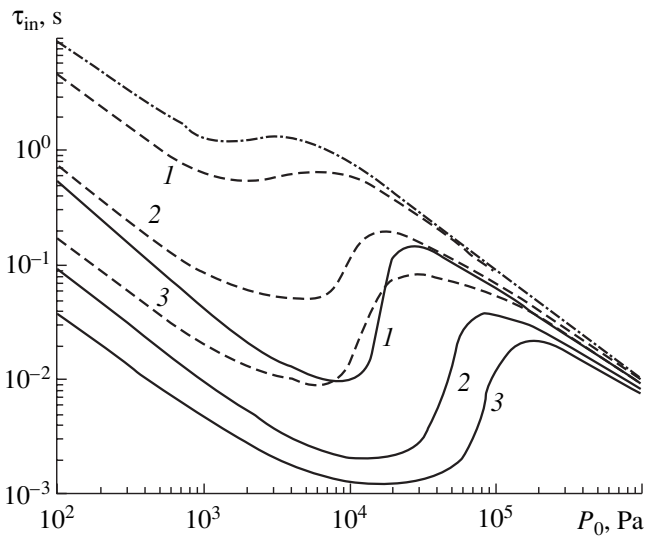

Fig. 4. Initial-pressure dependences of $\tau_{in}(P_0)$ for the $H_2/O_2 = 2/1$ mixture at $T_0 = 600$ K (solid lines) when O_2 molecules are excited to the $b^1\Sigma_g^+$ state by 762-nm radiation and (dotted lines) when all the absorbed energy is spent on gas heating for E_{in} = (*1*) 1, (*2*) 5, and (*3*) 10 J/cm^2. The dashed line is $\tau_{in}(P_0)$ for $E_{in} = 0$.

When O_2 molecules are excited to the $b^1\Sigma_g^+$ state with the emission of 762-nm radiation, the basic chain-initiation reactions are reaction nos. 6 and 10 yielding OH radicals and H atoms, respectively. Under 762-nm radiation, $O_2(a^1\Delta_g)$ molecules, along with $O_2(b^1\Sigma_g^+)$ molecules, arise in the mixture. Therefore, at the initial stage of the process, O atoms are predominantly formed in chain-branching reaction nos. 3 and 4. For low T_0 temperatures (<600 K), reaction nos. 29 and 30 also considerably contribute to the formation of O atoms. The appearance of these new intense channels of the formation of chain-mechanism carriers accelerates chain reactions and reduces τ_{in}.

The method based on the excitation of O_2 molecules by laser radiation is much more efficient for the initiation of combustion than the method of direct heating of the reacting mixture by laser radiation (all radiation energy absorbed by the gas is spent on the heating of the medium), which is now extensively discussed. This is illustrated in Fig. 4, where τ_{in} is shown as a function of the initial pressure of the H_2/O_2 mixture for various E_{in} values in these two cases. As is seen, the τ_{in} value for the excitation of O_2 molecules by 762-nm radiation can be equal to one-seventieth to one-tenth of that for the pure thermal action of laser radiation. It is also seen that, for every E_{in} value, when a certain boundary value P_{0b} is exceeded, radiation does not reduce τ_{in} compared to the case $I_0 = 0$. The P_{0b} value increases with E_{in} or I_0. In particular, $P_{0b} = 2 \times 10^4$ and 2×10^5 Pa for the excitation of O_2 molecules with $\tau_p = 10^{-3}$ s and $E_{in} = 1$ and 10 J/cm^2, respectively. The boundary value P_{0b} exists due both to the intense formation of chemically inert hydrogen peroxide (Fig. 3) for quite low T_0 at $P_0 > P_{0b}$ and to a decrease in the concentration of H atoms and OH radicals.

Thus, the excitation of O_2 molecules to the $b^1\Sigma_g^+$ state by 762-nm laser radiation opens new channels of the formation of active O and H atoms and OH radicals. This considerably reduces both the induction period and ignition temperature of hydrogen–oxygen mixtures. These components are carriers of the chain mechanism for the oxidation of other gases. Therefore, this method of intensifying combustion is expected to be very efficient for hydrocarbon fuels.

ACKNOWLEDGMENTS

This work was supported by the Russian Foundation for Basic Research, project nos. 02-01-00703 and 02-02-16915.

REFERENCES

1. B. Raffel, J. Warnatz, and J. Wolfrum, J. Appl. Phys. **37** (4), 189 (1985).
2. P. D. Ronney, Opt. Eng. **33** (2), 510 (1994).
3. M. A. Tanoff, M. D. Smooke, R. E. Teets, and J. A. Sell, Combust. Flame **103** (4), 253 (1995).
4. M.-S. Chou and T. J. Zukowski, Combust. Flame **87** (2), 191 (1991).
5. T. X. Phuoc and F. P. White, Combust. Flame **119** (3), 203 (1999).
6. J. X. Ma, D. R. Alexander, and D. E. Poulain, Combust. Flame **112** (4), 492 (1998).
7. C. Amiot and J. Verges, Can. J. Phys. **59** (9), 1391 (1981).
8. V. I. Grabovskiĭ and A. M. Starik, Kvant. Élektron. **31** (4), 356 (1994).
9. A. M. Starik and N. S. Titova, Khim. Fiz. **19** (9), 61 (2000).
10. A. M. Starik and N. S. Titova, Khim. Fiz. **20** (5), 17 (2001).
11. V. D. Rusanov and A. A. Fridman, *Physics of a Chemically Active Plasma* (Nauka, Moscow, 1984).
12. M. S. Chou, F. E. Fendell, and H. W. Beherens, Proc. SPIE **1862**, 45 (1993).

Translated by R. Tyapaev

Doklady Physics, Vol. 48, No. 8, 2003, pp. 405–408. Translated from Doklady Akademii Nauk, Vol. 391, No. 5, 2003, pp. 610–613.

PHYSICS

On the Phenomenological Description of Crystallization in Melts

S. O. Gladkov

Presented by Academician O.A. Bannykh September 30, 2002

Received October 15, 2002

The properties of melts were apparently first investigated by Fogel [1] and Fulcher [2]. In these pioneering studies, they measured the viscosity of substances η in the vicinity of the crystallization temperature T_{cr}. It was shown empirically that viscosity must obey the law

$$\eta = \eta_0 \exp\frac{\Delta}{T - T_{cr}},$$

where η_0 and Δ are certain constants and T is a parameter equivalent to the thermostat temperature. More recently, Ya.I. Frenkel (see collected articles [3]) studied crystallization in liquids and melting in solid-phase structures using the free-volume model. This model was later applied in a modified form to study the nonequilibrium properties of glassy materials [4–9]. In addition to the above investigations, some aspects of crystallization theory were considered in [10, 11], where an analytical explanation of the empirical Fogel–Fulcher law was proposed. A rigorous mathematical model of melting was described in detail in [12], where a theory of melting of solid crystal structures was constructed on the basis of the gradual breaking of the long-range crystal order.

In this study, I propose an alternative model of crystallization, which provides rigorous calculation of the growth of the crystallization region as a function of the deviation of the current temperature T from the crystallization temperature T_{cr}.

Let us consider a melted substance that is slowly cooled to the crystallization temperature T_{cr}. We describe the growth of locally formed crystallization regions with allowance for heat transfer. To mathematically describe an increase in the average size of a nucleus of the crystalline phase, we use the Smoluchowski equation modified for the case under consideration. The evolution of the crystallization regions is assumed to be similar to that of a nuclear chain reaction. The process is schematically shown in Fig. 1, which illustrates an increase in randomly nucleated crystallization regions $\{A\} = A, A', A'', \ldots$ in a geometric sequence with the multiplier $q = 2$. The regions $\{A\}$ are numbered by the superscript ν. Let the temperature of the region A be $T_0 = T_{cr}$ and the temperatures of the adjacent regions $A_1, A_2, A_3, \ldots, A_k$ be $T_1 < T_2 < T_3 < \ldots < T_k$, respectively. The regions A_i are uncrystallized regions in the liquid melt rather than solid phases. The last, kth, region is determined by the condition that $(k + 1)$-th region is absent and that the regions with a linear size ρ, into which the entire conditional area L^2 of the melt is uniformly divided, overlap.

The size ρ can be estimated from the step d in the radial direction of the nucleus growth of the crystalline phase (Fig. 2). We have $\rho \approx k_{max}d$, where k_{max} is introduced below [formula (3)].

For each of the regions I, II, III, …, the heat conduction equation should be introduced. The most complete system of equations that takes into account both the latent heat of crystallization (as is known, it is proportional to the crystallization rate $\mathbf{v}_{cr}$) and the purely hydrodynamic flow of a very viscous liquid to the nucleus itself can be represented in the following finite-

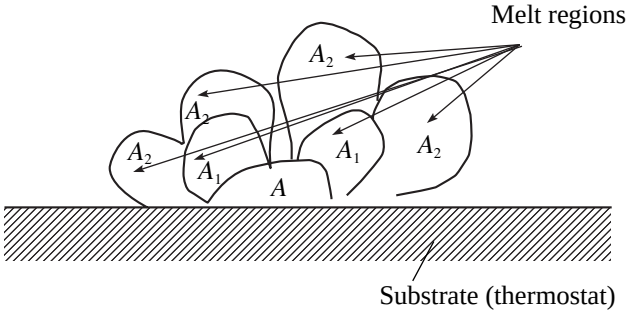

Fig. 1. Schematic representation of crystallization as the growth of regions in a geometric sequence with the multiplier $q = 2$.

Moscow State Regional University,
ul. Radio 10a, Moscow, 105005 Russia
e-mail: sglad@newmail.ru

1028-3358/03/4808-0405$24.00 © 2003 MAIK "Nauka/Interperiodica"

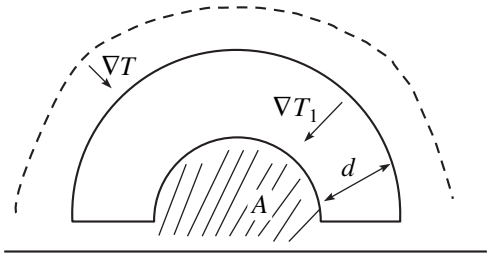

Fig. 2. Simplified model of the growth of the crystallization region shown schematically in Fig. 1. The regions $\{A\} = A$, A', A'', … are the attractors specified by the superscript ν in Eq. (4). Thermal flows along the temperature gradients to the corresponding attractor are conventionally shown by arrows.

difference form:

$$\frac{\partial T_i^{(\nu)}}{\partial t} = \alpha_i(T_{i+1}^{(\nu)} - T_i^{(\nu)}) + \frac{\mathbf{v}_{cr}}{c_v}\nabla P + q_{cr}, \qquad (1a)$$

$$\frac{\partial \mathbf{v}_{cr}}{\partial t} + (\mathbf{v}_{cr}\nabla)\mathbf{v}_{cr} = -\frac{\nabla P}{\rho} + \rho^{-1}\sum_{n=1}^{3}\frac{\partial}{\partial x_n}\frac{\eta\partial \mathbf{v}_{cr}}{\partial x_n}. \qquad (1b)$$

Here, $\alpha_i = \frac{\kappa s_i}{\delta}$ is the heat-transfer coefficient, where κ is the thermal conductivity, δ is the size of the heat-exchange area (the liquid-to-crystal transition region), and s_i is the contact area between the ith and $(i + 1)$-th regions; $i = 1, \ldots, k$; ν = I, II, III, …; c_v is the heat capacity per unit volume of the crystal; $\frac{dq_{cr}}{dt}$ is the latent heat of crystallization; the Boltzmann constant k_B is hereafter taken to be equal to unity; and ∇P is the pressure gradient between the crystalline phase and the surrounding liquid melt. Strictly speaking, ∇P would also be written in the finite-difference form, i.e., as $\nabla P = \frac{P_{i+1} - P_i}{\delta}$. However, this is not necessary for the following reason. Since the crystallization rate is low, the nonlinear term in Eq. (1b) can be omitted. The remaining linear equation shows that, when the second term with the dynamic viscosity η on the right-hand side of Eq. (1b) is disregarded, the crystallization rate is proportional to the pressure gradient. Therefore, the penultimate term on the right-hand side of Eq. (1a) is proportional to $(\nabla P)^2$. We ignore this term of second-order smallness and consider that the crystallization heat depends implicitly on time and is virtually independent of coordinates. Then, it can be introduced on the left-hand side of Eq. (1a). Introducing the new renormalized temperature (retaining the earlier notation T), we finally arrive at the following approximate linear finite-difference equation:

$$\frac{\partial T_i^{(\nu)}}{\partial t} = \alpha_i(T_{i-1}^{(\nu)} - T_i^{(\nu)}).$$

Equations (1a) and (1b) represent a complete closed system of linear differential equations written for individual regions I, II, III, …. This is physically clear: each region of the initial crystalline phase A, A', A'', … is an attractor to which temperature gradients are directed. In our case, the heat-transfer coefficient in Eq. (1) has the quite unconventional dimension [s^{-1}], whereas the ordinary dimension of this coefficient is [W/m^2 K]. However, since [W/m^2 K] = [J/s m^2 K] = [kg/s^3 K] = 10^3 (g/s^3)(10^{16}/1.38 Erg) ≈ 8×10^{18} (1/s cm^2) = α*, the relation between α and α* is evident: $\alpha_i = \alpha_i^* s_i$.

It should be noted that, in our model, we do not take into account the effect of the $(i - 1)$-th region on temperature in the ith region, because the $(i - 1)$-th region in our model is treated as already crystallized and considered thereby as the ith region.

The temperature hierarchy for each of the given regions ν is as follows:

$$T < T_0 = T_{cr} < T_1 < T_2 < T_3 < \ldots < T_k, \qquad (2)$$

where T is the thermostat temperature (or the supercooling temperature kept constant).

The simplest approximation of variation in temperature can, for example, have the form

$$T_k^{(\nu)} = T_0 + k\, e^{-\gamma k}\delta T, \qquad (3)$$

where $\delta T = T_0 - T$ and the exponential factor is the cutoff factor limiting the growth of the number of the attachment zones. Hence, it is seen that $k_{max} = \frac{1}{\gamma}$. The coefficient γ is assumed to be small ($\gamma \ll 1$).

Next, it is necessary to modify the Smoluchowski equation for our particular case and to write it in convenient terms. Let us introduce a time-continuous variation of the ith size l_i, which is related to the probabilistic pattern of the growth of the crystallization region $\{A\}$. Then, in accordance with our scheme (Fig. 1), the evolution of the νth region must obey the phenomenological equation

$$\frac{\partial l_i^{(\nu)}}{\partial t} = d^{-1}\sum_{i'=2i+1}^{2i-2} l_{i'}^{(\nu)}[W(T_{i'}^{(\nu)})l_i^{(\nu)} - W(T_i^{(\nu)})l_{i'}^{(\nu)}]. \qquad (4)$$

Here, $W(T) = \omega e^{-\Delta/T}$, where ω is the characteristic frequency of the tunneling transition from the liquid to crystal region through the potential barrier; $\Delta = U_2 - U_1$ is the barrier height, where U_1 and U_2 are the energies per particle in the liquid and solid phases, respectively; and the subscript i varies from 0 to k. The term proportional to $W(T_i^{(\nu)})$ on the right-hand side of Eq. (4) cor-

responds to the possibility of the ith crystallization region drifting to another crystal i'. It is easy to see that temperature hierarchy (2) leads to the following evident, easily verifiable hierarchy for the transition frequencies:

$$W_0 < W_1 < W_2 < \ldots < W_k. \tag{5}$$

The physical meaning of inequality (5) is quite clear. Thermal fluctuations in the liquid phase (melt) increase with temperature. This means that the thermal barrier decreases and the tunneling probability (according to the Arrhenius law of tunneling transition) increases. This behavior is expressed as hierarchy (5) of the frequency probabilities.

Finally, it is necessary to set the phase size l_i as a function of the number i. It is quite reasonable to assume that

$$l_i = l_0 + \frac{id}{i+1}. \tag{6}$$

As a result, Eqs. (1), (3), (4), and (6) can be combined into the unified system

$$\frac{\partial l_k}{\partial t} = d^{-1}\{l_{2k+1}[W(T_{2k+1})l_k - W(T_k)l_{2k+1}] + l_{2k+2}[W(T_{2k+2})l_k - W(T_k)l_{2k+2}]\}, \tag{7a}$$

$$\frac{\partial T_k}{\partial t} = \alpha(T_{k-1} - T_k), \tag{7b}$$

$$T_k = T_0 + ke^{-\gamma k}\delta T, \tag{7c}$$

$$l_k = l_0 + \frac{kd}{k+1}, \tag{7d}$$

where the superscript ν is omitted and the heat-transfer coefficient is assumed to be constant in the ith region.

To solve this system of equations and to find the relation between the size l_0 and T_{cr}, we divide Eq. (7a) by Eq. (7b) and take into account Eqs. (7c) and (7d). As a result, we arrive at the rather awkward equation

$$\frac{\partial l_0}{\partial T_0} = (\delta T d\alpha)^{-1}\left\{-\frac{l_0 d W_0\left(k^* + \frac{7}{4}\right)}{(k^*+1)\left(k^* + \frac{3}{3}\right)} - \frac{d^2 W_0 f_1(k^*)}{2} + \frac{\partial W_0}{\partial T_0} + 2l_0^2\delta T\frac{\partial W_0}{\partial T_0}(k^*+1) + l_0 d\delta T f_2(k^*) + d^2\delta T k^* f_3(k^*)\right\}, \tag{8}$$

where

$$f_1(k^*) = \frac{k^* + \frac{1}{2}}{(k^*+1)^2} + \frac{k^*+2}{\left(k^* + \frac{3}{2}\right)^2},$$

$$f_2(k^*) = k^* + \frac{1}{2} + \frac{(k^*+1)^2}{k^* + \frac{3}{2}} + \frac{k^*}{k^*+1}\left(k^* + \frac{1}{2} + \frac{k^{*2} + 2k^* + \frac{1}{2}}{k^* + \frac{3}{2}}\right), \tag{9}$$

$$f_3(k^*) = \frac{\left(k^* + \frac{1}{2}\right)^2}{(k^*+1)^2} + \frac{k^{*2} + 2k^* + \frac{1}{2}}{\left(k^* + \frac{3}{2}\right)^2}.$$

Here, $k^* = ke^{-\gamma k}$.

It is seen that the solution of Eq. (8) for small δT can be found by omitting the terms proportional to δT in curly brackets. As a result, for $k^* \gg 1$, we have $f_1 \approx \frac{2}{k^{*2}}$, $f_2 \approx 4k^*$, $f_3 \approx 2$, and

$$\frac{\partial l_0}{\partial T_0} \simeq -(l_0 + d)\frac{W_0}{\delta T \alpha k^*}. \tag{10}$$

From this simple differential equation, the size of the crystallization region can be determined as a function of the deviation of $T_0 = T_{cr}$ from T. Actually, it follows from Eq. (10) that

$$l_0 \approx l^*\left(\frac{T}{T_{cr} - T}\right)^\beta, \tag{11}$$

where $\beta = \frac{\delta\omega e^{-\Delta T}}{s^*\kappa k^*}$, l^* is an integration constant having the dimension of length, and s^* is a certain average contact area.

Formula (11) is the solution of the problem.

Using the above analysis and calculating the exponent β, one can compare its value with the numerical calculation based on percolation theory. According to this theory, the exponent is independent of any physical parameter of a substance and introduced as a geometric

factor inherent in all structures independent of their nature.

REFERENCES

1. H. Fogel, Phys. Z. **22**, 645 (1921).
2. G. S. Fulcher, J. Am. Ceram. Soc. **8**, 339 (1925).
3. J. Frenkel, *Kinetic Theory of Liquids* (Nauka, Leningrad, 1975; Clarendon Press, Oxford, 1946).
4. D. Turnbul and M. H. Cohen, J. Chem. Phys. **343** (1), 120 (1961).
5. M. H. Cohen and G. S. Grest, Phys. Rev. B: Condens. Matter **20** (3), 1077 (1979).
6. S. O. Gladkov, Physica B (Amsterdam) **162**, 181 (1990).
7. S. O. Gladkov, Physica B (Amsterdam) **167**, 145 (1990).
8. D. Turnbul and M. H. Cohen, J. Chem. Phys. **31** (1), 1164 (1959).
9. M. H. Cohen and G. S. Grest, Solid State Commun. **39**, 143 (1981).
10. S. O. Gladkov, Physica B (Amsterdam) **160**, 211 (1989).
11. S. O. Gladkov, *Physics of Composites: Thermodynamic and Dissipative Properties* (Nauka, Moscow, 1999).
12. A. Z. Patashinskiĭ and B. I. Shumilo, Zh. Éksp. Teor. Fiz. **89** (7), 315 (1985) [Sov. Phys. JETP **62**, 177 (1985)].

Translated by Yu. Vishnyakov

Doklady Physics, Vol. 48, No. 8, 2003, pp. 409–413. Translated from Doklady Akademii Nauk, Vol. 391, No. 5, 2003, pp. 614–618.

PHYSICS

Landau–Lifshitz Equations for Magnetic Systems with Constant and Variable Memory

Ya. L. Kobelev[1,*], L. Ya. Kobelev[2], and Corresponding Member of the RAS E. P. Romanov[1,]**

Received March 27, 2003

The Landau–Lifshitz equation

$$\frac{\partial}{\partial t}\mathbf{M} = -g[\mathbf{M}\mathbf{H}_{\text{eff}}] \quad (1)$$

describes the dynamics of the macroscopic dissipation-free motion of the magnetization vector of a ferromagnet in a magnetic field. Here, $\mathbf{M}(\mathbf{r}, t)$ is the magnetization per unit volume of the ferromagnet and g is the gyromagnetic ratio. When only the exchange interaction and the magnetic-anisotropy energy are taken into account, the effective magnetic field $\mathbf{H}_{\text{eff}}$ can be written in the form

$$\mathbf{H}_{\text{eff}} = \frac{1}{2}\alpha_{ik}\frac{\partial^2\mathbf{M}}{\partial x_i \partial x_k} - \frac{\partial W(\mathbf{M})}{\partial \mathbf{M}} + \mathbf{H}, \quad (2)$$

where the first, second, and third terms are the exchange-interaction contribution, anisotropic-energy contribution, and external magnetic field, respectively. We allow both uniform and nonuniform spin distributions over the ferromagnet, as well as the existence of magnetic clusters, domain walls, etc. The dimension of the above formations is taken to be topological. However, memory (both time memory and memory about past trajectories) in certain physical systems can vary both in time and in space. Available experimental data show that the fractal dimension of physical objects depends on the parameters of the surrounding (temperature, pressure, etc.) and internal parameters characterizing a system (elasticity, strength, etc.).

Fractal structures are observed in many physical phenomena, including those in solids. This indicates that the momentum and coordinate distributions of magnetically ordered systems (or magnetic clusters) of the electron magnetic moments can be quite well described in terms of fractal representations (in particular, Levi-type distributions for magnetic glasses). In this case, the distribution over a system of such clusters will have a fractal or multifractal dimension. The latter implies the existence of time or spatial memory (including that varying in time or with spatial distribution, e.g., with motion of domain walls, temperature, etc.) in the magnetic-moment system (consisting of magnetic clusters). To describe such magnetic systems, the Landau–Lifshitz phenomenological equations must be extended to fractal or multifractal sets involving ion, atomic, molecular, or electron clusters; i.e., they must be expressed in terms of fractional derivatives. In any case, this must be done when magnetic moments undergo anomalous diffusion caused by the fractal structure of the surroundings.

Anomalous diffusion, i.e., diffusion for which the mean squared displacement of a particle is proportional to a fractional power of time ($\langle x^2\rangle \sim t^\beta$, where β is a fractional number), has been actively studied in recent years. It is observed in aerosols, gels, spin glasses, certain disordered systems, aperiodic crystals, electron–ion plasma, in systems described by the statistical physics of open systems [1], and apparently in magnetically ordered systems under certain conditions. Anomalous diffusion (or fractal relaxation) was described theoretically by using fractal geometry [2] in numerous works (see [3]). Diffusion equations in fractional derivatives [4, 5] are usually used in these works. Experiments [6–8] show that the fractal dimension depends on physical parameters, and anomalous diffusion is important in this case.

In this work, we study magnetically ordered systems (by an example of a ferromagnet) with fractal or multifractal properties. These systems are apparently quite common, because the fractal structure of ion or atomic clusters plays an important role in polycrystalline solids [8]. To take into account the effect of fractal struc-

[1] *Institute of Metal Physics, Ural Division, Russian Academy of Sciences, ul. S. Kovalevskoĭ 18, Yekaterinburg, 620219 Russia*

* *e-mail: yakov@imp.uran.ru*

** *e-mail: romanov@prn.uran.ru*

[2] *Ural State University, pr. Lenina 51, Yekaterinburg, 620083 Russia*
e-mail: leonid.kobelev@usu.ru

1028-3358/03/4808-0409$24.00

tures on the magnetic properties of the system, the Landau–Lifshitz equations and equations for spin waves are written in the fractal space with constant and variable memory, and the corresponding spectra of spin waves are found. We analyze the effect of the fractal force found in [9, 10] on the behavior of magnetic moments, spin-wave spectrum, and the behavior of the magnetic system as a whole. This force was studied for anomalous diffusion in [11], is proportional to the coordinate gradient of the multifractal dimension, and is induced by the multifractal medium.

FRACTIONAL VARIABLE-ORDER DERIVATIVES AND INTEGRALS

Equations with fractional derivatives describe non-Markovian processes with constant memory. Dynamic processes in systems with time- and coordinate-dependent memory cannot be described in terms of Riemann–Liouville fractional derivatives that do not reproduce variations in the fractal dimension of the variable-memory physical system under consideration. For this reason, it is necessary to use variable-order fractional derivatives generalizing fractional Riemann–Liouville derivatives and integrals for the dynamics of multifractal objects (i.e., objects whose fractal dimension depends on time and coordinates). One of us (L.Ya.K.) introduced such a technique in [9–12].

To describe the behavior of magnetic moments in a medium with coordinate- and time-dependent multifractal dimension (or in a physical system with such fractal properties), one must use the generalized Riemann–Liouville fractional derivatives that were introduced in [9] and used in a number of works (see, e.g., [12]). These derivatives are defined as (for left-side derivatives; for more detail, see [9])

$$\frac{\partial^{1+\varepsilon_t}}{\partial t^{1+\varepsilon_t}} \equiv D_{+,t}^{d_t} f(t) f$$

$$= \left(\frac{d}{dt}\right)^n \int_a^t dt' \frac{f(t')}{\Gamma(n-d_t(t'))(t-t')^{d_t(t')-n+1}},$$

$$\frac{\partial^{1+\varepsilon_x}}{\partial x^{1+\varepsilon_t}} f \equiv D_{+,x}^{d_x} f(x) \tag{3}$$

$$= \left(\frac{d}{dx}\right)^n \int_a^x dx' \frac{f(x')}{\Gamma(n-d_x(x'))(x-x')^{d_x(x')-n+1}}.$$

Here, Γ is the Euler gamma function; $n = \{d\} + 1$, where $\{d\}$ is the integer part of d for $d \geq 0$ (i.e., $(n-1) \leq d < n$) and $n = 0$ for $d < n$; $d_t = 1 + \varepsilon(t)$; and $d_x = 1 + \varepsilon(x)$. The integral operators defined above for fractional orders d_t and d_x depending on coordinates and time can be expressed in terms of ordinary derivatives and integrals [9, 12] for $|\varepsilon| \ll 1$. In this case, generalized Riemann–Liouville fractional derivatives satisfy the approximate relations (we present here only relations for derivatives)

$$D^{1+\varepsilon_t} f(x,t) = (1+\varepsilon_t)\frac{\partial}{\partial t} f(x,t) + \frac{\partial \varepsilon_t}{\partial t} f(x,t),$$
$$D^{1+\varepsilon_x} f(x,t) = (1+\varepsilon_x)\frac{\partial}{\partial x} f(x,t) + \frac{\partial \varepsilon_x}{\partial x} f(x,t). \tag{4}$$

These relations make it possible to describe the dynamics of a system including the effect of changes in the fractal dimension (if they are much smaller than unity) on the behavior of the physical system by means of ordinary differential and integral equations.

LANDAU–LIFSHITZ EQUATION FOR MAGNETIC MEDIA WITH VARIABLE MEMORY

Variable memory can be taken into account by replacing the derivatives in Eqs. (1) and (2) with generalized fractional derivatives (3). This replacement leads to the following integro-differential equations for the magnetic moment:

$$\frac{\partial^{d_t(\mathbf{r},t)}}{\partial t^{d_t(\mathbf{r},(t))}} \mathbf{M} = -g[\mathbf{M}\mathbf{H}_{\text{eff}}], \tag{5}$$

$$\mathbf{H}_{\text{eff}} = \frac{1}{2}\alpha_{ik}\frac{\partial^{d_i(x)}}{\partial x_i^{d_i(x)}}\frac{\partial^{d_k(x)}\mathbf{M}}{\partial x_k^{d_k(x)}} - \frac{\partial^{d_M(x)} W(\mathbf{M})}{\partial \mathbf{M}^{d_M(x)}} + \mathbf{H}, \tag{6}$$
$$x = \mathbf{r}, t.$$

Hereafter, we use the scale for which dimensional factors arising due to the presence of fractional derivatives are equal to unity. Time fractal dimension d_t and spatial fractal dimension $d_\mathbf{r}$ characterizing time and spatial memory, respectively, do not generally coincide with each other, i.e., $d_t \neq d_\mathbf{r}$. These dimensions can also be different in different directions of crystallographic or magnetic structures, but this fact is disregarded. The Landau–Lifshitz equations for magnetic systems with constant or partially constant memory are a particular case of these equations for constant fractal dimensions or one of these fractal dimensions. The following cases must be distinguished: (i) d_t = const and $d_\mathbf{r}$ is variable and (ii) $d_\mathbf{r}$ = const and d_t is variable. Completely constant memory corresponds to constant d_t and $d_\mathbf{r}$ values, which, as was mentioned above, can differ from each other, in any case for different directions of the crystallographic axes.

SPIN-WAVE EQUATIONS IN A FRACTAL MEDIUM WITH CONSTANT AND VARIABLE MEMORY

Phenomenological equations for spin waves in a nonfractal medium follow from the Landau–Lifshitz equations when determining the effective magnetic field and linearizing magnetic moments and magnetic field near their equilibrium values [13]. Since this work aims to illustrate the application of the new mathematical technique (variable-order fractional derivatives) to magnetically ordered systems, we analyze the effect of the fractal properties of the system on spin waves only for a uniaxial ferromagnet. Let

$$\mathbf{M}(\mathbf{r}, t) = \mathbf{M}_0 + \mathbf{m}(\mathbf{r}, t)$$

and

$$\mathbf{H}^{(i)}(\mathbf{r}, t) = \mathbf{H}_0^{(i)} + \mathbf{h}(\mathbf{r}, t).$$

Equations for spin waves in a fractal magnetic medium can be derived from Eqs. (5) and (6). They can also be derived from equations for spin waves [13] by replacing ordinary derivatives with generalized fractional derivatives. This method is simplest and, carefully applied, yields correct equations (although they, as well as the Landau–Lifshitz phenomenological equations, can be derived from first principles). The linearized equation of motion for the magnetic moment density $\mathbf{m}$ in a variable-memory fractal medium (the equation for spin waves in a variable-memory magnetic medium described by fractal dimensions d_t and $d_\mathbf{r}$) for a uniaxial ferromagnet has the form

$$\frac{\partial^{d_t(\mathbf{r}, t)}}{\partial t^{d_t(\mathbf{r}, (t))}}\mathbf{m} = g\left(\mathbf{M}_0 \times \left[\mathbf{h} + \alpha_{ik}\frac{\partial^{d_i(x)}}{\partial x_i^{d_i(x)}}\frac{\partial^{d_k(x)}\mathbf{m}}{\partial x_k^{d_k(x)}} + \beta'\mathbf{n}(\mathbf{mn}) - \frac{1}{M_0^2}(\mathbf{M}_0\mathbf{H}_0^i + \beta'(\mathbf{M}_0\mathbf{n})^2)\mathbf{m}\right]\right). \quad (7)$$

The linearized spin-wave equations for "easy axis" or "easy plane" magnetic anisotropy are written as

$$\frac{\partial^{d_t(\mathbf{r}, t)}}{\partial t^{d_t(\mathbf{r}, (t))}}\mathbf{m} = g\left(\mathbf{M}_0 \times \left[\mathbf{h} + \alpha_{ik}\frac{\partial^{d_i(x)}}{\partial x_i^{d_i(x)}}\frac{\partial^{d_k(x)}\mathbf{m}}{\partial x_k^{d_k(x)}} + \beta'\mathbf{n}(\mathbf{mn}) - \left(\beta' + \frac{H_0^{(i)}}{M_0}\right)\mathbf{m}\right]\right), \quad (8)$$

$$\frac{\partial^{d_t(\mathbf{r}, t)}}{\partial t^{d_t(\mathbf{r}, (t))}}\mathbf{m} = g\left(\mathbf{M}_0 \times \left[\mathbf{h} + \alpha_{ik}\frac{\partial^{d_i(x)}}{\partial x_i^{d_i(x)}}\frac{\partial^{d_k(x)}\mathbf{m}}{\partial x_k^{d_k(x)}} + \beta'\mathbf{n}(\mathbf{mn}) - \frac{H_0^{(i)}}{M_0}\mathbf{m}\right]\right). \quad (9)$$

The boundary conditions in a magnetic medium with memory have the form

$$\left(\alpha_{kj}\frac{\partial^{d_j} m_i}{\partial x_j^{d_j}} + \gamma_{ik;\,l}m_l\right)\nu_k\Big|_S = 0, \quad (10)$$

in the absence of dissipative processes,

$$\varepsilon_{rpi}\mathbf{M}_{0p}\left(\alpha_{kl}\frac{\partial^{d_l} m_i}{\partial x_l^{d_l}} + \gamma_{ik;\,l}m_l\right)\nu_k\Big|_S = 0 \quad (11)$$

or in the presence of a symmetry center of the crystal lattice,

$$\nu_k\alpha_{kl}\frac{\partial^{d_l}\mathbf{m}}{\partial x_l^{d_l}} = 0. \quad (12)$$

The above equations, together with the boundary conditions, describe the propagation of spin waves in a variable-memory magnetic medium. Below, we consider a more simple case of constant memory in an isotropic ferromagnet.

SPIN-WAVE EQUATIONS FOR A CONSTANT-MEMORY UNIAXIAL FERROMAGNET

In this case, and with allowance for only exchange-energy contribution for the uniaxial ferromagnet ($\beta_x = \beta_y = \beta_z = \beta$), the spin-wave equation has the form ($d_t = \alpha$ = const, $d_\mathbf{r} = \beta_\mathbf{r}$ = const)

$$\frac{\partial^\alpha}{\partial t^\alpha}\mathbf{m} = g\left(\mathbf{M}_0 \times \left[\mathbf{h} + \alpha_{ik}\frac{\partial^{2\beta}\mathbf{m}}{\partial x_i^\beta \partial x_k^\beta} + \beta'\mathbf{n}(\mathbf{mn}) - \frac{1}{M_0^2}(\mathbf{M}_0\mathbf{H}_0^i + \beta'(\mathbf{M}_0\mathbf{n})^2)\mathbf{m}\right]\right). \quad (13)$$

It is easy to obtain the following relation between the energy and wavenumber of spin-wave spectra:

$$E \sim (\alpha_{il}k_i^\beta k_l^\beta)^{\frac{1}{\alpha}}. \quad (14)$$

SPIN-WAVE EQUATIONS IN THE APPROXIMATION OF WEAK VARIABLE MEMORY

In the approximation of weak variable memory, fractional derivatives can be replaced with ordinary derivatives by using Eqs. (4) and writing Eq. (7) in the form

$$\frac{\partial}{\partial t}[(1+\varepsilon_t(\mathbf{r},t))\mathbf{m}] = \mathbf{M}_0 \times \alpha_{ik}\frac{\partial}{\partial x_i}\left\{(1+\varepsilon_x)\frac{\partial[(1+\varepsilon_{x_i})\mathbf{m}]}{\partial x_k}\right\}. \quad (15)$$

This equation is similar to the equation for anomalous diffusion with variable memory, which is analyzed in [11]. After reduction to the form

$$\frac{\partial \mathbf{m}}{\partial t} = \frac{\partial}{\partial x_i}\left[D_{ik}(x,t)\frac{\partial}{\partial x_k}\mathbf{m} - F_i\mathbf{m}\right] + A\mathbf{m}, \quad (16)$$

typical for diffusion equations, where [for $D_{ik}(\mathbf{r}, t) = \text{const}$]

$$F_i(x) = -D_{ik}\left(\frac{\partial \varepsilon_x}{\partial x_k} + \frac{\partial \varepsilon_t}{\partial x_k}\right),$$
$$A = -\left(D_{ik}\frac{\partial \varepsilon_t}{\partial x_i}\frac{\partial \varepsilon_t}{\partial x_k} + \frac{\partial \varepsilon_t}{\partial t}\right), \quad (17)$$

similar to [11], the spin-wave equation involves two new terms: (i) a force (which will be referred to as the "fractal force") proportional to the gradients of fractal coordinate dimensions and (ii) terms proportional to $\mathbf{m}$ corresponding to the appearance of a gap in the spin-wave spectrum for certain types of the coordinate dependence of the fractal dimension. We emphasize that fractal structures of this type can in principle be formed technologically. We will seek the solution in the form $\mathbf{m} = \mathbf{m}_0 + \varepsilon\mathbf{m}_1$ for $|\varepsilon < 1|$. In this case, $\mathbf{m}_1$ satisfies a diffusion-type equation with variable coefficients of the term proportional to $\mathbf{m}_1$, and $\mathbf{m}_0$ has the ordinary spin-wave spectrum.

FRACTAL-FORCE EFFECT ON THE BEHAVIOR OF SPIN WAVES

We consider the fractal-force effect on the behavior of the magnetic moment in more detail. As follows from Eq. (17), the fractal force has the form $F \sim \frac{\partial \varepsilon_{\mathbf{r}}}{\partial x_i}$. For constant ε, this force vanishes. Depending on sign (which is always opposite to the sign of forces that act on magnetic moments and are proportional to ε), this force can lead both to dissipation of the ordering of magnetic moments and to an increase in this ordering. Its magnitude depends on the type of the coordinate dependence of the fractal dimension. In particular, for $\varepsilon_x = \varepsilon_0 x$, this force, as well as the energy gap, is constant, i.e., $E_0 F \sim \varepsilon_0$ and $E_0 \sim \varepsilon_0$. The last quantities are proportional to the derivative with respect to ε. For the fractal structure approximated by $\varepsilon_x \sim a_1 x + a_2 x^3$, discrete frequencies appear in the spin-wave spectrum. If ε depends periodically on time and coordinates with frequencies ω_t and ω_x, respectively, and can be approximated by $\sin\omega_t t$ and $\sin\omega_x x_i$, then the equation for spin waves involves terms with variable coefficients responsible for interesting properties of spin waves.

CONCLUSIONS

The new results following from the existence of variable memory in magnetic systems are as follows.

First, there is the appearance of the fractal force, which disappears in the absence of memory or in the presence of constant memory (in essence, it is a new-type magnetic hysteresis) and is proportional to the coordinate gradient of fractal dimension. Can a fractal medium with constant or variable memory (in the latter case, determined by time and coordinate variations in the fractal dimension) be used to write information? Can the fractal dimension be used to control variation in information? Since the behavior of the multifractal dimension can be controlled by varying external forces, this is apparently possible. The fractal dimension can apparently be used as memory. There is only a question of whether this use is economically and technically appropriate.

Second, a gap appears in the spin-wave spectrum due to variable memory (it disappears for constant memory). The spin-wave spectrum in a magnetic system is more complex and can vary in time in certain cases. The latter property is caused by the fact that variable-memory systems are open and therefore always lose (or acquire) energy on dissipation processes.

ACKNOWLEDGMENTS

This work was supported in part by INTAS (grant no. 00-0847), the Russian Foundation for Basic Research (project no. 00-02-16285), and the US Civilian Research and Development Foundation for the Independent States of the Former Soviet Union (grant no. REC-005).

REFERENCES

1. Yu. L. Klimontovich, *Statistical Physics of Open Systems* (Yanus, Moscow, 1995; Kluwer, Dordrecht, 1995), Vol. 1.
2. B. Mandelbrot, *The Fractal Geometry of Nature* (Freeman, New York, 1982).
3. A. V. Chechkin, R. Gorenflo, and I. M. Sokolov, Phys. Rev. E **66**, 046129 (2002).

4. S. G. Samko, A. A. Kilbas, and O. I. Marichev, *Fractional Integrals and Derivatives, Theory and Applications* (Nauka i Tekhnika, Minsk, 1987; Gordon and Breach, Amsterdam, 1993).
5. I. M. Gelfand and G. E. Shilov, *Generalized Functions* (Academic, New York, 1964).
6. V. Ya. Shur, S. A. Negashev, and E. L. Rumyantsev, Ferroelectrics **169**, 63 (1995).
7. P. V. Korolev and S. N. Kul'kov, Perspekt. Mater., No. 3, 21 (1997).
8. V. S. Ivanova, A. S. Balankin, I. Zh. Bunin, and A. A. Oksogoev, *Synergetics and Fractals in Materials Science* (Nauka, Moscow, 1994).
9. L. Ya. Kobelev, *Fractal Theory of Time and Space*, Available from VINITI, No. 189-B99 (1999).
10. L. Ya. Kobelev, in *Proceedings of 24th International Workshop on High Energy Physics and Field Theory, 27–29 June, Protvino, 2001*, pp. 126–152; http://dbserv.ihep.su/~pubs.
11. Ya. L. Kobelev, L. Ya. Kobelev, and Yu. L. Klimontovich, Dokl. Akad. Nauk **390** (5), 605 (2003) [Dokl. Phys. **48**, 264 (2003)].
12. Ya. L. Kobelev, L. Ya. Kobelev, and E. P. Romanov, Dokl. Akad. Nauk **372**, 177 (2000) [Dokl. Phys. **45**, 194 (2000)].
13. A. I. Akhiezer, V. G. Bar'yakhtar, and S. V. Peletminskii, *Spin Waves* (Nauka, Moscow, 1967; North-Holland, Amsterdam, 1968).

Translated by R. Tyapaev

Doklady Physics, Vol. 48, No. 8, 2003, pp. 414–417. Translated from Doklady Akademii Nauk, Vol. 391, No. 5, 2003, pp. 619–622.

PHYSICS

Guided Modes in Photonic Crystal Fibers

V. I. Krivenkov

Presented by Academician V.V. Osiko April 29, 2003

Received December 25, 2002

Photonic crystal (PC) light guides represent are a 2D periodic set of close-packed hollow glass fibers; i.e., they actually have a 2D photonic-crystal structure. They exhibit a number of remarkable properties, such as the presence of photonic gaps, which are characteristic only for periodic structures, and the possibility of both realizinge the single-mode regime and forming dispersion in a wide spectral range. These fibers are exceptionally efficient for solution of actual problems of nonlinear optics, physics of photonic crystals, quantum electrodynamics, and many other problems. The field of their use is continuously being extended. The fabrication technology, properties, and application prospects of PC fibers weare reviewed in detail in [1, 2].

Available methods of numerically solving the problem of eigenfunctions and eigenvalues for light guides with an intricate section shape such as hole light guides was briefly reviewed in [2], where PC fibers were treated as a particular case of hole light guides, for which the periodic-structure requirement is optional. These methods applied to PC fibers either provide only a general representation about their properties, as the approximate method of replacing the index of refraction of a hole shell by an effective index of refraction [3], or requires significant computational resources, as in the case of numerical integration of the Maxwell equations by the finite-difference technique, because these methods ignore the features of the PC-fiber mode structure.

In this study, we describe a rigorous method of solving the problem of natural waves in a general-type PC fiber with the inclusion of the feature of its mode structure. For all guided modes of this fiber, exact expressions for the field components, as well as the dispersion relations, which are simple compared to the general case of a fiber with an intricate section [4], and the equations for critical wavelengths are obtained. The dispersion relations and the equations for critical wavelengths are represented as the equality to zero for a determinant, whose order is minimal and depends only on the mode structure of the PC fiber under consideration for a given accuracy.

Moscow State Academy of Instrumentation Engineering and Informatics, ul. Stromynka 20, Moscow, 107846 Russia

As a generalized PC-fiber model, we consider an infinite, transversely periodic, dielectric structure that is homogeneous along a certain z axis and includes a core and an infinitely thick shell ($r \geq a$) with a constant permittivity $\varepsilon_{00} < \max\varepsilon(r, \varphi)$. Without loss of generality, the core permittivity $\varepsilon(r, \varphi)$, as well as $\varepsilon^{-1}(r, \varphi)$, in the cylindrical coordinate system r, φ, z can be represented in the form

$$\varepsilon^i(r, \varphi) = \sum_{n=0}^{\infty} \varepsilon_n^i(r)\cos(nN\varphi),$$
$$0 \leq r < a, \quad i = 0, \pm 1.$$

Here, $N \in \{1, 2, \ldots\}$ is the parameter specifying the structure periodicity, a is the core radius, and

$$\varepsilon_n^i(r) = \frac{2^{-\delta(n)}}{\pi}\int_0^{2\pi} \varepsilon^i(r, \varphi)\cos(nN\varphi)d\varphi,$$
$$n = 0, 1, \ldots, \quad i = 0, \pm 1$$
$$(\delta(x \neq 0) = 0, \delta(0) = 1)$$

are generally the piecewise continuous functions, which can be represented as [5]

$$\varepsilon_n^i(r) = \sum_{k=0}^{\infty} \varepsilon_{nk}^{il}\left(\frac{r - r_{l-1}}{r_l - r_{l-1}}\right)^k,$$
$$r_{l-1} \leq r < r_l, \quad l = 1, 2, \ldots, L,$$

after determining the discontinuity points r_1, r_2, …, r_{L-1}. Here, $\varepsilon_{nk}^{i1} = 0$, $k = 0, 1, \ldots$; $n = 1, 2, \ldots$; $i = 0, \pm 1$; $r_0 = 0$, $r_L = a$.

The dependence of the electric field $\mathbf{E} = (E_r, E_\varphi, E_z)$ and magnetic field $\mathbf{H} = (H_r, H_\varphi, H_z)$ for the guided mode in the fiber under consideration on time t and longitudinal coordinate z is specified in the form $\exp[j(\omega t - \beta z)]$ (it will be omitted below), where ω and β are the circular frequency and the longitudinal-propagation constant for the mode. In this case, from the Maxwell equations for a nonmagnetic dielectric medium, we obtain

1028-3358/03/4808-0414$24.00

the following set of first-order partial differential equations:

$$r\frac{\partial \mathbf{h}^{\alpha}}{\partial r} = \mathbf{A}^{\alpha}(r, \varphi)\mathbf{h}^{1-\alpha}, \quad \alpha = 0, 1,$$

where

$$\mathbf{h}^{0} = \begin{pmatrix} j\sqrt{\varepsilon_0}E_z \\ k_0 r\sqrt{\mu_0}H_r \end{pmatrix}, \quad \mathbf{h}^{1} = \sqrt{\mu_0}\begin{pmatrix} jH_z \\ k_0 r H_{\varphi} \end{pmatrix},$$

$$\mathbf{A}^{\alpha}(r, \varphi) = \begin{pmatrix} (-1)^{1-\alpha}\left(\frac{\varepsilon(r, \varphi)}{\gamma}\right)^{2\alpha-1}\frac{\partial}{\partial\varphi} & \frac{\gamma^2 - \varepsilon(r, \varphi)}{\gamma^{\alpha}\varepsilon^{1-\alpha}(r, \varphi)} \\ k_0^2 r^2 \gamma^{1-\alpha}\varepsilon^{\alpha}(r, \varphi) & (-1)^{1-\alpha}\frac{\partial}{\partial\varphi} \end{pmatrix},$$

$\gamma = \frac{\beta}{k_0}$, $k_0 = \omega\sqrt{\varepsilon_0\mu_0}$, ε_0 and μ_0 are the permittivity and permeability of free space, respectively.

By using the substitution

$$\mathbf{h}^{\alpha}(r, \varphi) = (-1)^{\mu\alpha}\sum_{m=-M}^{\infty}\mathbf{S}^{|\alpha-\mu|}_{|mN+\nu|}(\varphi)\mathbf{h}^{\alpha}_{m}(r), \quad \alpha = 0, 1,$$

$$\mu \in \{0, 1\}, \quad \nu \in \{0, 1, \ldots, N-1\},$$

$$M = \begin{cases} 0, & \text{if} \quad 2\nu = 0, N \\ \infty, & \text{if} \quad 2\nu \neq 0, N, \end{cases}$$

where

$$\mathbf{S}^{\alpha}_{m}(\varphi) = \begin{pmatrix} \sin\left(m\varphi + \alpha\frac{\pi}{2}\right) & 0 \\ 0 & \sin\left[m\varphi + (\alpha-1)\frac{\pi}{2}\right] \end{pmatrix},$$

which corresponding to even modes ${}_eHE_{mn}$ and ${}_eEH_{mn}$ for $\mu = 0$ and to odd modes ${}_oHE_{mn}$ and ${}_oEH_{mn}$ for $\mu = 1$ with the azimuth subscript $m = |kN + \nu|$, $k = 0, \pm1, \ldots$, this set of equations can be transformed into the infinite set of first-order ordinary differential equations

$$r\frac{d\mathbf{h}^{\alpha}_{m}(r)}{dr} = \frac{1}{2}\left[\sum_{j=0}^{|m|-1+\delta(|m|-m)}\mathbf{A}^{\alpha}_{m-\vartheta(m)j, j}(r)\mathbf{h}^{1-\alpha}_{m-\vartheta(m)j}(r)\right.$$

$$+\sum_{j=0}^{\infty}\mathbf{A}^{\alpha}_{m+\vartheta(m)j, j}(r)\mathbf{h}^{1-\alpha}_{m+\vartheta(m)j}(r)$$

$$-(-1)^{\alpha+\mu}(1-\delta(m+M))\mathbf{I}$$

$$\left.\times\sum_{j=|m|+\delta(|m|+m)}^{\infty}\mathbf{A}^{\alpha}_{m+\vartheta(-m)j, j}(r)\mathbf{h}^{1-\alpha}_{-m-\vartheta(-m)j}(r)\right],$$

$$\alpha = 0, 1, \quad m = (\pm1)^{(1-\delta(M))(0, 1, \ldots)},$$

where

$$\mathbf{A}^{\alpha}_{mn}(r) = \begin{pmatrix} \frac{|mN+\nu|\varepsilon_n^{2\alpha-1}(r)}{\gamma^{2\alpha-1}} & \gamma^{\alpha}\left(\frac{\varepsilon_n^{2\alpha-1}(r)}{\gamma^{2(2\alpha-1)}} - \delta(n)\right) \\ (-\gamma)^{1-\alpha}k_0^2 r^2\varepsilon_n^2(r) & |mN+\nu|\delta(n) \end{pmatrix},$$

$$\mathbf{I} = \begin{pmatrix} 1 & 0 \\ 0 & -1 \end{pmatrix}, \quad \vartheta(m) = \frac{m}{|m|} \quad (\vartheta(0) = 1).$$

We represent the continuous solution to of the last set of equations, which decreases faster than r^{-1} for $r \longrightarrow \infty$, in the form

$$\mathbf{h}^{\alpha}_{m}(r) = \sum_{i=0}^{1}\sum_{n=-M}^{\infty}\sum_{k=0}^{\infty}a_n^i\mathbf{h}^{\alpha i l}_{mnk}\left(\frac{r-r_{l-1}}{r_l - r_{l-1}}\right)^{\delta(l-1)|mN+\nu|+k},$$

$$r_{l-1} \le r < r_l, \quad l = 1, 2, \ldots, L,$$

$$\begin{pmatrix} \mathbf{h}^{0}_{m}(r) \\ \cdots\cdots\cdots \\ \mathbf{h}^{1}_{m}(r) \end{pmatrix} = b_m^0\begin{pmatrix} 1 \\ \varepsilon_{00}|mN+\nu|u^{-2} \\ 0 \\ \varepsilon_{00}F_{|mN+\nu|}(r) \end{pmatrix}$$

$$+ b_m^1\begin{pmatrix} 0 \\ \gamma F_{|mN+\nu|}(r) \\ -1 \\ \gamma|mN+\nu|u^{-2} \end{pmatrix}, \quad r_L \le r < \infty,$$

$$\alpha = 0, 1, \quad m = (\pm1)^{1-\delta(M)}(0, 1, \ldots),$$

where $a_0^{\mu} = b_0^{\mu} = 0$, if $\nu = 0$,

$$\mathbf{h}^{\alpha i 1}_{mn0} = \delta(m-n)\begin{pmatrix} (1-\delta(|m|+\nu+|1-\alpha-i|))\gamma^{|\alpha-i|}(\varepsilon_{00}^{i1})^{\alpha} \\ (i-1)|mN+\nu| \end{pmatrix},$$

$$\mathbf{h}^{\alpha i1}_{mnk} = \frac{\sum_{j=0}^{k-1}[(|mN+\nu|+k)\mathbf{A}^{\alpha 1}_{m,0,k-j}\mathbf{h}^{1-\alpha,i,1}_{mnj} + \mathbf{A}^{\alpha 1}_{m00}\mathbf{A}^{1-\alpha,1}_{m,0,k-j}\mathbf{h}^{\alpha i1}_{mnj}]}{k(2|mN+\nu|+k)}, \quad k = 1, 2, \ldots,$$

$$\mathbf{h}^{\alpha il}_{mn0} = \sum_{k=0}^{\infty}\mathbf{h}^{\alpha,i,l-1}_{mnk}, \quad l = 2, 3, \ldots, L,$$

$$\mathbf{h}^{\alpha il}_{m,n,k+1} = \frac{1}{\rho_l(k+1)}\left\{-k\mathbf{h}^{\alpha il}_{mnk} + \frac{1}{2}\sum_{p=0}^{k}\left[\sum_{j=0}^{|m|-1+\delta(|m|-m)}\mathbf{A}^{\alpha l}_{m-\vartheta(m)j,j,k-p}\mathbf{h}^{1-\alpha,i,l}_{m-\vartheta(m)j,n,p} + \sum_{j=0}^{\infty}\mathbf{A}^{\alpha l}_{m+\vartheta(m)j,j,k-p}\mathbf{h}^{1-\alpha,i,l}_{m+\vartheta(m)j,n,p}\right.\right.$$

$$\left.\left. - (-1)^{\mu+\alpha}(1-\delta(m+M))\mathbf{I}\sum_{j=|m|+\delta(|m|+m)}^{\infty}\mathbf{A}^{\alpha l}_{m+\vartheta(-m)j,j,k-p}\mathbf{h}^{1-\alpha,i,l}_{-m-\vartheta(-m)j,n,p}\right]\right\}, \quad k = 0, 1, \ldots, \quad l = 2, 3, \ldots, L,$$

$$\mathbf{A}^{\alpha l}_{mnk} = \begin{pmatrix} \dfrac{|mN+\nu|\varepsilon^{2\alpha-1,l}_{nk}}{\gamma^{2\alpha-1}} & \gamma^{\alpha}\left(\dfrac{\varepsilon^{2\alpha-1,l}_{nk}}{\gamma^{2(2\alpha-1)}} - \delta(n+k)\right) \\ (-\gamma)^{1-\alpha}k_0^2(r_l - r_{l-1})^2\sum_{j=0}^{2}2^{\delta(1-j)}\rho_l^{2-j}\varepsilon^{\alpha l}_{n,k-j} & |mN+\nu|\delta(n+k) \end{pmatrix},$$

$$F_m(r) = \frac{r\dfrac{d}{dr}[K_m(k_0 ur)]}{u^2 K_m(k_0 u r_L)}, \quad u^2 = \gamma^2 - \varepsilon_{00} > 0, \quad \rho_l = \frac{r_{l-1}}{r_l - r_{l-1}} \quad (\varepsilon^{\alpha l}_{n,-1} = \varepsilon^{\alpha l}_{n,-2} = 0).$$

Here, $K_m(x)$ is the modified Bessel function of the second kind and the constants a^i_n, b^i_n, $i = 0, 1$; $n = (\pm 1)^{1-\delta(M)}(0, 1, \ldots)$ are the nontrivial solution of the homogeneous linear set of equations

$$\sum_{i=0}^{1}\sum_{n=-M}^{\infty}\sum_{k=0}^{\infty}a^i_n\mathbf{h}^{\alpha iL}_{mnk} = \sum_{i=0}^{1}b^i_m\mathbf{h}^{\alpha i}_m,$$

$$\alpha = 0, 1, \quad m = (\pm 1)^{1-\delta(M)}(0, 1, \ldots),$$

where

$$\mathbf{h}^{ii}_m = \begin{pmatrix} (-1)^i \\ \varepsilon_{00}^{1-i}\gamma^i|mN+\nu|u^{-2} \end{pmatrix},$$

$$\mathbf{h}^{i,1-i}_m = \begin{pmatrix} 0 \\ \varepsilon^i_{00}\gamma^{1-i}F_{|mN+\nu|}(r_L) \end{pmatrix}, \quad i = 0, 1.$$

Equating the determinant of this set of equations to zero, after simple transformations, we obtain the equation with respect to an unknown phase constant γ:

$$\det(\mathbf{PQ}) = 0,$$

where

$$\mathbf{P} = (\mathbf{P}_{mn}), \quad \mathbf{Q} = (\mathbf{Q}_{mn}),$$

$$(m, n) = (\pm 1)^{1-\delta(M)}(0, 1, \ldots),$$

$$\mathbf{Q}_{mn} = \sum_{k=0}^{\infty}\left(\begin{array}{c:c} \mathbf{h}^{00L}_{mnk} & \mathbf{h}^{01L}_{mnk} \\ \hdashline \mathbf{h}^{10L}_{mnk} & \mathbf{h}^{11L}_{mnk} \end{array}\right), \quad |n| + \nu \neq 0,$$

$$\mathbf{Q}_{m0} = \sum_{k=0}^{\infty}\begin{pmatrix} \mathbf{h}^{0,1-\mu,L}_{m0k} \\ \hdashline \mathbf{h}^{1,1-\mu,L}_{m0k} \end{pmatrix}, \quad \nu = 0,$$

$$\mathbf{P}_{mn} = \delta(m-n)$$

$$\times\begin{pmatrix} -\varepsilon_{00}F_{|mN+\nu|}(r_L) & 0 & \gamma|mN+\nu|u^{-2} & 1 \\ -\varepsilon_{00}|mN+\nu|u^{-2} & 1 & \gamma F_{|mN+\nu|}(r_L) & 0 \end{pmatrix},$$

$$|m| + \nu \neq 0,$$

$$\mathbf{P}_{0n} = \delta(n)(-\mu\varepsilon_{00}F_0(r_L), 1-\mu, (1-\mu)\gamma F_0(r_L), \mu),$$

$$\nu = 0,$$

$$\mu \in \{0, 1\}, \quad \nu \in \{0, 1, \ldots, N-1\},$$

which is the dispersion relation for either even modes ${}_eHE_{mn}$ and ${}_eEH_{mn}$ for $\mu = 0$ or odd modes ${}_oHE_{mn}$ and ${}_oEH_{mn}$ for $\mu = 1$ with the azimuth subscript $m = |kN + \nu|$, $k = 0, \pm 1, \ldots$.

In the limiting case of $\gamma \longrightarrow \sqrt{\varepsilon_{00}}$, we obtain the equation for the unknown wavelength $\lambda = \frac{2\pi}{k_0}$:

$$\det[\mathbf{RQ}(\gamma = \sqrt{\varepsilon_{00}})] = 0,$$

where

$$\mathbf{R} = (\mathbf{R}_{mn}), \quad m, n = (\pm 1)^{1-\delta(M)}(0, 1, \ldots),$$

$$\mathbf{R}_{mn} = \delta(m-n)\begin{pmatrix} \sqrt{\varepsilon_{00}} & 0\ 1\ 0 \\ \dfrac{4\pi^2\varepsilon_{00}r_L^2}{\lambda^2(|mN+\nu|-1)} & 1\ 0\ 1 \end{pmatrix},$$

$$|mN + \nu| \neq 0, 1,$$

$$\mathbf{R}_{mn} = \delta(m-n)\begin{pmatrix} 1\ 0\ 0\ 0 \\ 0\ 0\ 1\ 0 \end{pmatrix}, \quad |mN + \nu| = 1,$$

$$\mathbf{R}_{0n} = \delta(n)(\mu,\ 0,\ 1-\mu,\ 0), \quad \nu = 0,$$

$$\mu \in \{0, 1\}, \quad \nu \in \{0, 1, \ldots, N-1\},$$

which is the equation for the critical wavelengths for either even modes ${}_eHE_{mn}$ and ${}_eEH_{mn}$ for $\mu = 0$ and odd modes ${}_oHE_{mn}$ and ${}_oEH_{mn}$ for $\mu = 1$ with the azimuth subscript $m = |kN + \nu|$, $k = 0, \pm 1, \ldots$.

The order of the determinants on the left-hand side of the resulting equations is actually equal to twice the number of terms in the Fourier expansion for the mode-field components. It is evident that the number of these terms is minimal for the given accuracy due to the inclusion of the feature of the mode structure of the PC fiber under consideration.

REFERENCES

1. A. S. Biryukov and E. M. Dianov, Volokonno-Opt. Tekhnol., Mater. Ustroĭstva, No. 5, 6 (2002).
2. A. M. Zheltikov, Usp. Fiz. Nauk **170**, 1203 (2000) [Phys. Usp. **43**, 1125 (2000)].
3. A. S. Belanov, A. V. Belov, E. M. Dianov, *et al.*, Kvant. Élektron. (Moscow) **32** (5), 425 (2002).
4. V. I. Krivenkov, Dokl. Akad. Nauk **387**, 184 (2002) [Dokl. Phys. **47**, 9 (2002)].
5. V. I. Krivenkov, Dokl. Akad. Nauk **378**, 751 (2001) [Dokl. Phys. **46**, 407 (2001)].

Translated by V. Bukhanov

Doklady Physics, Vol. 48, No. 8, 2003, pp. 418–421. Translated from Doklady Akademii Nauk, Vol. 391, No. 5, 2003, pp. 623–627.

PHYSICS

Effect of the High Rate of Avalanche Ionization behind a Shock Wave in a Monatomic Gas

Corresponding Member of the RAS V. M. Fomin, B. V. Postnikov*, and V. I. Yakovlev

Received September 16, 2002

After first investigations [1], a kinetic model of ionizing monatomic gases in shock waves has been developed [2]. However, this model only partially describes the actual process of ionization relaxation: certain experimental results, e.g., [3–6], are not explained in this model. Tumakaev [3] revealed an energy imbalance for electrons in monatomic gases (mercury vapors, argon): energy spent on the ionization and radiative losses in the greater part of the relaxation zone are not compensated by the heating of electrons due to Coulomb (electron–ion) collisions. Schneider and Park [4] showed that variation in electron temperature behind the shock front at the initial stage of an avalanche is undetermined. Under the same initial conditions in argon, this temperature was both considerably below atomic temperature and close to atomic temperature, which contradicts the energy balance equation for electrons. Moreover, the activation energy determined using the known temperature dependence of the rate of avalanche ionization was almost one-tenth the expected value. The electron temperature determined in [5] by using this temperature dependence for electrons in the relaxation zone coincides with the atomic temperature immediately behind the shock front even in the avalanche region. At the same time, according to the energy balance equation for electrons, this parameter must decrease due to increasing energy losses of electrons inelastically colliding with atoms. McIntyre *et al.* [6] revealed anomalies in the distribution of excited states of neon and argon atoms behind the shock front.

These facts enable one to assume (as in [3]) the possibility of the existence of additional (compared to the commonly accepted model) channels of energy exchange between particles in the relaxation zone. The structure of a shock wave was calculated with allowance for additional kinetic mechanisms (involving metastable particles, molecular ions, and radiative processes), because the conditions of irregular variation in the flow parameters behind ionizing shock waves in monatomic (and even molecular) gases were observed in certain ranges [7, 8]. These calculations and the approaches used in them were reviewed in [9, 10]. Conclusive experimental evidence of the determining role of these processes has not been obtained. For this reason, other mechanisms of the formation of unstable flow regimes were also proposed (see, e.g., [9–11]). In this case, the general analysis [9] of the flow structure behind the shock front, as well as the detailed analysis [11] of the ionization relaxation zone based on the traditional model, is used. The role of radiation was analyzed in [10]. We emphasize that, although the available hypotheses are considerably different, some authors consider that instability is fundamentally associated with the presence of the nonequilibrium (relaxation) zone behind the shock front (see, e.g., [9, 11]). Therefore, in spite of numerous available results, investigation of the flow structure and the physics of processes in ionizing shock waves is of current interest.

In this work, we analyze the flow structure for a monatomic gas (argon) behind the front of ionizing shock waves for Mach numbers 10.5–12.5, which correspond to stable flow regimes. Irregular variation in detected signals (interference and plasma glow) was observed for M < 10.5–10.7. For an initial argon pressure of 400 and 666.5 Pa (3 and 5 Torr), the equilibrium parameters of the plasma varied in the following ranges: electron density $N_e \approx (1–3) \times 10^{16}$ cm^{-3}, ionization degree $\alpha \approx (1–5) \times 10^{-2}$, and temperature $T \approx$ 0.9–1.2 eV.

In contrast to the frequently applied approach based on comparison between measurements and calculations of the electron density profiles and length (duration) of the relaxation zone, the method [12] that we used is based on comparison between measured and calculated distributions of the rate of avalanche ionization (source of electrons S_e in terms and notation proposed in [2]) behind the shock front. The only ionization mechanism (electron–atom collisions) dominates in the avalanche region. Therefore, justified analysis of mechanisms of energy exchange between particles is possible, because the rate of avalanche ionization is determined by the rate of energy exchange between electrons and heavy

Institute of Theoretical and Applied Mechanics, Siberian Division, Russian Academy of Sciences, ul. Institutskaya 4/1, Novosibirsk, 630090 Russia

** e-mail: boris@itam.nsc.ru*

1028-3358/03/4808-0418$24.00

particles according to the energy balance equation [1, 2]. Thus, the novelty of the method is in the possibility of experimentally testing the adequacy of the model used for the kinetics of electron heating and the actual process.

Measurements of the ionization rate behind the front are used as a method of investigation in, e.g., [4] only when analyzing the initial stage of the relaxation zone, where initial ionization depends on several factors (impurities, radiation, atom–atom collisions) and only slightly affects the gasdynamic parameters of the flow. In [12], it was shown that the application of conservation laws and the measured time dependence of the electron density $N_e(t)$ makes it possible to determine the distributions of gasdynamic parameters and the rate of avalanche ionization behind the front in the approximation of a one-dimensional or quasi-one-dimensional (with allowance for the boundary layer) flow. For the quasi-one-dimensional case, S_e is related to the rate $\frac{dN_e}{dt}$ of variation in the electron density as

$$S_e = \left\{1 - \frac{2\alpha E_\mathrm{I}}{5kT_1 + \left(\frac{5}{3}kT_1\mathrm{M}^2\right)\left(1 - 4\left(\frac{u}{u_1}\right)^2\right)}\right\} \times \frac{u}{u_1}\frac{dN_e}{dt} - S_e^*$$

or

$$S_e = K_s\frac{u}{u_1}\frac{dN_e}{dt} - S_e^*,$$

where E_I is the atom ionization energy, k is Boltzmann's constant, u is the flow velocity with respect to the shock front moving with the velocity u_1, and T_1 is the gas temperature before the front. The second term S_e^* represents the geometry of the shock-tube channel and boundary-layer character and is less than 10% of the first term under the experimental conditions. The factor K_s varied in the range 0.8–1.0 because $\alpha \ll 1$. The dominant effect of the boundary layer is in a decrease in the relative velocity $\frac{u}{u_1}$ (to 30% compared to the one-dimensional solution) and in the corresponding decrease in S_e.

The application of IR interferometry with a wavelength of 10.6 μm [13] and a sensitivity of 2.8×10^{14} cm^{-3} (one tenth of the interference band) enabled us to measure the electron density distribution behind the shock front with a high accuracy. Figure 1 shows typical measured distributions $N_e(t)$ (t is the time from the passage of the shock front), which were used to determine the experimental ionization rates. As is seen in Fig. 1, the measured rates S_e of argon ionization

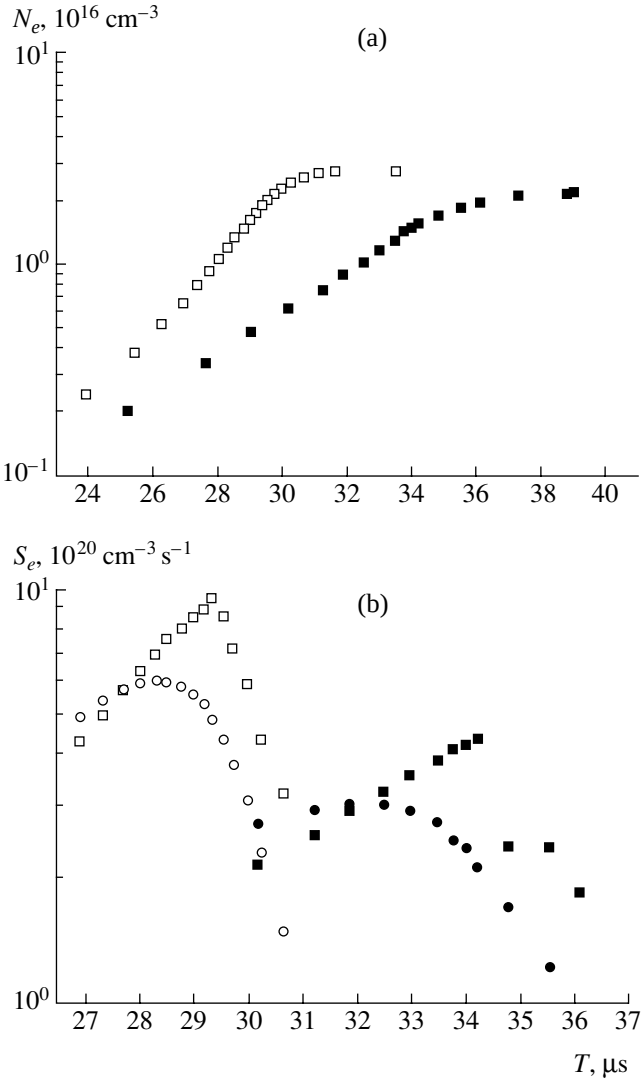

Fig. 1. (a) Electron density measured for M = (closed squares) 11.94 and (open squares) 12.47 and (b) ionization rate distribution that is measured for M = (closed squares) 11.94 and (open squares) 12.47 and is calculated for M = (closed circles) 11.94 and (open circles) 12.47 in the avalanche region behind the shock front in argon for an initial pressure of 3 Torr.

exceed the calculated results S_e^{cal} by a factor of 2–3 at the maximum.

Calculations were based on the known relation [2]

$$S_e^{\mathrm{cal}} = \beta(T_e)N_eN_a - \alpha^*(T_e)N_e^3$$

or

$$S_e^{\mathrm{cal}} = \beta(T_e)N_eN_a\left[1 - \frac{N_e^2}{N_a}K(T_e)\right],$$

where $\beta(T_e)$, $\alpha^*(T_e)$, and $K(T_e)$ are the ionization rate, recombination rate, and ionization-equilibrium constant, respectively. In the instantaneous-ionization

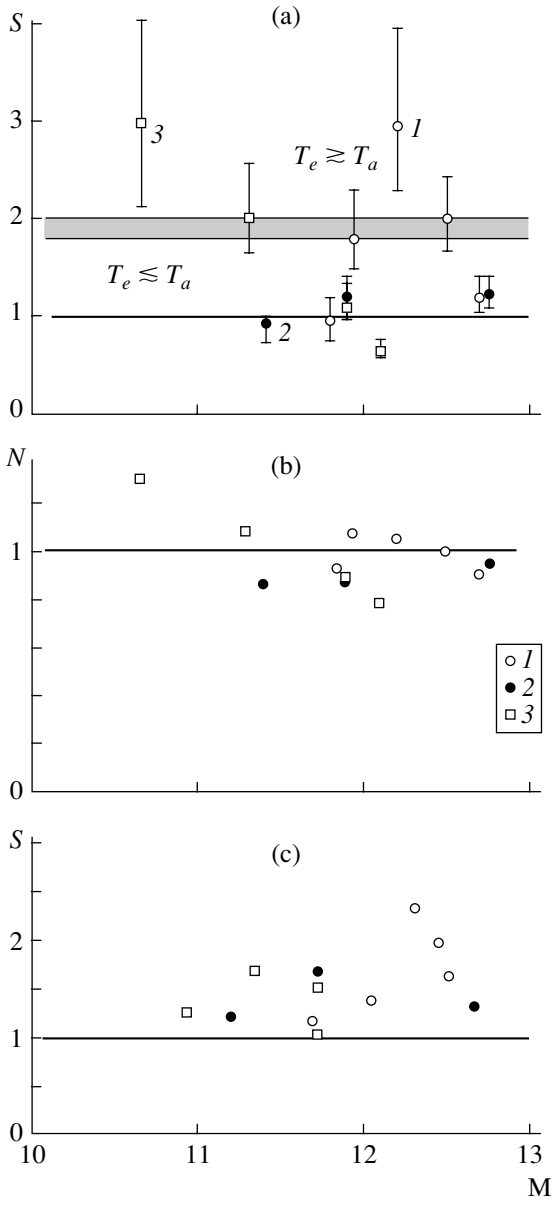

Fig. 2. Experimental results in argon vs. the Mach number when pressure before the shock front is equal to (*1*, *2*) 3 and (*3*) 5 Torr and the impurity level is equal to (*1*, *3*) 10^{-4} and (*2*) 10^{-3}.

approximation (single-level model of the atom), we have

$$\beta(T_e) = C_e\left(2 + \frac{\Delta E}{T_e}\right)T_e^{3/2}\exp\left(-\frac{\Delta E}{T_e}\right),$$

where ΔE is the difference between the ionization energy and the energy of the first excited atomic level and C_e is the constant determining the cross section for atom excitation by an electron impact. According to [1, 8], the values $C_e = (4.7\text{–}7.0) \times 10^{-18}$ cm^2/eV are used. Calculation of $\beta(T_e)$ with allowance for multilevel atomic structure in the modified diffusion approximation [2] indicates that the effective value is equal to $C_e \approx 9 \times 10^{-18}$ cm^2/eV in the parameter range under consideration. Temperature T_e is calculated by using a procedure developed in [12, 15] from the equation of local energy balance for electrons [2]:

$$1.5kT_eS_e^{\text{cal}} = Q_{\text{el}} - Q_{\text{in}}$$

or

$$1.5kT_e\beta(T_e)N_eN_a\left[1 - \frac{N_e^2}{N_a}K(T_e)\right] = Q_{\text{el}} - Q_{\text{in}},$$

where the parameters $\beta(T_e)$, Q_{el} (rate of electron heating under elastic collisions), and Q_{in} (rate of energy loss under inelastic collisions) are known functions of electron temperature and parameters of the plasma state. For conditions under consideration ($\alpha \ll 1$), the effect of the energies of radiation and excited states is disregarded, because their contributions to the total energy balance are relatively small.

Figure 2a shows the ratio $S = \dfrac{S_e}{S_e^{\text{cal}}}$ of the measured and calculated rates of avalanche ionization for argon near the S_e maximum as a function of the Mach number of the shock wave for various initial conditions such as gas pressure and gas purity. For most experiments, $S > 1$; i.e., the maximum measured rates of avalanche ionization exceed the calculated rates. It was found that the electron temperature is equal to and higher than the atomic temperature for $S \approx 1.8\text{–}2$ and higher S values, respectively. However, these states, as well as states with $S = 1$, are rarely observed.

Since the result is novel, additional analysis of data was carried out to determine S values more precisely by increasing the accuracy of the calculation of S_e^{cal}. This accuracy is primarily determined by the accuracy of the calculation of the integral temperature parameter [12] from the energy conservation law by using measured velocity (or Mach number M with a relative error of about 0.8%). The parameter S can be calculated more accurately due to measurements of the electron density distribution both in the relaxation zone and in the equilibrium state (with an accuracy of 3%). This parameter is the most sensitive indicator of the equilibrium state of the ionized gas behind the shock front, because it depends most strongly on temperature (according to the Saha equation) and correspondingly on the Mach number of the shock wave. Figure 2b shows the measured-to-calculated ratio of the electron density N as a function of the Mach number for various experimental conditions. As was shown in [13], $N = 1 \pm \delta$ ($\delta \ll 1$) for most experiments; i.e., measured and calculated electron density coincide with each other in the equilibrium state. Assuming that the spread δ in experimental data is primarily attributed to the error in measurements of the Mach number, its new value in correction is chosen

from the condition that $\delta = 0$, i.e., that the measured and calculated electron densities are equal to each other. The refined M values (except two of them) agree with the measured values within the indicated error (0.8%) of the velocity measurement. Figure 2c shows the results of such a correction of data. Virtually the same effect is observed: the desired parameter varies within the range $S = 1–2.3$ and often exceeds unity. Since the range of M variation is narrow and the number of experiments is small, the dependence of S on the Mach number (and other parameters) is not definitely determined. We emphasize that the results are analyzed with the maximum constant $C_e \approx 9 \times 10^{-18}$ cm^2/eV, which is larger than the values used in other similar investigations by a factor of 1.3–1.5. The use of its commonly accepted values leads to a more pronounced effect (increase in S by an additional factor of 1.5–2).

Thus, complex analysis of data (including measurements of the electron density in the ionization equilibrium region) corroborates the preliminary conclusion [12] that the rate of avalanche ionization of argon (and krypton) exceeds that calculated in the traditional model. The basic result obtained for the first time is that the relative excess in the rate in this case is not fixed and varies in the range $S = 1–3$. Various phases of the dynamic structure of ionization relaxation are possibly detected in experiments; i.e., indications of the oscillation development of this process are manifested even in the stable flow regime. This conclusion is indirectly corroborated in [14], where the auto-oscillating variation in plasma radiation behind the front and the length of the relaxation zone were studied for developed instability of shock waves.

It is difficult to observe the revealed effect by the frequently used method of comparing measurements and calculations of the variation in the electron density behind the shock front, because one tries to fit (by varying kinetic parameters) an integral parameter, the length of the relaxation zone, which depends strongly on processes proceeding at the initial stage. Indeed, similar analysis of the data of previous experiments [5, 8] showed that they also exhibit a high rate of avalanche ionization of argon with $S = 1.8$ (M = 11.5) for data from [5] and $S = 2.9$, 3.5, and 1 (M = 16.5, 16.2, and 13) for data from [8].

In [15], we attempted to attribute the observed high rate of avalanche ionization to the existence of an additional channel of energy exchange between particles due to the associative ionization of excited atoms in collisions with unexcited particles. The general form of the energy balance equation for electrons was found with allowance for the multilevel structure of the atomic energy terms. In this equation, additional energy fluxes due to associative ionization (and the inverse process) of excited levels are taken into account in addition to the energy fluxes in electron–atom collisions. The structure of the equation shows that energy fluxes of electrons can in principle be redistributed when electrons transit from bound states to continuum. Estimates made in [15] for the flow region, where ionization dominates (until the S_e maximum), indicate that the energy expenses of electrons decrease and are primarily attributed to the transition to the first excited level. Moreover, the energy fluxes in transitions between excited states and to continuum (the latter and former are of the same order) are ensured by avalanche ionization of excited atoms. As a result, the electron temperature increases (by no more than 10% under the experimental conditions), which noticeably increases the rate of avalanche ionization due to its strong temperature dependence. The causes of the variation in the rate of the process must be determined by further analysis of the connection between mechanisms of ionization and energy exchange between particles in the refined model (equations) of ionization relaxation kinetics behind the shock front.

ACKNOWLEDGMENTS

This work was supported by the Russian Foundation for Basic Research, project nos. 00-01-00829a and 03-01-00902.

REFERENCES

1. H. Petschek and S. Byron, Ann. Phys. (New York) **1** (3), 270 (1957).
2. L. M. Biberman, A. Kh. Mnatsakanyan, and I. T. Yakubov, Usp. Fiz. Nauk **102**, 431 (1970) [Sov. Phys. Usp. **13**, 728 (1971)].
3. G. K. Tumakaev, Candidate's Dissertation in Physics and Mathematics (Leningrad, 1971).
4. K.-P. Schneider and C. Park, J. Phys. Fluids **18** (8), 969 (1975).
5. C. O. Weiss and B. Kotzan, J. Appl. Phys. **7** (3), 203 (1975).
6. T. J. McIntyre, A. F. P. Houwing, R. J. Sandeman, and H.-A. Bachor, J. Fluid Mech. **227**, 617 (1991).
7. R. W. Griffith, R. J. Sandeman, and H. J. Hornung, J. Appl. Phys. **9** (12), 1681 (1976).
8. I. I. Glass and W. S. Liu, J. Fluid Mech. **84**, Part 1, 55 (1978).
9. N. M. Kuznetsov, Khim. Fiz. **14** (9), 3 (1995).
10. S. A. Egorushkin and V. S. Uspenskiĭ, Khim. Fiz. **11** (4), 1013 (1992).
11. M. Mond, I. Rutkevich, and E. Toffin, Phys. Rev. E **56** (5), 5968 (1997).
12. P. V. Grigor'ev, Yu. P. Makarov, and V. I. Yakovlev, Pis'ma Zh. Tekh. Fiz. **26** (17), 105 (2000) [Tech. Phys. Lett. **26**, 803 (2000)].
13. R. I. Soloukhin, Yu. A. Yacobi, and V. I. Yakovlev, Arch. Mech. **26**, 637 (1974).
14. G. K. Tumakaev, Z. A. Stepanova, and P. V. Grigor'ev, Zh. Tekh. Fiz. **64** (4), 46 (1994) [Tech. Phys. **39**, 373 (1994)].
15. B. V. Postnikov and V. I. Yakovlev, Pis'ma Zh. Tekh. Fiz. **28** (17), 82 (2002).

Translated by R. Tyapaev

Doklady Physics, Vol. 48, No. 8, 2003, pp. 422–426. Translated from Doklady Akademii Nauk, Vol. 391, No. 6, 2003, pp. 749–753.

PHYSICS

On the Diffraction of Waves by an Apodized Periodic Structure

V. F. Kravchenko* and Corresponding Member of the RAS V. I. Pustovoĭt**

Received November 15, 2002

1. The engineering of selective reflecting setups with a high reflectance or separation of narrow-band radiation from wide-band radiation is always a problem of current interest for both electromagnetic and acoustic waves. Various spectral-selection methods based on interference and diffraction of waves [1, 2] and on parametric interaction of waves in media with parameters periodically varying in space [3–6] are extensively used in practice. The creation of high-contrast optical and acoustic filters, where a signal beyond the transmission band is suppressed by 6–8 orders of magnitude and, what is particularly important, side (parasitic) transmission windows are absent, is a rather difficult problem, which is not necessarily solvable in practice. This problem is particularly pressing in Raman spectroscopy, when intense laser radiation must be suppressed to measure rather weak Raman scattering, which is weaker than the exciting laser radiation by 7–10 orders of magnitude and is spaced from the laser-radiation line by only 50–100 cm^{-1} for certain substances (the so-called notch-filter problem).

Contrary to most approaches to this problem, which are based on the diffraction of waves by the periodic structure of varying medium properties, we will consider the diffraction of waves by an apodized periodic structure, where variation in the medium properties depends exponentially on coordinates. The propagation and diffraction of waves by unapodized periodic structures were analyzed in detail for acoustic waves in [7], for light waves in [8, 9], where various types of optical filters on this basis were considered, and for X-rays in [10]. Extensively used in acoustoelectronic devices based on surface acoustic waves [11], various spatial-apodization methods [12] enabled one, in particular, to design electromagnetic-radiation filters with ideal selective properties (see, e.g., [12, Ch. 3]).

* *Institute of Radio Engineering and Electronics, Russian Academy of Sciences, ul. Mokhovaya 18, Moscow, 103907 Russia*

** *Scientific and Technological Centre of Unique Instrumentation, Russian Academy of Sciences, ul. Butlerova 15, Moscow, 117342 Russia*

Contrary to [13, 14], where spatially periodic media with sharp boundaries were considered and the problem of the propagation of waves in such media was solved by matching solutions for various homogeneous layers (i.e., by using boundary conditions), we will consider a medium with smoothly varying parameters, which vary negligibly at wavelength distances. We emphasize that the concepts and approaches considered below are applicable to both acoustic and electromagnetic waves.

2. We consider the problem of the collinear diffraction of a wave by an apodized spatially periodic structure of variation in the permittivity of a medium. For simplicity, we analyze the electrodynamic problem of the propagation of a plane electromagnetic wave in an isotropic medium, whose permittivity varies as

$$\varepsilon(x) = \varepsilon_0 + \alpha e^{-\gamma x}\cos(qx), \tag{1}$$

where ε_0 is unperturbed permittivity, α is the amplitude of variation in permittivity, γ^{-1} is the characteristic spatial scale of this variation, and q is the "wave vector" of the spatial structure and satisfies the condition $\left|\frac{\gamma}{q}\right| \ll 1$.

Substituting permittivity (1) into the Maxwell equations, we arrive at the following set of equations for two interacting electromagnetic waves:

$$E_+(x, t) = \frac{1}{2}E_1 e^{i\omega_1 t - ik_1 x} + \text{c.c.},$$

$$E_-(x, t) = \frac{1}{2}E_2 e^{i\omega_2 t + ik_2 x} + \text{c.c.},$$

propagating in opposite directions:

$$\begin{aligned} \frac{dE_1}{dx} &= i\Gamma e^{(i\Delta k - \gamma)x}E_2, \\ \frac{dE_2}{dx} &= -i\Gamma e^{(i\Delta k - \gamma)x}E_1. \end{aligned} \tag{2}$$

Here, $\Gamma = \frac{k\alpha}{\sqrt{\varepsilon_0}}$, $\Delta k = k_1 + k_2 - q$ is the wave detuning, which is equal to $\Delta k = 2k - q$, because $\omega_1 = \omega_2$ and $k_1 =$

1028-3358/03/4808-0422$24.00 © 2003 MAIK "Nauka/Interperiodica"

$k_2 \equiv k$. The set of Eqs. (2) was derived using the conditions

$$\Delta k \ll k, \quad \left|\frac{d^2E_{1,2}}{dx^2}\right| \ll \left|k\frac{dE_{1,2}}{dx}\right|.$$

These are ordinary requirements of slow variation in wave amplitudes near the synchronism conditions, which are usually used when deriving the set of Eqs. (2) from the Maxwell equations. The only difference of the set of Eqs. (2) from the sets of equations for nonlinear or parametric interacting waves is the presence of the exponential factor $e^{-\gamma x}$ describing the "apodization" of the periodic structure. The condition

$$\frac{d}{dx}\{|E_1|^2 - |E_2|^2\} = 0, \tag{3}$$

meaning the conservation of the total flux of wave energies at every point x follows from the set of Eqs. (2). We emphasize that relation (3), in contrast to a similar relation for a spatially periodic medium without apodization, i.e., for $\gamma = 0$, follows from Eqs. (2) also for $\gamma \neq 0$.

Near the Bragg conditions, i.e., for $\Delta k = 0$, two waves, rather than one wave, propagate with slightly different velocities in each direction in a homogeneous periodic medium. It is easy to show that the wavenumber k and frequency ω of these waves are related as

$$k_{1,2} = \omega\sqrt{\varepsilon_0}\sqrt{1 \pm \frac{\alpha}{\varepsilon_0}} \simeq \omega\sqrt{\varepsilon_0}\left(1 \pm \frac{\alpha}{2\varepsilon_0}\right).$$

We note that the relation between ω and k for

$$k_1 \ll k \ll k_2$$

is complex. Therefore, waves propagating in this direction are attenuated and a so-called gap in eigenvalues ω arises. This attenuation value and width of the gap depend strongly on the amplitude of variation in the medium properties. Since we consider variations in the medium properties such that $|\alpha e^{-\gamma x}| \ll \varepsilon_0$, the above effects will be disregarded.

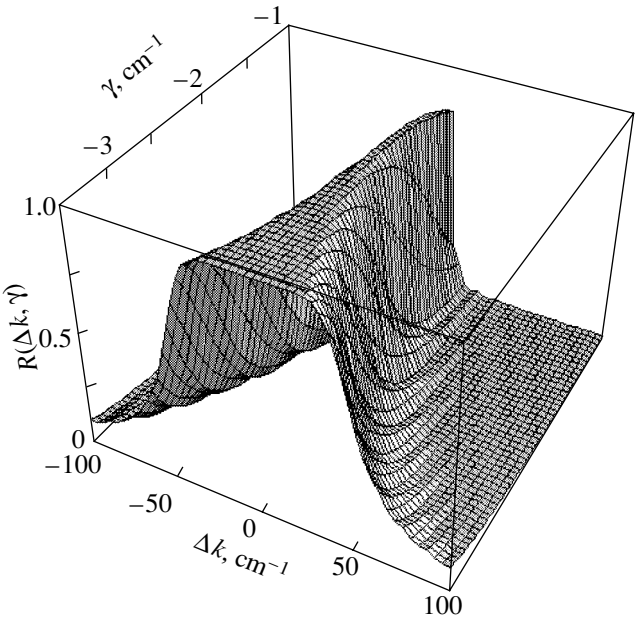

Fig. 1. General form of the function $R(\Delta k, \gamma)$ for $\gamma < 0$.

From Eqs. (2), we derive the equation for one of the waves, for example, for the reflected wave E_2:

$$\frac{d^2E_2}{dx^2} + (i\Delta k + \gamma)\frac{dE_2}{dx} - \Gamma^2 e^{-2\gamma x}E_2 = 0. \tag{4}$$

The boundary conditions for the reflected wave obviously have the form

$$E_2(L) = 0, \quad \left.\frac{dE_2}{dx}\right|_{x=0} = -i\Gamma E_1(0), \tag{5}$$

where L is the length of interaction between waves or the characteristic scale of the periodic structure.

To solve Eq. (4), it is necessary to change the variable as $u = e^{-\gamma x}$. In this case, the solution of Eq. (4) with boundary conditions (5) is obtained in the general form

$$E_2(x) = iE_1\Gamma e^{-(\gamma + i\Delta k)x}\frac{I_{-\frac{1}{2}-\frac{\Delta k}{\gamma}}\left(\frac{\Gamma}{\gamma}e^{-\gamma x}\right)I_{\frac{1}{2}+\frac{\Delta k}{\gamma}}\left(\frac{\Gamma}{\gamma}e^{-\gamma L}\right) - I_{-\frac{1}{2}-\frac{\Delta k}{\gamma}}\left(\frac{\Gamma}{\gamma}e^{-\gamma L}\right)I_{\frac{1}{2}+\frac{\Delta k}{\gamma}}\left(\frac{\Gamma}{\gamma}e^{-\gamma x}\right)}{I_{\frac{1}{2}-\frac{\Delta k}{\gamma}}\left(\frac{\Gamma}{\gamma}\right)I_{\frac{1}{2}+\frac{\Delta k}{\gamma}}\left(\frac{\Gamma}{\gamma}e^{-\gamma L}\right) - I_{-\frac{1}{2}-\frac{\Delta k}{\gamma}}\left(\frac{\Gamma}{\gamma}e^{-\gamma L}\right)I_{-\frac{1}{2}+\frac{\Delta k}{\gamma}}\left(\frac{\Gamma}{\gamma}\right)}, \tag{6}$$

where $I_\nu(x)$ is the modified Bessel function.

Solution (6) describes the amplitude of the diffracted wave propagating towards the incident wave. This expression enables one to determine the intensity of the reflected wave at the point $x = 0$ and then to calculate reflectance $R(\Delta k) = \left|\frac{E_2(0)}{E_1(0)}\right|^2$ for the apodized periodic structure:

$$R(\Delta k, \gamma) = \left| \frac{I_{-\frac{1}{2}-\frac{\Delta k}{\gamma}}\left(\frac{\Gamma}{\gamma}e^{-\gamma x}\right) I_{\frac{1}{2}+\frac{\Delta k}{\gamma}}\left(\frac{\Gamma}{\gamma}e^{-\gamma L}\right) - I_{-\frac{1}{2}-\frac{\Delta k}{\gamma}}\left(\frac{\Gamma}{\gamma}e^{-\gamma L}\right) I_{\frac{1}{2}+\frac{\Delta k}{\gamma}}\left(\frac{\Gamma}{\gamma}e^{-\gamma x}\right)}{I_{\frac{1}{2}-\frac{\Delta k}{\gamma}}\left(\frac{\Gamma}{\gamma}\right) I_{\frac{1}{2}+\frac{\Delta k}{\gamma}}\left(\frac{\Gamma}{\gamma}e^{-\gamma L}\right) - I_{-\frac{1}{2}-\frac{\Delta k}{\gamma}}\left(\frac{\Gamma}{\gamma}e^{-\gamma L}\right) I_{-\frac{1}{2}+\frac{\Delta k}{\gamma}}\left(\frac{\Gamma}{\gamma}\right)} \right|^2. \quad (7)$$

The intensity of the transmitted wave is obviously determined by the quantity

$$T(\Delta k, \gamma) = 1 - R(\Delta k, \gamma), \quad (8)$$

which is the ratio of the intensity of the transmitted wave at the point $x = L$ to the intensity of the incident wave at the point $x = 0$. Expression (8) determines the efficiency of the suppression of radiation at the exit from the apodized periodic structure and is a direct consequence of condition (3).

It is very difficult to determine the asymptotic behavior of solution (6) for $\gamma \longrightarrow 0$, because initial equation (4) is solved by changing the variable x to u, which is meaningless for $\gamma \longrightarrow 0$. Fortunately, Eq. (4) is easily solved for $\gamma = 0$. According to this solution, reflectance has the form

$$R_{\gamma = 0}(\Delta k) = \left| \frac{\sinh(L\Gamma\sqrt{1-\xi^2})}{i\sqrt{1-\xi^2}\cosh(L\Gamma\sqrt{1-\xi^2}) - \xi\sinh(L\Gamma\sqrt{1-\xi^2})} \right|^2, \quad (9)$$

where $\xi = \dfrac{\Delta k}{2\Gamma}$. Formula (9) gives the wave transmittance for the sinusoidal periodic structure without apodization.

3. Thus, we obtain exact solutions of the problem of the diffraction of incident radiation by a periodic structure with exponential apodization. These solutions make it possible to determine the reflectance and transmittance of the wave by such a structure. We emphasize that the reflectance $R(\Delta k)$ and transmittance $T(\Delta k)$ of the apodized structure under consideration are independent of the sign of γ and have the necessary symmetry; i.e., they are the same for waves incident on this periodically apodized structure both from the left and from the right. Indeed, expression (7) is invariant under the formal replacement

$$\gamma \to -\gamma, \quad \Gamma \to \Gamma e^{-\gamma L}, \quad (10)$$

where the latter condition arises due to the necessity of satisfying boundary conditions (5).

Further analysis can be only numerical. To this end, we plot function $R(\Delta k, \gamma)$ (7) (see Fig. 1). As is seen, apodization strongly changes the character of the reflection and transmission of the wave by such structure. Figure 2 shows two lines for different γ values and demonstrates that apodization strongly reduces the amplitude of side maxima.

To use periodic structures as cutoff filters in Raman spectroscopy, it is very important to estimate the possible degree of the suppression of radiation. Figure 3 shows reflectance $R(\Delta k, -3\ \text{cm}^{-1})$ as a function of detuning Δk near the maximum at the point $\Delta k = 0$. In particular, $R(0, -3\ \text{cm}^{-1}) = 0.9999880813$ and $R(5\ \text{cm}^{-1}, -3\ \text{cm}^{-1}) = 0.9999702333$. Therefore, suppression can easily achieve 10^{-5} and can be considerably stronger for larger interaction scales L.

For the practical quality of a cutoff filter, the light-energy fraction that infiltrates through all side maxima and leads to the parasitic exposure of a photoreceiver is very important. This energy obviously depends on the spectrum of incident radiation. We estimate this energy for apodized and unapodized periodic structures and for uniform-spectrum incident radiation. For the

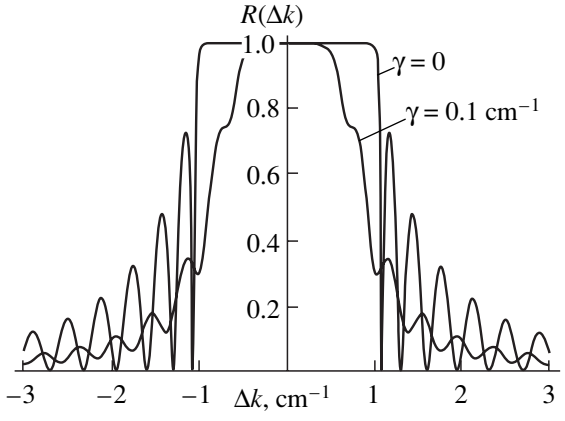

Fig. 2. Reflectance $R(\Delta k)$ of the apodized periodic medium vs. the wave detuning Δk as calculated by Eqs. (7) and (8) for interaction length $L = 15\ \text{cm}^{-1}$, coupling constant $\Gamma = 0.1\ \text{cm}^{-1}$, and γ values indicated in the figure. The plot for the transmittance $T(\Delta k) = 1 - R(\Delta k)$ of this structure is obvious.

reflecting fraction of radiation, the problem reduces to the calculation of the ratio of the integrals

$$\int_{\Delta k_{\min}}^{\Delta k_{\max}} R(\Delta k)d\Delta k, \qquad \int_{\Delta k_{\min}}^{\Delta k_{\max}} h_{\gamma=0}(\Delta k)d\Delta k, \qquad (11)$$

where $\Delta k_{\min}$ and $\Delta k_{\max}$ are, respectively, the minimum and maximum wavenumbers determined by both the spectral range of radiation and the position of the nearest maximum to the wavenumber satisfying the synchronism conditions, i.e., $k = 2q$. For simplicity, we take $\Delta k_{\max} = \infty$ and $\Delta k_{\min} = \dfrac{\pi}{2\Gamma L}$, which is the position of the nearest minimum to the phase-synchronism point $k = 2q$. In this case, integrals are calculated numerically and the ratio of the second integral to the first one is equal to 1.75 for the periodic-structure parameters shown in Fig. 2.[1] This means that the reflected-energy fraction in all side maxima, or beyond the fundamental band, for the apodized periodic structure is smaller than that for the unapodized structure by a factor of 1.75.

4. Further, we discuss possible applications of such periodically apodized structures and some concepts of technology for their manufacture. Amplitude apodization was shown to strongly suppress side maxima in the transmission function of the filter and to conserve strong suppression of the wave-transmission amplitude near the synchronism conditions. This is physically attributed to the fact that the amplitude of a wave diffracted by such a structure is determined by a new characteristic scale γ^{-1} [see Eq. (6)] rather than by the interaction length or characteristic size of the system. The application of these filters to suppression of an intense laser-radiation line, as well to ensuring the absence of side maxima, provides the possibility of measuring rather weak Raman scattering near the intense laser-radiation line. Therefore, the set of substances that can be studied by Raman spectroscopy can be considerably extended. We note that the apodization of a periodic structure is widely used in so-called opposing-pin converters for surface acoustic waves [12]. Apodization provides filters with almost ideal selective properties, which are extensively used in various fields of science and engineering.

Such periodically apodized structures can find interesting applications for the radio band, where wavelengths are significantly longer than in optics and technological requirements for the production of such structures are weaker. In particular, such structures can provide the production of parabolic mirror antennas for a certain wavelength range with a very high gain. The selective properties of these antennas are determined not only by sizes of a mirror but also by the period of the structure. Since, as was shown above, media with periodically varying properties can provide very high reflectance in a certain wavelength range, such antennas can apparently be applied in the submillimeter wavelength range, where it is difficult to find materials with large reflectance. We note that radiation beyond this wavelength range, where diffraction is small, is transmitted unchanged through such an antenna, and radiation in a different wavelength range can be separated form this flux. This antenna is schematically shown in Fig. 4.

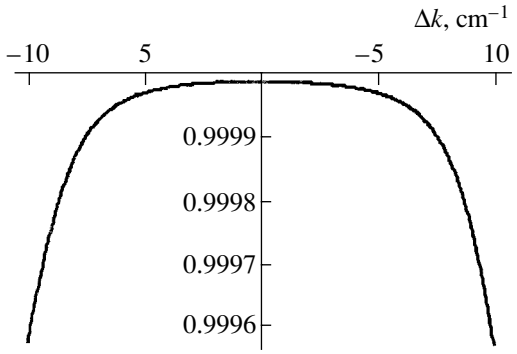

Fig. 3. Reflectance $R(\Delta k, -3\ \mathrm{cm}^{-1})$ vs. the wave detuning Δk near the maximum at $\Delta k = 0$. In particular, $R(0, -3\ \mathrm{cm}^{-1}) = 0.9999880813$ and $R(5\ \mathrm{cm}^{-1}, -3\ \mathrm{cm}^{-1}) = 0.9999702333$. Therefore, such structures can have very high reflectance.

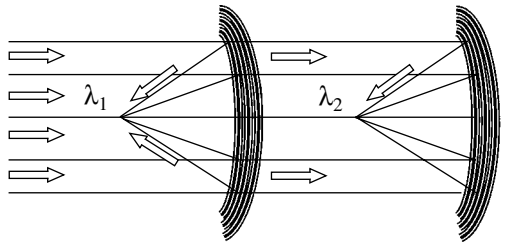

Fig. 4. Schematic representation of a selective antenna. The incident radiation passes through the parabolic periodically apodized structure, which reflects and focuses radiation near a certain wavelength λ_1. The remaining radiation passes further and can be focused by the following parabolic structure with a different periodic scale.

5. In conclusion, we emphasize that the amplitude of variation in optical properties or parameter α in Eq. (1) can be complex. This means that a periodically apodized structure can be formed due to variation of the conductivity of the medium, which opens new possibilities for the technology of the production of such structures. In this case, the above mathematical analysis is valid with the replacement of α^2 with $|\alpha^2|$ in the resulting formulas.

[1] All calculations were carried out by using the Mathematica 4.2 software package.

REFERENCES

1. G. S. Landsberg, *Optics* (Nauka, Moscow, 1976).
2. E. Hecht, *Optics* (Addison-Wesley, Reading (Mass), 1990).
3. E. G. Anan'ev, V. E. Pozhar, and V. I. Pustovoit, Opt. Spektrosk. **62**, 159 (1987) [Opt. Spectrosc. **62**, 97 (1987)].
4. V. I. Pustovoĭt and V. V. Timoshenko, Radiotekh. Élektron. **43** (4), 461 (1998).
5. V. I. Pustovoĭt and V. E. Pozhar, Radiotekh. Élektron. **43** (1), 121 (1998).
6. V. I. Pustovoĭt, Dokl. Akad. Nauk **365**, 39 (1999) [Dokl. Phys. **44**, 132 (1999)].
7. L. M. Brekhovskikh, *Waves in Layered Media* (Akad. Nauk SSSR, Moscow, 1957; Academic, New York, 1960).
8. A. Yariv and P. Yeh, *Optical Waves in Crystals: Propagation and Control of Laser Radiation* (Wiley, New York, 1984; Mir, Moscow, 1987).
9. P. Yeh, A. Yariv, and C. S. Hong, J. Opt. Soc. Am. **67**, 423 (1977).
10. *X-Ray Grazing-Incidence Optics*, Ed. by A. V. Vinogradov (Mashinostroenie, Leningrad, 1989).
11. Yu. V. Gulyaev and V. I. Pustovoĭt, Zh. Éksp. Teor. Fiz. **46**, 1386 (1964) [Sov. Phys. JETP **19**, 937 (1964)].
12. E. A. Ash, in *Acoustic Surface Waves* (Springer-Verlag, Berlin, 1978; Mir, Moscow, 1981).
13. G. V. Morozov, R. Gr. Maev, and G. W. F. Drake, Phys. Rev. E **60**, 4860 (1999).
14. G. V. Morozov, R. Gr. Maev, and G. W. F. Drake, Phys. Rev. E **63**, 056601 (2001).

Translated by R. Tyapaev

Doklady Physics, Vol. 48, No. 8, 2003, pp. 427–431. Translated from Doklady Akademii Nauk, Vol. 391, No. 4, 2003, pp. 478–482.

TECHNICAL PHYSICS

Universal Asymptotic Behavior of the Power Spectrum of $\frac{1}{f}$ Noise

A. G. Budarin

Presented by Academician A.F. Andreev April 10, 2003

Received March 31, 2003

The goal of this work is to determine the asymptotic behavior of the power spectrum of $\frac{1}{f}$ noise attributed to continuous large-scale fluctuations of a measured-parameter field. Estimates [1, 2] of the effect of fluctuations on the $\frac{1}{f}$ spectrum in the theory of $\frac{1}{f}$ processes testify to the existence of this asymptotic behavior. However, the asymptotic behavior itself was not studied in these works, because they were devoted to finding the mathematical form of the physical field that can turn into a random process with the $\omega^{-\alpha}$ spectrum in the course of measurements. As follows from the solution of an inverse statistical problem [1, 2], the desired form is specified by a train of Poisson pulse processes $S(x, t)$ and $R(x, t)$ substantially depending on the coordinates. The processes are formed by K pulses $a_i s(x - x_i)\delta(t - t_i)$ and $a_i r(x - x_i, t - t_i)$, where a_i are the amplitudes; $x_i \in (0, L)$ and $t_i \in (0, T)$ are, respectively, the position and time of the ith fluctuation; and $r(x - x_i, t - t_i)$ is the solution of the diffusion equation $r_t = Vr_x + \kappa r_{xx}$ under the initial condition $r(x - x_i, 0) = s(x - x_i)$ and homogeneous boundary conditions. In this case, the flux $J(x, t) = -\kappa Rx(x, t)$ formed by the contributions $j_i = j(x - x_i, t - t_i) = -\kappa r_x(x - x_i, t - t_i)$ represents the measured field that turns into $\frac{1}{f}$ noise. According to [1, 2], only weighted sums of the random number of singularities $(x - x_i)^{-\beta}$ or $(x_i - x)^{-\beta}$ can serve as processes $S(x, t)$ that have the spectrum $F(\omega) \sim \omega^{-\alpha}$ and are consistent with experiments. Here, $\beta = \frac{3}{2} - \alpha$, $\beta \in (0, 1)$, and $\alpha \in (0.5, 1.5)$. If the basic parameter of the theory is small, i.e., $h = \frac{\pi}{L}\left(\frac{\kappa}{\omega}\right)^{1/2} \ll 1$, then the spectrum $F(\omega)$ has the form

$$F(\omega) = 2\nu\langle a^2\rangle\langle\langle j(x - x_i, t - t_i)\rangle\rangle_{x, x_i}$$
$$= \nu L\langle a^2\rangle\kappa^2\sum_{n=1}^{\infty}\langle b_n^2\rangle k_n^2(\lambda_n^2 + \omega^2)^{-1} \sim \omega^{-\alpha}. \quad (1)$$

Here, b_n are the Fourier components for the spatial dependence of the function $r(x - x_i, t - t_i)$, $k_n = \frac{\pi n}{L}$, $\lambda_n = \kappa k_n^2$, and $\nu = \frac{\langle K\rangle}{TL}$.

It is clear that the singular form of the process $S(x, t)$ describing physical sources of $\frac{1}{f}$ noise in the theory presented in [1, 2] is a model assumption. Noise is actually formed in the field of continuous fluctuations of a parameter being measured and is accompanied by these fluctuations [3]. For this reason, we generalize the form of $S(x, t)$ as a sequence of power singularities over a continuous functional background. As will be shown below, a nontrivial consequence of such a generalization is the appearance of the universal asymptotic behavior of the model $\frac{1}{f}$ spectrum. This behavior is independent of the form of pulses in the process $S(x, t)$ responsible for $\frac{1}{f}$ noise.

We now estimate the spectrum $F(\omega)$ in the generalized model with $\langle K\rangle = 1$, when the process $S(x, t)$ has only one singularity $(x - x_i)^{-\beta}$. With a given accuracy ε, the continuous function $s(x - x_i)(x - x_i)^{\beta}$ is approximated by a polynomial as

$$s(x - x_i) = \sum_{m=0}^{M} C_{mi}(x - x_i)^{m-\beta}, \quad M = M(\varepsilon); \quad (2)$$

1028-3358/03/4808-0427$24.00

$$b_n = \sum_{m=0}^{M} C_{mi} b_{nm},$$
$$b_{nm} = \frac{2}{L}\int_0^L (x - x_i)^{m-\beta} \sin(k_n x)\,dx; \quad (3)$$

$$\langle b_n^2 \rangle = \sum_{m=0}^{M} \sum_{m'=0}^{M} C_{mm'} \langle b_{nm} b_{nm'} \rangle, \quad C_{mm'} = \langle C_{mi} C_{m'i} \rangle. \quad (4)$$

Changing the variables in Eq. (3) as $y = k_n(x - x_i)$, $\zeta_i = \frac{x_i}{L}$, $\varphi = \varphi_{ni} = \pi n \zeta_i$, $\psi = \psi_{ni} = \pi n(1 - \zeta_i)$, and $a_{nm} = \frac{2}{L k_n^{m+1-\beta}}$, we obtain

$$b_{nm} = a_{nm}[\sin\varphi_{ni} I_{cm}(\psi_{ni}) + \cos\varphi_{ni} I_{sm}(\psi_{ni})], \quad (5)$$

where

$$I_{cm}(t) = \int_0^t y^{m-\beta} \cos y\,dy$$

and

$$I_{sm}(t) = \int_0^t y^{m-\beta} \sin y\,dy.$$

We substitute $v = \frac{t^{m-\beta}}{(1-\beta)_m}$ and $u = \sin t$ or $u = \cos t$ into the general formula

$$\int u v^{(m)} dt = \sum_{k=0}^{m-1} (-1)^k u^{(k)} v^{(m-k-1)} + (-1)^m \int v u^{(m)} dt. \quad (6)$$

Using the identities $u^{(k)} = \sin\left(k\frac{\pi}{2} + t\right)$, $u^{(k)} = \cos\left(k\frac{\pi}{2} + t\right)$, and Eq. (6), we obtain

$$\int t^{-\beta} \sin t\,dt = \sum_{k=1}^{m} (-1)^k t^{k-\beta} (1-\beta)_k^{-1} \cos\left(k\frac{\pi}{2} + x\right) + (-1)^m (1-\beta)_m^{-1} s_m(\beta, x),$$

$$\int t^{-\beta} \cos t\,dt = -\sum_{k=1}^{m} (-1)^k t^{k-\beta} (1-\beta)_k^{-1} \sin\left(k\frac{\pi}{2} + x\right) + (-1)^m (1-\beta)_m^{-1} c_m(\beta, x),$$

$$s_m(\beta, x) = \int t^{m-\beta} \sin\left(m\frac{\pi}{2} + t\right) dt,$$

$$c_m(\beta, x) = \int t^{m-\beta} \cos\left(m\frac{\pi}{2} + t\right) dt.$$

For $m = 2l$, we have $s_m(\beta, x) = (-1)^l I_{sm}(x)$ and $c_m(\beta, x) = (-1)^l I_{cm}(x)$; for $m = 2l + 1$, we have $s_m(\beta, x) = (-1)^l I_{cm}(x)$ and $c_m(\beta, x) = (-1)^{l+1} I_{sm}(x)$. As follows from these formulas and Eq. (5),

$$b_{nm} = (-1)^{l+n+1} a_{nm} \sum_{k=1}^{m} (-1)^k u_{mk}(\beta) \psi^{k-\beta} \cos\left(k\frac{\pi}{2}\right) + (-1)^l v_m(\beta) b''_{n0}, \text{ for } m = 2l,$$

$$b_{nm} = (-1)^{l+n} a_{nm} \sum_{k=1}^{m} (-1)^k u_{mk}(\beta) \psi^{k-\beta} \sin\left(k\frac{\pi}{2}\right) + (-1)^l v_m(\beta) b'_{n0}, \text{ for } m = 2l + 1,$$

$$b''_{n0} = a_{n0} \int_0^\psi y^{-\beta} \sin(\varphi + y)\,dy,$$

$$b'_{n0} = a_{n0} \int_0^\psi y^{-\beta} \cos(\varphi + y)\,dy,$$

where $u_{mk}(\beta) = \frac{(1-\beta)_m}{(1-\beta)_k}$ and $v_m(\beta) = (1-\beta)_m k_n^{-m}$.

For $m = 2l$ and $m' = 2l'$, we obtain

$$\langle b_{nm} b_{nm'} \rangle = e_{n0} + e_{n1} + e'_{n1} + e_{n2},$$

where

$$e_{n0} = (-1)^{l+l'} a_{nm} a_{nm'} \times \sum_{k=2}^{m}{}'' \sum_{k'=2}^{m'}{}'' (-1)^{(k+k')/2} u_{mk}(\beta) u_{m'k'}(\beta) \langle \psi^{k+k'-2\beta} \rangle,$$

$$e_{n1} = (-1)^{l+l'+n+1} a_{nm} \times \sum_{k=2}^{m}{}''(-1)^{k/2} u_{mk}(\beta) v_{m'}(\beta) \langle \psi^{k-\beta} b''_{n0} \rangle,$$

$$e'_{n1} = (-1)^{l+l'+n+1} a_{nm'} \times \sum_{k'=2}^{m'}{}''(-1)^{k'/2} u_{m'k'}(\beta) v_{m}(\beta) \langle \psi^{k'-\beta} b''_{n0} \rangle,$$

$$e_{n2} = (-1)^{l+l'} v_m(\beta) v_{m'}(\beta) \langle b''^2_{n0} \rangle.$$

The average quantities entering into these formulas are estimated as $e_{n0} - e_{n2}$: $\langle \psi^{k+k'-2\beta} \rangle = (\pi n)^{k+k'-2\beta}(k + k' + 1 - 2\beta)^{-1}$, $\langle b''^2_{n0} \rangle \sim \langle b'^2_{n0} \rangle \sim a_{n0}^2 \Gamma^2 \frac{1-\beta}{2}$, $\langle \psi^{k-\beta} b''_{n0} \rangle = a_{n0}(\pi n)^{k+1-2\beta} P$, where

$$P = \iint_{0 \le \zeta + \eta \le 1} (1-\zeta)^{k-\beta} \eta^{-\beta} \sin[\pi n(\zeta + \eta)] d\zeta d\eta.$$

Changing the variables $\zeta = st$, $\eta = s(1-t)$, and $\mu = r + 2 - \beta$, we reduce the integral P to the form

$$P = \int_0^1 \int_0^1 (1-st)^{k-\beta} s^{1-\beta} (1-t)^{-\beta} \sin(\pi n s) ds dt$$

$$= (1-\beta)^{-1} \int_0^1 s^{1-\beta} \sin(\pi n s) {}_2F_1(\beta - k, 1; 2-\beta; s) ds$$

$$= \sum_{r=0}^{\infty} (\beta - k)_r (1-\beta)_{r+1} \int_0^1 s^{r+1-\beta} \sin(\pi n s) ds$$

$$= (2i)^{-1} \sum_{r=0}^{\infty} (\beta - k)_r (1-\beta)^{-1}_{r+1} \times \mu^{-1} [{}_1F_1(\mu, \mu+1, i\pi n) - {}_1F_1(\mu, \mu+1, -i\pi n)]. \quad (7)$$

Substituting the asymptotic behavior of the hypergeometric function ${}_1F_1(\mu, \mu+1, z) \sim \mu z^{-1} \exp z$ into Eq. (7), we obtain

$$P \sim (-1)^{n+1} [(\pi n)(k + 1 - 2\beta)]^{-1},$$

$$\langle \psi^{k-\beta} b''_{n0} \rangle \sim a_{n0} (-1)^{n+1} (k + 1 - 2\beta)^{-1} (\pi n)^{k-2\beta}.$$

Similarly, for $m = 2l + 1$ and $m' = 2l' + 1$, the quantities $\langle b_{nm} b_{nm'} \rangle$ are given by the formulas

$$\langle b_{nm} b_{nm'} \rangle = o_{n0} + o_{n1} + o'_{n1} + o_{n2},$$

where

$$o_{n0} = (-1)^{l+l'+1} a_{nm} a_{nm'} \times \sum_{k=1}^{m}{}' \sum_{k'=1}^{m'}{}' (-1)^{(k+k')/2} u_{mk}(\beta) u_{m'k'}(\beta) \langle \psi^{k+k'-2\beta} \rangle,$$

$$o_{n1} = (-1)^{l+l'+n+1} a_{nm} \times \sum_{k=1}^{m}{}' (-1)^{(k-1)/2} u_{mk}(\beta) v_{m'}(\beta) \langle \psi^{k-\beta} b'_{n0} \rangle,$$

$$o'_{n1} = (-1)^{l+l'+n+1} a_{nm'} \times \sum_{k'=1}^{m'}{}' (-1)^{(k'-1)/2} u_{m'k'}(\beta) v_{m}(\beta) \langle \psi^{k'-\beta} b'_{n0} \rangle,$$

$$o_{n2} = (-1)^{l+l'} v_m(\beta) v_{m'}(\beta) \langle b'^2_{n0} \rangle.$$

The estimates of the average quantities entering into these expressions have the form $\langle \psi^{k-\beta} b'_{n0} \rangle = a_{n0}(\pi n)^{k+1-2\beta} Q$, where

$$Q = \iint_{0 \le \zeta + \eta \le 1} (1-\zeta)^{k-\beta} \times \eta^{-\beta} \cos[\pi n(\zeta + \eta)] d\zeta d\eta.$$

Changing the variables similarly to the above case for P, we write out the integral Q in a form similar to Eq. (7):

$$Q = \frac{1}{2} \sum_{r=0}^{\infty} (\beta - k)_r (1-\beta)^{-1}_{r+1} \mu^{-1} \times [{}_1F_1(\mu, \mu+1, i\pi n) + {}_1F_1(\mu, \mu+1, -i\pi n)]. \quad (8)$$

Therefore, $Q \sim (-1)^{n+1} (\sqrt{2}\,\pi n)^{-2}$ and $\langle \psi^{k-\beta} b'_{n0} \rangle \sim \frac{a_{n0}}{2} (-1)^{n+1} (\pi n)^{k-1-2\beta}$.

For $m = 2l$ and $m' = 2l' + 1$, we obtain

$$\langle b_{nm} b_{nm'} \rangle = w_{n0} + w_{n1} + w'_{n1} + w_{n2},$$

where

$$w_{n0} = (-1)^{l+l'} a_{nm} a_{nm'} \times \sum_{k=2}^{m}{}'' \sum_{k'=1}^{m'}{}' (-1)^{(k+k'+1)/2} u_{mk}(\beta) u_{m'k'}(\beta) \langle \psi^{k+k'-2\beta} \rangle,$$

$$w_{n1} = (-1)^{l+l'+n+1} a_{nm} \times \sum_{k=2}^{m}{}'' (-1)^{k/2} u_{mk}(\beta) v_{m'}(\beta) \langle \psi^{k-\beta} b'_{n0} \rangle,$$

$$w'_{n1} = (-1)^{l+l'+n+1} a_{nm'} \times \sum_{k'=1}^{m'}{}' (-1)^{(k'-1)/2} u_{m'k'}(\beta) v_{m}(\beta) \langle \psi^{k'-\beta} b''_{n0} \rangle,$$

$$w_{n2} = (-1)^{l+l'} v_m(\beta) v_{m'}(\beta) \langle b''_{n0} b'_{n0} \rangle.$$

Substituting the expressions for $\langle b_{nm} b_{nm'} \rangle$ into Eq. (4), we find $\langle b_n^2 \rangle$ for all $0 \le m$ and $m' \le M$. Substituting $\langle b_n^2 \rangle$ into Eq. (1), we arrive at the following estimate of the $\frac{1}{f}$ spectrum $F(\omega)$ in the presence of the continuous field of fluctuations:

$$F(\omega) \sim 4\nu L \left(\frac{\kappa}{\omega}\right)^2 \times \sum_{m=0}^{M} \sum_{m'=0}^{M} (-1)^{l+l'} C_{mm'} L^{m+m'-2-2\beta} \sum_{j=0}^{2} W_{jmm'}. \quad (9)$$

Here,

$$W_{0mm'}\big|_{m=2l,\, m'=2l'} = \sum_{k=2}^{m}{}'' \sum_{k'=2}^{m'}{}'' (-1)^{(k+k')/2} A_{mm'kk'} S(h, m+m'-k-k'),$$

$$W_{1mm'}\big|_{m=2l,\, m'=2l'} = \sum_{k=2}^{m}{}'' (-1)^{k/2} A_{mm'k0} S(h, m+m'-k),$$

$$W_{2mm'}\big|_{m=2l,\, m'=2l'} = \frac{1}{2}\Gamma^2(1-\beta) B_{mm'00} S(h, m+m'-2\beta),$$

$$W_{0mm'}\big|_{m=2l+1,\, m'=2l'+1} = -\sum_{k=1}^{m}{}' \sum_{k'=1}^{m'}{}' (-1)^{(k+k')/2} A_{mm'kk'} S(h, m+m'-k-k'),$$

$$W_{1mm'}\big|_{m=2l+1,\, m'=2l'+1} = \frac{1}{2} \sum_{k=1}^{m}{}' (-1)^{(k-1)/2} B_{mm'k0} S(h, m+m'+1-k),$$

$$W_{2mm'}\big|_{m=2l+1,\, m'=2l'+1} = \frac{1}{2}\Gamma^2(1-\beta) B_{mm'00} S(h, m+m'-2\beta),$$

$$W_{0mm'}\big|_{m=2l,\, m'=2l'+1} = \sum_{k=2}^{m}{}'' \sum_{k'=1}^{m'}{}' (-1)^{(k+k'-1)/2} A_{mm'kk'} S(h, m+m'-k-k'),$$

$$W_{1mm'}\big|_{m=2l,\, m'=2l'+1} = \frac{1}{2} \sum_{k=2}^{m}{}'' (-1)^{k/2} B_{mm'k0} S(h, m+m'+1-k),$$

$$W_{0mm'}\big|_{m=2l+1,\, m'=2l'} = \sum_{k=1}^{m}{}' \sum_{k'=2}^{m'}{}'' (-1)^{(k+k'-1)/2} A_{mm'kk'} S(h, m+m'-k-k'),$$

$$W_{1mm'}\big|_{m=2l+1,\, m'=2l'} = \sum_{k=1}^{m}{}' (-1)^{(k-1)/2} A_{mm'k0} S(h, m+m'-k),$$

$$W_{2mm'}\big|_{m=2l,\, m'=2l'+1} \sim W_{2mm'}\big|_{m=2l+1,\, m'=2l'} \sim o(W_{2mm'}\big|_{m=2l,\, m'=2l}),$$

$$B_{mm'kk'} = u_{mk}(\beta) u_{m'k'}(\beta),$$

$$A_{mm'kk'} = B_{mm'kk'}(k+k'+1-2\beta)^{-1},$$

$$S(h, q) = \lim_{N \to \infty} S_N(h, q),$$

$$S_N(h, q) = \sum_{n=1}^{N} [(\pi n)^q (1 + (hn)^4)]^{-1}.$$

The primes and double primes stand for summations over odd and even indices, respectively.

For $h = \left(\frac{\lambda_1}{\omega}\right)^{1/2} \ll 1$, the asymptotic estimates of the sums for $q = -2\beta$ and $q = 0$ give $S(h, -2\beta) \sim \left(4\sin\left(\pi\frac{\alpha}{2}\right)\right)^{-1} \times (\pi/h)^{1+2\beta}$ and $S(h, 0) \sim \frac{\sqrt{2}\pi}{4h}$, respec-

tively. For other q, Eq. (9) provides the estimate $\frac{S(h, q)}{S(h, 0)} \ll 1$. Indeed, this estimate is valid for $q = 1$, because

$$\frac{S(h, 1)}{S(h, 0)} \sim \frac{S_N(h, 1)}{S_N(h, 0)} \sim N^{-1}\sum_{n=1}^{N}(\pi n)^{-1} \sim \frac{\ln N}{N} \ll 1$$

for $N \gg 1$.

For $q > 1$, the same estimate holds, because $S(h, q) \sim$ const. For $m = m' = 0$, we obtain the spectrum

$$F(\omega) \sim \frac{1}{2}\Gamma^2\left(\alpha - \frac{1}{2}\right)\mathrm{cosec}\left(\pi\frac{\alpha}{2}\right)\nu C_{00}^2\left(\frac{\kappa}{\omega}\right)^{\alpha} \qquad (10)$$

from the model [1, 2] of the field formed by power singularities. For $q = 0$, we obtain the new component

$$F(\omega) \sim \sqrt{2}\nu D\left(\frac{\kappa}{\omega}\right)^{3/2}, \qquad (11)$$

associated with the generalization of the model [1, 2]. Here, D is the sum of the terms $\frac{C_{mm'}L^{-m-m'-2\beta}}{m + m' + 1 - 2\beta}$, except for $m = m' = 0$. A similar result can be obtained for the Fourier basis $\{\cos(k_n x)\}$.

The estimate of spectrum (11) remains valid for arbitrary homogeneous boundary conditions and for arbitrary $\langle K\rangle$. This estimate is universal due to the following reasons. For $h \ll 1$ $\left(\text{i.e., for } \omega^{-1} \ll \lambda_1^{-1} \text{ and } l_{\text{diff}} \sim \left(\frac{\kappa}{\omega}\right)^{1/2} \ll L\right)$, the $\frac{1}{f}$ spectrum is formed by the fluxes j_i originating in small neighborhoods $\delta_i = \{l_{\text{diff}}, \omega^{-1}\}_i$ of the points (x_i, t_i). As follows from the analysis of the diffusion equation for small δ_i [6], the fluxes are independent of boundary conditions and of each other. The first property leads to the insensitivity of the spectrum of fluxes $J(x, t)$ to the type of boundary conditions. The second property, along with the condition of independence of the points (x_i, t_i), results in additivity of the contributions of the fluxes j_i to the $\frac{1}{f}$ spectrum, and estimate (10) is therefore valid for arbitrary $\langle K\rangle$.

Thus, based on the mathematical theory of $\frac{1}{f}$ noise [1, 2], we show that continuous large-scale fluctuations affect the $\frac{1}{f}$ spectrum so that a spectral component having the universal asymptotic behavior $\omega^{-3/2}$ independent of the form of the fluctuations appears.

It is worth noting that the physical cause of asymptotic behavior (11) differs fundamentally from that of the asymptotic forms $\sim\omega^{-2\alpha}$ for $\alpha \le 1$ and $\sim\omega^{-2}$ for $\alpha > 1$, which were considered in [4] and were attributed to time correlations in the diffusion flux $J(x, t)$. Asymptotic behavior (11) exists in the case under consideration, because the field of the measured-parameter singularities is modulated by a continuous random background. Thus, the asymptotic forms found in [4] and those considered here are due to different and independent mechanisms. However, both these mechanisms are manifested only if the mechanism considered in [4] acts effectively. Otherwise, spectrum (10) will be observed. With an increase in the frequency ω, asymptotic behavior that approaches zero more slowly must be manifested. Hence, the dependence $\omega^{-3/2}$ should be expected for $\alpha = 1$.

REFERENCES

1. A. G. Budarin, Dokl. Akad. Nauk **359**, 615 (1998) [Dokl. Phys. **43**, 218 (1998)].
2. A. G. Budarin, Radiotekhnika (Moscow) **11**, 8 (1997).
3. A. G. Budarin, Dokl. Akad. Nauk **372**, 326 (2000) [Dokl. Phys. **45**, 208 (2000)].
4. A. G. Budarin, Pis'ma Zh. Éksp. Teor. Fiz. **73**, 763 (2001) [JETP Lett. **73**, 678 (2001)].
5. *Handbook of Mathematical Functions*, Ed. by M. Abramowitz and I. A. Stegun (Dover, New York, 1971; Nauka, Moscow, 1979).
6. Ya. B. Zel'dovich and A. D. Myshkis, *Principles of Mathematical Physics* (Nauka, Moscow, 1973).

Translated by V. Chechin

Doklady Physics, Vol. 48, No. 8, 2003, pp. 432–436. Translated from Doklady Akademii Nauk, Vol. 391, No. 6, 2003, pp. 754–758.

TECHNICAL PHYSICS

Suppression of the Residual Radiation of Ultrashort-Pulse Antennas in Packet Mode

Corresponding Member of the RAS L. D. Bakhrakh* and M. Ya. Izrailovich**

Received March 27, 2003

Pulses radiated by ultrashort-pulse antennas [1, 2] are significantly distorted compared to an input signal produced by an ultrashort-pulse generator and applied to the antenna input. In particular, the radiated signal is more prolonged. To suppress this residual radiation, we suggested in [3] application of an extra corrective pulse (corrective action) to the antenna input after the input pulse. This corrective pulse is calculated so that radiation is completely suppressed to a given time. The second problem of the correction of the output signal is the best fit of its time diagram to a given shape. This problem was solved in [4] also by using extra corrective pulses applied to the antenna input simultaneously with the input signal of the ultrashort-pulse generator.

We emphasize that only separate pulses were considered in [3, 4]. At the same time, ultrashort-pulse antennas operate most frequently in packet mode; i.e., they radiate finite sequences of repetitive pulses. In this case, the problem of correction of signals becomes much more complicated because of the overlap of distorted repetitive pulses.

When the procedures described in [3, 4] completely suppress the residual radiation following an input pulse before arrival of the next input pulse, the problem of correcting a sequence of repetitive pulses is identical to that for a single pulse. However, it is difficult to ensure such suppression, because it requires a corrective signal of a very high power, especially in the case of a short time interval between pulses.

In this paper, we present methods of determining limited-power corrective signals for ultrashort-pulse antennas operating in the packet mode. The methods solve the first problem of correction of output signals, namely, the problem of the suppression of residual radiation with allowance for the overlap of repetitive radiated signals.

* *Moscow Research Institute of Instrument Engineering, Kutuzovskiĭ prospect 34, Moscow, 121170 Russia*

** *Blagonravov Institute of Mechanical Engineering, Russian Academy of Sciences, ul. Bardina 4, Moscow, 117334 Russia*

1. ANALYSIS OF THE TIME PROFILES OF DISTORTED RADIATED SIGNALS

The dynamic response of an antenna [which represents the relation of an input signal $x_0(t)$ produced by an ultrashort-pulse generator to the corresponding signal $y_0(t)$ radiated by the antenna] is assumed to be described by a pulse transfer function. For a single pulse,

$$y_0(t) = \int_0^t h(t-\tau)x_0(\tau)d\tau, \quad t \in (0;\, T_1],$$
$$y_0(t) = \int_0^{T_1} h(t-\tau)x_0(\tau)d\tau, \quad t > T_1, \tag{1}$$

where T_1 is the duration of the input signal $x_0(t)$. For a sequence of n pulses repeated with the period T, the radiated signal has the form

$$y_0(t) = \sum_{i=1}^{l-1} \int_{(i-1)T}^{(i-1)T+T_1} h(t-\tau)x_0(\tau)d\tau + \int_{lT}^{t} h(t-\tau)x_0(\tau)d\tau,$$
$$t \in (lT;\, lT + T_1],$$
$$y_0(t) = \sum_{i=1}^{l} \int_{(i-1)T}^{(i-1)T+T_1} h(t-\tau)x_0(\tau)d\tau, \tag{2}$$
$$t \in (lT + T_1, (l+1)T],$$
$$l = 2, 3, \ldots, n-1,$$
$$y_0(t) = \sum_{i=1}^{n} \int_{(i-1)T}^{(i-1)T+T_1} h(t-\tau)x_0(\tau)d\tau, \quad t \in (nT; \infty).$$

As was shown in [5], by introducing new variables $\tau_i = \tau - (i-1)T$ and in view of the T periodicity of $x_0(t)$,

1028-3358/03/4808-0432$24.00

expressions (2) can be transformed to the form

$$y_0(t) = \int_0^{T_1} g_{l-1}(t-\tau)x_0(\tau)d\tau + \int_0^{t-lT} h(t-\tau-lT)x_0(\tau)d\tau,$$
$$t \in (lT;\ lT+T_1], \quad (3)$$
$$y_0(t) = \int_0^{T_1} g_l(t-\tau)x_0(\tau)d\tau, \quad t \in [lT+T_1, (l+1)T],$$
$$y_0(t) = \int_0^{T_1} g_n(t-\tau)x_0(\tau)d\tau, \quad t \in [(n-1)T+T_1, \infty),$$

where

$$g_l(t-\tau) = \sum_{i=0}^{l-1} h(t-\tau-iT).$$

This representation of the time profile of the radiated signal is convenient, because it allows us to estimate the residual radiation intensity for an arbitrary input signal $x_0(\tau)$.

2. GENERAL CASE OF THE SUPPRESSION OF RESIDUAL RADIATION

In order to suppress residual radiation described by expressions (3), a corrective pulse should be applied to the antenna input for the time interval from the end of an input pulse to the beginning of the next pulse:

$$u_l(t), \quad t \in (lT+T_1;\ (l+1)T).$$

In this case, the total radiation of the antenna is given by the expressions

$$y(t) = y_0(t) - \int_{T_1}^{t} h(t-\tau)u_1(\tau)d\tau, \quad t \in (T_1;\ T],$$
$$y(t) = y_0(t) - \sum_{i=1}^{l-1} \int_{(i-1)T+T_1}^{iT} h(t-\tau)u_i(\tau)d\tau,$$
$$t \in (lT;\ lT+T_1],$$
$$y(t) = y_0(t) - \sum_{i=1}^{l-1} \int_{(i-1)T+T_1}^{iT} h(t-\tau)u_i(\tau)d\tau - \int_{lT+T_1}^{t} h(t-\tau)u_l(\tau)d\tau, \quad (4)$$
$$t \in (lT+T_1;\ (l+1)T], \quad l = 2, 3, \ldots, n.$$

For the most complete suppression of the residual radiation of a sequence of pulses, the overlap of these pulses should be minimized. Hence, it is advisable to minimize the residual radiation intensity at the times $t = lT$, $l = 1, 2, \ldots$ just before the beginnings of subsequent pulses. As follows from Eqs. (4), the radiation intensity at these times is

$$y(lT) = y_0(lT) - \sum_{i=1}^{l} \int_{(i-1)T+T_1}^{lT} h(lT-t)u_i(t)dt, \quad (5)$$

where, according to Eqs. (3),

$$y_0(lT) = \int_0^{T_1} g_{l-1}(lT-t)x_0(t)dt.$$

It should be noted that the radiation intensity $y(lT)$ given by Eqs. (5) depends on the corrective signals $u_i(t)$, $i = 1, 2, \ldots, l$, which affect the antenna input after both the current input pulse $x_0(t)$, $t \in ((l-1)T;\ (l-1)T+T_1]$ and all preceding corrective pulses. Therefore, these corrective pulses cannot be determined separately for each repetitive pulse (when the residual radiation of the pulse is not completely suppressed before the arrival of the next pulse).

In view of this circumstance, the optimization criterion for the corrective action is taken in the form of the magnitude of the total residual radiation:

$$y_n = \sum_{l=1}^{n} y(lT) = \sum_{l=1}^{n} y_0(lT) - \sum_{l=1}^{n}\sum_{i=1}^{l} \int_{(i-1)T+T_1}^{iT} h(lT-t)u_i(t)dt$$
$$= \sum_{l=1}^{n} y_0(lT) - \sum_{i=1}^{n} \int_{(i-1)T+T_1}^{iT} \sum_{l=i}^{n} h(lT-t)u_i(t)dt. \quad (6)$$

The power of each corrective signal $u_i(t)$, $i = 1, 2, \ldots, n$ is assumed to be limited by the same value

$$\frac{1}{T-T_1} \int_{(i-1)T+T_1}^{iT} u_i^2 dt \le W. \quad (7)$$

For functional y_n (6) to be minimal, its second term must be maximal. It can be written in the form

$$I = \sum_{i=1}^{n} \int_{(i-1)T+T_1}^{iT} H_i(t)u_i(t)dt, \quad (8)$$

where

$$H_i(t) = \sum_{l=i}^{n} h(lT-t).$$

The problem of maximizing functional I (8) under restrictions (7) reduces to n independent identical problems:

$$\max I_i(u_i) = \int_{(i-1)T+T_1}^{iT} H_i(t)u_i(t)dt,$$
$$\frac{1}{T-T_1}\int_{(i-1)T+T_1}^{iT} u_i^2 dt \le W. \quad (9)$$

For each of these problems, the Euler–Lagrange equation has the form

$$-\frac{2\lambda_i}{T-T_1}u_i + H_i(t) = 0, \quad i = 1, 2, \ldots, n, \quad (10)$$

where λ_i are the Lagrange multipliers introduced for restrictions (7) to be met. It follows from Eqs. (10) that

$$u_i(t) = \frac{T-T_1}{2\lambda_i}H_i(t), \quad i = 1, 2, \ldots, n.$$

Substituting $u_i(t)$ into the corresponding restriction, we find λ_i and then the following final expressions for the corrective actions:

$$u_i^*(t) = \frac{\sqrt{(T-T_1)W}}{\|H_i\|}H_i(t), \quad t \in ((i-1)T+T_1; iT), \quad (11)$$

where

$$\|H_i\| = \left[\int_{(i-1)T+T_1}^{iT} H_i^2(t)dt\right]^{\frac{1}{2}}.$$

The corresponding minimum value of residual radiation intensities (6) is given by the expression

$$y_n^* = \sum_{l=1}^{n} y_0(lT) - \sum_{l=1}^{n}\|H_i\|\sqrt{(T-T_1)W}. \quad (12)$$

In this case, we assume that the quantity y_n^* given by Eq. (12) is nonnegative and the partial sums

$$y_m^* = \sum_{l=1}^{m} y_0(lT) - \sum_{l=1}^{m}\|H_i\|\sqrt{(T-T_1)W}$$

of the residual radiation intensities are positive. This assumption is valid when the duration $T - T_1$ of the corrective signal is sufficiently short.

3. SUPPRESSION OF RESIDUAL RADIATION BY A PERIODIC CORRECTIVE ACTION

Corrective actions $u_i^*(t)$ (11) ensuring the minimum intensity of residual radiation have different time profiles in time intervals between pulses, which results in some engineering problems. In order to simplify them, it may be advisable to use a periodic corrective signal that has a period T equal to the input-pulse duration and acts only in the time intervals $t \in [(l-1)T + T_1; lT]$, $l = 1, 2, \ldots, n$ between pulses. In this case, total residual radiation (6) is also used as the minimized criterion. Since the corrective action $u(t) - T$ is a periodic function, residual radiation at the times $t = lT$, $l = 1, 2, \ldots, n$ is determined by the expressions

$$y(lT) = y_0(lT) - \int_{T_1}^{T} g_{l-1}(lT-t)u(t)dt, \quad l = 1, 2, \ldots, n. \quad (13)$$

According to Eqs. (13), total residual radiation y_n (6) is given by the expression

$$y_n = \sum_{l=1}^{n} y(lT) = \sum_{l=1}^{n} y_0(lT) - \int_{T_1}^{T}\sum_{l=1}^{n} g_{l-1}(lT-t)u(t)dt. \quad (14)$$

We assume that restriction (7) is imposed on the corrective-pulse power at each time interval $[(l-1)T + T_1; lT]$, $l = 1, 2, \ldots, n$. Since $u_l(t) = u_{l-1}(t - T)$, restriction (7) reduces to the form

$$\frac{1}{T-T_1}\int_{T_1}^{T} u^2 dt \le W. \quad (15)$$

It is required to find a function $u^*(t)$ such that the functional

$$I = \int_{T_1}^{T}\sum_{l=1}^{n} g(lT-t)u(t)dt$$

is minimal under restriction (15). The Euler–Lagrange equation for this problem has the form

$$-\frac{2\lambda}{T-T_1}u + G_n(t) = 0. \quad (16)$$

Here, λ is the Lagrange multiplier introduced to satisfy restriction (15) and

$$G_n(t) = \sum_{l=1}^{n} g_{l-1}(lT-t).$$

As follows from Eq. (16),

$$u(t) = \frac{T-T_1}{2\lambda}G_n(t).$$

We substitute this expression into inequality (15),

determine λ, and then find

$$u^*(t) = \frac{\sqrt{(T-T_1)W}}{\|G_n\|}G_n(t),$$
$$\|G_n\| = \left[\int_{T_1}^{T} G_n^2(t)dt\right]^{\frac{1}{2}}. \quad (17)$$

According to Eqs. (14) and (17), the minimum of the total residual radiation intensity is given by the expression

$$y_n^* = \sum_{l=1}^{n} y_0(lT) - \|G_n\|\sqrt{(T-T_1)W}. \quad (18)$$

If the power

$$W_0 = \frac{1}{T_1}\int_0^{T_1} x_0^2 dt$$

of the input pulse $x_0(t)$ is given, the upper bound of y_n^* is found by applying the Cauchy–Schwarz inequality to the first term of Eq. (18):

$$\bar{y}_n^* = \|G_n^0\|\sqrt{T_1 W_0} - \|G_n\|\sqrt{(T-T_1)W},$$

where

$$\|G_n^0\| = \left[\int_0^{T_1} G_n^2(t)dt\right]^{\frac{1}{2}}.$$

4. CONTINUOUS PERIODIC CORRECTIVE ACTIONS

Corrective actions $u_i^*(t)$ (11) and $u^*(t)$ (17) are continuous functions of time inside the domain of their definition, i.e., in the time intervals $t \in ((i-1)T + T_1, iT)$. They take nonzero values at the boundary points: $u_i^*(iT + T_1) \neq 0$ and $u_i^*((i+1)T) \neq 0$ for function (11) and $u^*(T_1) \neq 0$ and $u^*(T) \neq 0$ for periodic function (17). This feature leads to some difficulties, because actual corrective signals must take zero values outside these time intervals. Therefore, the realization of the corrective actions described above requires their step change, which inevitably causes dynamic distortions. Hence, it is advisable to define corrective signals such that they satisfy the boundary conditions $u((i-1)T + T_1) = u(iT) = 0$. To this end, in addition to the quadratic integral restriction corresponding to the limiting power, a quantity characterizing the derivative $\dot{u}(t)$ should be used as a measure of the intensity of the function $u(t)$. The introduction of the corresponding integral quadratic term in the functional to be optimized is the most simple way to satisfy these boundary conditions for $u(t)$ [6]. In what follows, we consider the case of T-periodic corrective action.

Since the functional to be minimized is the second term on the right-hand side of Eq. (14), we introduce the generalized functional

$$I(u, \dot{u}) = \int_{T_1}^{T}\left[-\lambda G_n(t)u + \frac{1}{2}u^2 + \frac{1}{2}\alpha\dot{u}^2\right]dt, \quad (19)$$

where λ is the Lagrange multiplier and α is the weight factor characterizing the rate of change of the corrective signal $u(t)$. The Euler–Lagrange equation corresponding to functional (19) has the form

$$\alpha\ddot{u} - u = \lambda G_n(t). \quad (20)$$

The function $u(t)$ should satisfy the boundary conditions $u(T_1) = u(T) = 0$ and restriction (15). The solution of Eq. (20) with the condition $u(T_1) = 0$ has the form

$$u(t) = \frac{1}{\gamma}\sinh\gamma(t-T_1)\dot{u}(T_1) + \frac{1}{\gamma}\lambda_1\int_{T_1}^{t}\sinh\gamma(t-\tau)G_n(\tau)d\tau, \quad (21)$$

where $\gamma = \frac{1}{\sqrt{\alpha}}$ and $\lambda_1 = \frac{\lambda}{\alpha}$.

The quantity $\dot{u}(T)$ entering into Eq. (21) is found from the condition $u(T) = 0$:

$$\dot{u}(T_1) = -[\sinh\gamma(T-T_1)]^{-1}\lambda_1\int_{T_1}^{T}\sinh\gamma(T-t)G_n(t)dt. \quad (22)$$

Substituting $\dot{u}(T_1)$ given by Eq. (22) into Eq. (21) and then determining λ_1 from condition (15) (considered as an equality), we arrive at the final expression

$$u^*(t) = \eta^*\left[\sinh\gamma(T-T_1)\int_{T_1}^{t}\sinh\gamma(t-\tau)G_n(\tau)d\tau - \sinh\gamma(t-T_1)\int_{T_1}^{T}\sinh\gamma(T-\tau)G_n(\tau)d\tau\right],$$

where

$$\eta^* = \left\{ \int_{T_1}^{T} \left[\int_{T_1}^{t} \sinh\gamma(T - T_1)\sinh\gamma(t - \tau) G_n(\tau) d\tau \right. \right.$$

$$\left. \left. - \int_{T_1}^{T} \sinh\gamma(t - T)\sinh\gamma(t - \tau) G_n(\tau) d\tau \right]^2 dt \right\}^{-\frac{1}{2}} \sqrt{(T - T_1)}$$

REFERENCES

1. H. F. Harmuth, *Nonsinusoidal Waves for Radar and Radio Communication* (Academic, New York, 1981; Radio i Svyaz', Moscow, 1985).
2. L. D. Bakhrakh and A. A. Bliskovitskiĭ, Usp. Fiz. Nauk **162** (12), 51 (1992) [Sov. Phys. Usp. **35**, 1080 (1992)].
3. L. D. Bakhrakh and M. Ya. Izrailovich, Antenny **2** (48), 45 (2001).
4. L. D. Bakhrakh and M. Ya. Izrailovich, Dokl. Akad. Nauk **379**, 325 (2001) [Dokl. Phys. **46**, 491 (2001)].
5. M. Ya. Izrailovich, Probl. Mashinostr. Nadezhnosti Mash., No. 6, 10 (1995).
6. V. I. Babitskiĭ and M. Ya. Izrailovich, Mashinovedenie, No. 6, 45 (1967).

Translated by V. Chechin

Doklady Physics, Vol. 48, No. 8, 2003, pp. 437–440. Translated from Doklady Akademii Nauk, Vol. 391, No. 4, 2003, pp. 483–486.

MECHANICS

On Statically Definable Relationships in Ideal-Plasticity Theory

D. D. Ivlev

Presented by Academician A.Yu. Ishlinskiĭ August 12, 2002

Received August 27, 2002

The properties of statically definable relationships in ideal-plasticity theory [1–5] are discussed.

1. We consider the dissipative function

$$D = \varepsilon_x\varphi_1 + \varepsilon_y\varphi_2 + \varepsilon_z\varphi_3 + 2\varepsilon_{xy}\varphi_4 + 2\varepsilon_{yz}\varphi_5 + 2\varepsilon_{xz}\varphi_6, \quad (1.1)$$

where $\varphi_i = \varphi_i(n_1, n_2, n_3)$.

Let us assume that

$$n_1^2 + n_2^2 + n_3^2 = 1. \quad (1.2)$$

We consider the functional

$$J = \sigma_{ij} - D - \nu(\varepsilon_x + \varepsilon_y + \varepsilon_z) + \mu(n_1^2 + n_2^2 + n_3^2 - 1), \quad (1.3)$$

where ν and μ are the Lagrange multipliers.

The extremum conditions for functional (1.3) have the form

$$\frac{\partial J}{\partial \varepsilon_{ij}} = 0, \quad \frac{\partial J}{\partial n_i} = 0. \quad (1.4)$$

From extremum conditions (1.4) for functional (1.3) with dissipative function (1.1), it follows that

$$\begin{aligned} \sigma_x &= \nu + \varphi_1(n_1, n_2, n_3), \quad \tau_{xy} = \varphi_4(n_1, n_2, n_3), \\ \sigma_y &= \nu + \varphi_2(n_1, n_2, n_3), \quad \tau_{yz} = \varphi_5(n_1, n_2, n_3), \\ \sigma_z &= \nu + \varphi_3(n_1, n_2, n_3), \quad \tau_{xz} = \varphi_6(n_1, n_2, n_3), \end{aligned} \quad (1.5)$$

$$\nu = \sigma - \frac{1}{3}(\varphi_1 + \varphi_2 + \varphi_3), \quad (1.6)$$

$$\varepsilon_x\frac{\partial\varphi_1}{\partial n_1} + \varepsilon_y\frac{\partial\varphi_2}{\partial n_1} + \varepsilon_z\frac{\partial\varphi_3}{\partial n_1} + 2\varepsilon_{xy}\frac{\partial\varphi_4}{\partial n_1} + 2\varepsilon_{yz}\frac{\partial\varphi_5}{\partial n_1} + 2\varepsilon_{xz}\frac{\partial\varphi_6}{\partial n_1} = 2\mu n_1,$$

$$\varepsilon_x\frac{\partial\varphi_1}{\partial n_2} + \varepsilon_y\frac{\partial\varphi_2}{\partial n_2} + \varepsilon_z\frac{\partial\varphi_3}{\partial n_2} + 2\varepsilon_{xy}\frac{\partial\varphi_4}{\partial n_2} + 2\varepsilon_{yz}\frac{\partial\varphi_5}{\partial n_2} + 2\varepsilon_{xz}\frac{\partial\varphi_6}{\partial n_2} = 2\mu n_2, \quad (1.7)$$

$$\varepsilon_x\frac{\partial\varphi_1}{\partial n_3} + \varepsilon_y\frac{\partial\varphi_2}{\partial n_3} + \varepsilon_z\frac{\partial\varphi_3}{\partial n_3} + 2\varepsilon_{xy}\frac{\partial\varphi_4}{\partial n_3} + 2\varepsilon_{yz}\frac{\partial\varphi_5}{\partial n_3} + 2\varepsilon_{xz}\frac{\partial\varphi_6}{\partial n_3} = 2\mu n_3.$$

Associated flow rule (1.7) should be complemented by the incompressibility condition

$$\varepsilon_x + \varepsilon_y + \varepsilon_z = 0. \quad (1.8)$$

The equilibrium equations

$$\begin{aligned} \frac{\partial\sigma_x}{\partial x} + \frac{\partial\tau_{xy}}{\partial y} + \frac{\partial\tau_{xz}}{\partial z} &= 0, \\ \frac{\partial\tau_{xy}}{\partial x} + \frac{\partial\sigma_y}{\partial y} + \frac{\partial\tau_{xz}}{\partial z} &= 0, \\ \frac{\partial\tau_{xz}}{\partial x} + \frac{\partial\tau_{yz}}{\partial y} + \frac{\partial\sigma_z}{\partial z} &= 0 \end{aligned} \quad (1.9)$$

along with relationships (1.2), (1.5), and (1.6), determine the statically definable set of equations in ideal-plasticity theory.

In the general case of static definability (1.5), there are six independent functions φ_i.

We consider the case where relationships (1.5) can be represented in the form

$$\begin{aligned} \varphi_1 &= N_1^2, \quad \varphi_4 = N_1N_2, \\ \varphi_2 &= N_2^2, \quad \varphi_5 = N_2N_3, \\ \varphi_3 &= N_3^2, \quad \varphi_6 = N_1N_3. \end{aligned} \quad (1.10)$$

Relations (1.10) can be written in the form

$$N_1 = \sqrt{\varphi_1}, \quad N_2 = \sqrt{\varphi_2}, \quad N_3 = \sqrt{\varphi_3}, \quad (1.11)$$

$$\varphi_4 = \sqrt{\varphi_1\varphi_2}, \quad \varphi_5 = \sqrt{\varphi_2\varphi_3}, \quad \varphi_6 = \sqrt{\varphi_1\varphi_3}. \quad (1.12)$$

Chuvash State University,
Moskovskiĭ pr. 15, Cheboksary, 428015 Russia

1028-3358/03/4808-0437$24.00

According to Eqs. (1.12) under assumptions (1.10), only three of the six φ_i functions are independent.

The functions φ_4, φ_5, and φ_6 can be chosen as independent. In this case, it follows from Eqs. (1.12) that

$$\varphi_1 = \frac{\varphi_4\varphi_6}{\varphi_5}, \quad \varphi_2 = \frac{\varphi_4\varphi_5}{\varphi_6}, \quad \varphi_3 = \frac{\varphi_5\varphi_6}{\varphi_4}. \tag{1.13}$$

According to Eqs. (1.10), relationships (1.5) and (1.6) take the form

$$\begin{aligned} \sigma_x &= \nu + N_1^2, \quad \tau_{xy} = N_1N_2, \\ \sigma_y &= \nu + N_2^2, \quad \tau_{yz} = N_2N_3, \\ \sigma_z &= \nu + N_3^2, \quad \tau_{xz} = N_1N_3, \end{aligned} \tag{1.14}$$

$$\nu = \sigma - \frac{1}{2}(N_1 + N_2 + N_3). \tag{1.15}$$

Relations (1.10) provide the expressions

$$\begin{aligned} n_1 = F_1(N_1, N_2, N_3), \quad n_2 = F_2(N_1, N_2, N_3), \\ n_3 = F_3(N_1, N_2, N_3). \end{aligned} \tag{1.16}$$

According to Eqs. (1.2) and (1.16), we have

$$F_1^2 + F_2^2 + F_3^2 = 1. \tag{1.17}$$

From equilibrium equations (1.9) and relationships (1.14), we obtain

$$\begin{aligned} &\frac{\partial\nu}{\partial x} + 2N_1\frac{\partial N_1}{\partial x} + N_2\frac{\partial N_1}{\partial y} \\ &+ N_1\frac{\partial N_2}{\partial y} + N_3\frac{\partial N_1}{\partial z} + N_1\frac{\partial N_3}{\partial z} = 0, \\ &\frac{\partial\nu}{\partial y} + N_2\frac{\partial N_1}{\partial x} + N_1\frac{\partial N_2}{\partial y} \\ &+ 2N_2\frac{\partial N_2}{\partial y} + N_3\frac{\partial N_2}{\partial z} + N_2\frac{\partial N_3}{\partial z} = 0, \\ &\frac{\partial\nu}{\partial z} + N_3\frac{\partial N_1}{\partial x} + N_1\frac{\partial N_3}{\partial x} \\ &+ N_3\frac{\partial N_2}{\partial y} + N_2\frac{\partial N_3}{\partial z} + 2N_3\frac{\partial N_3}{\partial z} = 0. \end{aligned} \tag{1.18}$$

Complementing Eqs. (1.18) with the differential relationship

$$F_1dF_1 + F_2dF_2 + F_3dF_3 = 0, \tag{1.19}$$

following from Eq. (1.17), we obtain four equations—Eqs. (1.18) and Eq. (1.19)—for the four unknowns ν, N_1, N_2, and N_3.

Relationship (1.19) is represented as

$$adN_1 + bdN_2 + cdN_3 = 0, \tag{1.20}$$

where

$$a = F_1\frac{\partial F_1}{\partial N_1} + F_2\frac{\partial F_2}{\partial N_1} + F_3\frac{\partial F_3}{\partial N_1} = F_i\frac{\partial F_i}{\partial N_1},$$

$$b = F_i\frac{\partial F_i}{\partial N_2}, \text{ and } c = F_i\frac{\partial F_i}{\partial N_3}.$$

Let us introduce the characteristic surface $\Psi(x, y, z) = 0$ and denote

$$\begin{aligned} \mathrm{grad}\Psi &= \Psi_x\mathbf{i} + \Psi_y\mathbf{j} + \Psi_z\mathbf{k}, \\ \mathbf{N} &= N_1\mathbf{i} + N_2\mathbf{j} + N_3\mathbf{k}, \\ \mathbf{A} &= a\mathbf{i} + b\mathbf{j} + c\mathbf{k}. \end{aligned} \tag{1.21}$$

The characteristic determinant of the set of Eqs. (1.18) and (1.20) has the form

$$\begin{aligned} \Phi = [2\Phi\bar{\Phi} \\ -(\Psi_x^2 + \Psi_y^2 + \Psi_z^2)(aN_1 + b_{N_2} + cN_3)] = 0, \end{aligned} \tag{1.22}$$

$$\begin{aligned} \Phi &= N_1\Psi_x + N_2\Psi_y + N_3\Psi_z \\ &= (\mathbf{N}\cdot\mathrm{grad}\Psi) = |\mathbf{N}||\mathrm{grad}\Psi|\cos\theta_1, \end{aligned} \tag{1.23}$$

$$\begin{aligned} \bar{\Phi} &= a\Psi_x + b\Psi_y + c\Psi_z \\ &= (\mathbf{A}\cdot\mathrm{grad}\Psi) = |\mathbf{A}||\mathrm{grad}\Psi|\cos\theta_2, \end{aligned} \tag{1.24}$$

$$aN_1 + bN_2 + cN_3 = |\mathbf{A}||\mathbf{N}|\cos\alpha. \tag{1.25}$$

It follows from relationships (1.22)–(1.25) that

$$2\cos\theta_1\cos\theta_2 = \cos\alpha. \tag{1.26}$$

The angle α between the vectors $\mathbf{A}$ and $\mathbf{N}$ is determined according to Eqs. (1.10), (1.16), (1.21), and (1.25) by the assumptions about the properties of the limiting behavior of a material. According to Eq. (1.23), the angle between the normal $\mathrm{grad}\Psi$ to the characteristic surface and the vector $\mathbf{N}$ is θ_1. According to Eq. (1.24), the angle between the vectors $\mathrm{grad}\Psi$ and $\mathbf{A}$ is θ_2. Relationship (1.26) determines the totality of $\mathrm{grad}\Psi$ vectors and, thus, the totality of elements of characteristic surfaces.

We assume that relationships (1.10) have the form

$$\begin{aligned} \varphi_1 &= An_1^2 = N_1^2, \quad \varphi_4 = Fn_1n_2 = N_1N_2, \\ \varphi_2 &= Bn_2^2 = N_2^2, \quad \varphi_5 = Gn_2n_3 = N_2N_3, \\ \varphi_3 &= Cn_3^2 = N_3^2, \quad \varphi_6 = Hn_1n_3 = N_1N_3, \end{aligned} \tag{1.27}$$

where A, B, C, F, G, and H are constants.

From Eqs. (1.27), we obtain

$$F = \sqrt{AB}, \quad G = \sqrt{BC}, \quad H = \sqrt{AC}, \tag{1.28}$$

$$A = \frac{FH}{G}, \quad B = \frac{FG}{H}, \quad C = \frac{GH}{F}, \tag{1.29}$$

$$n_1 = \frac{N_1}{\sqrt{A}}, \quad n_2 = \frac{N_2}{\sqrt{B}}, \quad n_3 = \frac{N_3}{\sqrt{C}}, \tag{1.30}$$

$$N_1 = \sqrt{A}n_1, \quad N_2 = \sqrt{B}n_2, \quad N_3 = \sqrt{C}n_3. \tag{1.31}$$

According to Eqs. (1.21) and (1.31), we have

$$\mathbf{N} = \sqrt{A}n_1\mathbf{i} + \sqrt{B}n_2\mathbf{j} + \sqrt{C}n_3\mathbf{k} \tag{1.32}$$

and, according to Eqs. (1.20), (1.30), and (1.31),

$$a = \frac{n_1}{\sqrt{A}}, \quad b = \frac{n_2}{\sqrt{B}}, \quad c = \frac{n_3}{\sqrt{C}}, \tag{1.33}$$

$$\mathbf{A} = \frac{n_1}{\sqrt{A}}\mathbf{i} + \frac{n_2}{\sqrt{B}}\mathbf{j} + \frac{n_3}{\sqrt{C}}\mathbf{k}. \tag{1.34}$$

From Eqs. (1.25), (1.32), and (1.34), it follows that

$$\cos\alpha = \frac{1}{|\mathbf{N}||\mathbf{A}|}, \tag{1.35}$$

where

$$|\mathbf{N}| = \sqrt{An_1^2 + Bn_2^2 + Cn_3^2}, \quad |\mathbf{A}| = \sqrt{\frac{n_1^2}{A} + \frac{n_2^2}{B} + \frac{n_3^2}{C}}.$$

For the case of ideal plasticity, $\sigma_1 = \sigma_2$, $\sigma_3 = \sigma_1 - 2k$, $\cos\alpha = 1$ and $\theta_1 = \theta_2 = 0$ in relationships (1.26) and (1.35).

We consider the case of ideal plasticity [3] for an anisotropic plastic solid:

$$\varphi_i = k(n_1, n_2, n_3). \tag{1.36}$$

According to Eqs. (1.14) and (1.36), we have

$$N_1 = \sqrt{k}n_1, \quad N_2 = \sqrt{k}n_2, \quad N_3 = \sqrt{k}n_3. \tag{1.37}$$

According to Eqs. (1.37), the vector **N** coincides in direction with the vector **n** specifying the direction of the third principal stress σ_3 for ideal-plasticity condition (1.36).

From Eqs. (1.2) and (1.37), we write

$$N_1^2 + N_2^2 + N_3^2 - k = 0. \tag{1.38}$$

From Eq. (1.38), it follows that

$$N_1dN_1 + N_2dN_2 + N_3dN_3 - \frac{dk}{2} = 0, \tag{1.39}$$

$$dk = \frac{\partial k}{\partial n_1}dn_1 + \frac{\partial k}{\partial n_2}dn_2 + \frac{\partial k}{\partial n_3}dn_3. \tag{1.40}$$

From relationships (1.37) and (1.40), we obtain

$$\begin{aligned}
dN_1 &= \left(\sqrt{k} + \frac{n_1}{2\sqrt{k}}\frac{\partial k}{\partial n_1}\right)dn_1 \\
&+ \frac{n_1}{2\sqrt{k}}\frac{\partial k}{\partial n_2}dn_2 + \frac{n_1}{2\sqrt{k}}\frac{\partial k}{\partial n_3}dn_3, \\
dN_2 &= \frac{n_2}{2\sqrt{k}}\frac{\partial k}{\partial n_1}dn_1 \\
&+ \left(\sqrt{k} + \frac{n_2}{2\sqrt{k}}\frac{\partial k}{\partial n_2}\right)dn_2 + \frac{n_2}{2\sqrt{k}}\frac{\partial k}{\partial n_3}dn_3, \\
dN_3 &= \frac{n_3}{2\sqrt{k}}\frac{\partial k}{\partial n_1}dn_1 \\
&+ \frac{n_{31}}{2\sqrt{k}}\frac{\partial k}{\partial n_2}dn_2 + \left(\sqrt{k} + \frac{n_3}{2\sqrt{k}}\frac{\partial k}{\partial n_3}\right)dn_3.
\end{aligned} \tag{1.41}$$

From the set of Eqs. (1.41), it follows that

$$\begin{aligned}
dn_1 &= \frac{1}{\Delta}(a_{11}dN_1 + a_{12}dN_2 + a_{13}dN_3), \\
dn_2 &= \frac{1}{\Delta}(a_{21}dN_1 + a_{22}dN_2 + a_{23}dN_3), \\
dn_3 &= \frac{1}{\Delta}(a_{31}dN_1 + a_{32}dN_2 + a_{33}dN_3),
\end{aligned} \tag{1.42}$$

where Δ is the determinant of the set of Eqs. (1.41) and a_{ij} are determined in terms of coefficients (1.41).

From Eqs. (1.20), (1.37), (1.39), (1.40), and (1.41), we find

$$\begin{aligned}
a &= \sqrt{k}n_1 - \frac{1}{2\Delta}\left(\frac{\partial k}{\partial n_1}a_{11} + \frac{\partial k}{\partial n_2}a_{21} + \frac{\partial k}{\partial n_3}a_{31}\right), \\
b &= \sqrt{k}n_2 - \frac{1}{2\Delta}\left(\frac{\partial k}{\partial n_1}a_{12} + \frac{\partial k}{\partial n_2}a_{22} + \frac{\partial k}{\partial n_3}a_{32}\right), \\
c &= \sqrt{k}n_3 - \frac{1}{2\Delta}\left(\frac{\partial k}{\partial n_1}a_{13} + \frac{\partial k}{\partial n_2}a_{23} + \frac{\partial k}{\partial n_3}a_{33}\right).
\end{aligned} \tag{1.43}$$

2. If relationships (1.14) are met for an incompressible medium satisfying condition (1.8), the dissipative function has the form

$$\begin{aligned}
D &= \sigma_{ij}\varepsilon_{ij} = \varepsilon_xN_1^2 + \varepsilon_yN_2^2 + \varepsilon_zN_3^2 \\
&+ 2\varepsilon_{xy}N_1N_2 + 2\varepsilon_{yz}N_2N_3 + 2\varepsilon_{xz}N_1N_3.
\end{aligned} \tag{2.1}$$

Let us consider the functional

$$\begin{aligned}
J &= \sigma_{ij}\varepsilon_{ij} - D - \nu(\varepsilon_x + \varepsilon_y + \varepsilon_z) \\
&+ \mu(F_1^2 + F_2^2 + F_3^2 - 1),
\end{aligned} \tag{2.2}$$

similar to functional (1.3) under conditions (1.8) and (1.17). Here, the quantity D is determined according to Eq. (2.1).

From the extremum conditions

$$\frac{\partial J}{\partial \varepsilon_{ij}} = 0, \quad \frac{\partial J}{\partial N_i} = 0 \tag{2.3}$$

for functional (2.2) follow relationships (1.14) and the expressions

$$\begin{aligned}
\varepsilon_x N_1 + \varepsilon_{xy} N_2 + \varepsilon_{xz} N_3 &= \mu F_i \frac{\partial F_i}{\partial N_1} = \mu a, \\
\varepsilon_{xy} N_1 + \varepsilon_y N_2 + \varepsilon_{yz} N_3 &= \mu F_i \frac{\partial F_i}{\partial N_2} = \mu b, \\
\varepsilon_{xz} N_1 + \varepsilon_{yz} N_2 + \varepsilon_z N_3 &= \mu F_i \frac{\partial F_i}{\partial N_3} = \mu c
\end{aligned} \tag{2.4}$$

for the associated-flow rule. Eliminating the quantity μ from Eqs. (2.4), we have

$$\begin{aligned}
&c(\varepsilon_x N_1 + \varepsilon_{xy} N_2 + \varepsilon_{xz} N_3) \\
&- a(\varepsilon_{xz} N_1 + \varepsilon_{yz} N_2 + \varepsilon_z N_3) = 0, \\
&c(\varepsilon_{xy} N_1 + \varepsilon_y N_2 + \varepsilon_{yz} N_3) \\
&- b(\varepsilon_{xz} N_1 + \varepsilon_{yz} N_2 + \varepsilon_z N_3) = 0.
\end{aligned} \tag{2.5}$$

Complementing Eqs. (2.5) with incompressibility condition (1.8) and passing to displacement-velocity components, we obtain a set of three equations—Eq. (1.8) and Eqs. (2.5)—for the three variables u, v, w. Equations (1.8) and (2.5) are a hyperbolic system, whose characteristic varieties are determined according to Eqs. (1.22)–(1.26).

REFERENCES

1. A. Yu. Ishlinskiĭ, Prikl. Mat. Mekh. **8** (3), 201 (1944).
2. D. D. Ivlev, Prikl. Mat. Mekh. **22** (1), 90 (1958).
3. A. Yu. Ishlinskiĭ and D. D. Ivlev, *Mathematical Theory of Plasticity* (Fizmatlit, Moscow, 2001).
4. A. Yu. Ishlinskiĭ, *Applied Problems of Mechanics* (Nauka, Moscow, 1986), Vol. 1, pp. 17–42.
5. D. D. Ivlev, *Mechanics of Plastic Media* (Fizmatlit, Moscow, 2001), Vol. 1, pp. 5–19.

Translated by V. Bukhanov

Doklady Physics, Vol. 48, No. 8, 2003, pp. 441–446. Translated from Doklady Akademii Nauk, Vol. 391, No. 5, 2003, pp. 628–633.

MECHANICS

Three-Wave Resonant Interaction Involving Unstable Wave Packets

S. Yu. Annenkov* and N. N. Romanova**

Presented by Academician V.E. Zakharov October 16, 2002

Received October 24, 2002

In this work, we derive the evolution equations for spectrally narrow, resonantly interacting wave packets weakly unstable in terms of linear theory. We consider the following two cases. In the first case, the system is linearly unstable due to the weak coupling of two modes whose energies have opposite signs. As an example of such a system, we analyze the model of a three-layer two-dimensional shear flow, where both the density and vorticity of the undistorted flow have jumps at the layer interfaces and are uniform inside the layers. In the second case, we consider the linear instability of an individual mode. The instability of capillary–gravity waves in a weakly supercritical flow described by the Kelvin–Helmholtz model is an example of this instability. The evolution equations are different for these two cases. The equations are derived in the Hamiltonian formalism, which allows us to consider wave processes disregarding the features of a particular problem. We prove that bounded solutions of the evolution equations exist in both cases. In other words, waves unstable in terms of the linear theory can be stabilized due to their interaction with neutral waves.

1. EVOLUTION EQUATIONS FOR A RESONANT TRIPLET INVOLVING AN UNSTABLE MODE IN THE MODEL OF A THREE-LAYER SHEAR FLOW

As was shown in [1], the dynamic equations describing wave disturbances in stratified shear flows have the form

$$\frac{\partial}{\partial x}\dot{\phi}_j(x,t) = -\frac{\partial}{\partial x}\frac{\delta H}{\delta \eta_j(x,t)} + \nu_j\frac{\delta H}{\delta \phi_j(x,t)}, \qquad (1)$$

$$\dot{\eta}_j(x,t) = \frac{\delta H}{\delta \phi_j(x,t)}. \qquad (2)$$

Here, $\eta_j(x, t)$ are the disturbances of the interfaces and $\phi_j(x, t)$ is the dynamic variable serving as the potential difference of the disturbances in neighboring layers. We consider the two-layer case, i.e., $j = 1, 2$. In order to simplify the calculation of the interaction coefficients, we solve the problem in the Boussinesq approximation. This simplification does not restrict the results obtained below. In terms of Fourier transforms, Eqs. (1) and (2) can be written out in the vector form

$$\mathcal{J}(k)\dot{\mathbf{d}}(k,t) = -\frac{\delta H}{\delta \mathbf{d}(-k,t)},$$

where $\mathbf{d} = (\phi_1, \phi_2, \eta_1, \eta_2)$ is the vector of the dependent variables. The matrix $\mathcal{J}(k)$ has the following (not canonical) form:

$$\mathcal{J}(k) = \begin{pmatrix} 0 & 0 & -1 & 0 \\ 0 & 0 & 0 & -1 \\ 1 & 0 & \dfrac{i\nu_1}{k} & 0 \\ 0 & 1 & 0 & \dfrac{i\nu_2}{k} \end{pmatrix}.$$

The first term in the expansion of the Hamiltonian is

$$H_2 = \frac{1}{2}\int (\mathbf{d}^*(k,t), \hat{h}(k)\mathbf{d}(k,t))\,dk,$$

where

$$\hat{h}(k) = \begin{pmatrix} \dfrac{|k|}{2} & \dfrac{\varepsilon|k|}{2} & -ikV_1 & 0 \\ \dfrac{\varepsilon|k|}{2} & \dfrac{|k|}{2} & 0 & -ikV_2 \\ ikV_1 & 0 & N_1^2 - V_1\nu_1 & 0 \\ 0 & ikV_2 & 0 & N_2^2 - V_2\nu_2 \end{pmatrix}.$$

* *Shirshov Institute of Oceanology, Russian Academy of Sciences, ul. Krasikova 23, Moscow, 117218 Russia*
e-mail: serge@wave.sio.rssi.ru

** *Obukhov Institute of Atmospheric Physics, Russian Academy of Sciences, Pyzhevskiĭ per. 3, Moscow, 109017 Russia*
e-mail: nata@omega.ifran.ru, romnatal@mtu-net.ru

1028-3358/03/4808-0441$24.00

The matrices $\hat{h}(k)$ and $\mathcal{J}(k)$ satisfy the conditions

$$\mathcal{J}^*(k) = \mathcal{J}(-k), \quad \mathcal{J}^*(k) = -\mathcal{J}'(k),$$

$$\hat{h}^*(k) = \hat{h}(-k), \quad \hat{h}^*(k) = \hat{h}'(k).$$

In this case, the dispersion relation has the form $D_1D_2 = \frac{\varepsilon^2 k^2}{4}$, where

$$D_j = \frac{\Omega_j}{b_j} - \frac{|k|}{2}, \quad \Omega_j = \omega - kV_j,$$

$$b_j = \frac{N_j^2}{\Omega_j} + \frac{\nu_j}{k}, \quad N_j^2 = \frac{g\Delta\rho_j}{\rho}.$$

Here, ω is the frequency, $\varepsilon = \exp(-2|k|h)$, and $\Delta\rho_j$ and ν_j are the jumps in the unperturbed density and vorticity, respectively. The parameter ε, serving as the weak coupling constant of the modes, is assumed to be small, of about nonlinearity. As follows from the condition $(\mathbf{Z}^*, \mathcal{J}\mathbf{Z}) = -i$, the normalized eigenvector is given by the expression

$$\mathbf{Z} = \left(\frac{\sqrt{D_2}}{\sqrt{L}}, -\frac{\sqrt{D_1}}{\sqrt{L}}, \frac{i\sqrt{D_2}}{b_1\sqrt{L}}, -\frac{i\sqrt{D_1}}{b_2\sqrt{L}}\right), \tag{3}$$

where $L = D'_{1\omega}D_2 + D'_{2\omega}D_1$.

For wavenumbers corresponding to the stability region, the transformation to the usual canonical variables $a_{1,2}$ has the form

$$\mathbf{d}(k, t) = \sum_{j=1}^{2} \mathbf{Z}_j(k)a_j(k, t) + \mathbf{Z}_j^*(-k)a_j^*(-k, t), \tag{4}$$

where $\mathbf{Z}_j(k)$ is eigenvector (3) corresponding to the eigenfrequency $\omega_j(k)$. The dynamic system written out in terms of these variables is well known [2, 3]:

$$\dot{a}_j(k, t) = -i\frac{\delta H}{\delta a_j^*(k, t)}. \tag{5}$$

The first term H_2 of the expansion of the Hamiltonian in terms of the small nonlinearity parameter is

$$H_2 = \int \sum_{j=1}^{2} \omega_j a_j a_j^* dk.$$

This transformation is inapplicable in the instability region, where the quantity L is small. In this case, the eigenvector $\mathbf{Z}_j(k)$ in Eq. (4) must be replaced by the eigenvector

$$\mathbf{Z}(\omega_1) = \left(\frac{\sqrt{D_2}}{\sqrt{L}}, 0, i\frac{\sqrt{D_2}}{b_1\sqrt{L}}, 0\right),$$
$$\mathbf{Z}(\omega_2) = \left(0, \frac{-\sqrt{D_1}}{\sqrt{L}}, 0, \frac{-i\sqrt{D_1}}{b_2\sqrt{L}}\right), \tag{6}$$

corresponding to the case of zero intermode coupling constant ε. The dynamic system also has form (5), but the quadratic term of the expansion of the Hamiltonian involves additional components [5]:

$$H_2 = \int\left(\sum_{j=1}^{2} \omega_j a_j(k)a_j^*(k)\right.$$
$$\left. + (s(k)a_1(k)a_2(-k) + q(k)a_1(k)a_2^*(k) + \text{c.c.})\right)dk, \tag{7}$$

where

$$s(k) = \frac{\varepsilon(k)}{\sqrt{D_1(k)D_2(-k)}}, \quad q(k) = \frac{\varepsilon(k)}{\sqrt{D_1(k)D_2(k)}}.$$

It is easy to prove that resonant interactions of the type under consideration exist in this model. In this case, the following two synchronism conditions are satisfied:

$$k_{01} + \hat{k}_{02} + k_{03} = 0, \quad \omega_1(k_{01}) + \omega_1(\hat{k}_{02}) + \omega_2(k_{03}) = 0;$$
$$\hat{k}_{02} = -\hat{k}_{02}; \tag{8}$$

$$k_{01} - k_{02} + k_{03} = 0,$$
$$\omega_1(k_{01}) - \omega_2(k_{02}) + \omega_2(k_{03}) = 0. \tag{9}$$

The spectral width of the interacting wave packets under consideration is taken as small. Under conditions (8) and (9), the variables $a_{1,2}(k)$ can be written out in the form

$$a_1(k) = a_1(k_{01} + \kappa) + a_1(\hat{k}_{02} + \kappa),$$
$$a_2(k) = a_2(k_{02} + \kappa) + a_2(k_{03} + \kappa).$$

We now consider the cubic term H_3 of the expansion, retaining only the terms that cannot be eliminated by a suitable canonical transformation. In the case of weak intermode coupling, the cubic term associated with interactions (8) of the "burst" type can be omitted, because it is of a higher order in the small parameter ε. As a result, we arrive at the following equation for the cubic term H_3 of the Hamiltonian:

$$H_3 = \frac{\mathcal{B}(k_{01}, k_{02}, k_{03})}{\sqrt{2\pi}}\int a_1^*(k_{01} + \kappa)a_2(k_{02} + \kappa)$$
$$\times a_2^*(k_{03} + \kappa)\delta(\kappa_1 - \kappa_2 + \kappa_3)\Pi d\kappa_j + \text{c.c.}$$

Expanding the eigenfrequencies in the vicinity of the wavenumbers k_{01}, k_{02}, $\hat{k}_{02}$, and k_{03}, we obtain

$$\omega_1(k_{01}+\kappa) = \omega_1(k_{01}) + v_{1gr}\kappa, \quad v_1 = \frac{d\omega_1}{dk}k_{01},$$

$$\omega_1(\hat{k}_{02}+\kappa) = \omega_1(\hat{k}_{02}) + \hat{v}_{2gr}\kappa, \quad \hat{v}_2 = \frac{d\omega_1}{dk}\hat{k}_{02},$$

$$\omega_2(k_{02}+\kappa) = \omega_2(k_{02}) + v_{2gr}\kappa, \quad v_2 = \frac{d\omega_2}{dk}k_{02},$$

$$\omega_2(k_{03}+\kappa) = \omega_2(k_{03}) + v_{3\mathrm{gr}}\kappa, \quad v_3 = \frac{d\omega_2}{dk}k_{03}.$$

We then introduce the variables $A_j(\kappa, \varepsilon t)$ serving as amplitudes slowly varying in time:

$$a_1(k_{01}+\kappa, t) = \exp(-i\omega_1(k_{01})t)A_1(\kappa, T),$$

$$a_2(k_{02}+\kappa, t) = \exp(-i\omega_2(k_{02})t)A_2(\kappa, T),$$

$$a_2(k_{03}+\kappa, t) = \exp(-i\omega_2(k_{03})t)A_3(\kappa, T),$$

$$a_1^*(-k_{02}-\kappa, t) = \exp(i\omega_1(-k_{02})t)A_4(\kappa, T).$$

Using Eq. (5), where only the two first dominant terms are retained in the expansion of the Hamiltonian, we obtain a system of equations in the variables $A_j(\kappa, T)$ and then perform the inverse Fourier transform

$$C_j(X, T) = \frac{1}{\sqrt{2\pi}}\int A_j(\kappa, T)\exp(i\kappa X)d\kappa.$$

As a result, we arrive at the following evolution equations for the slowly varying amplitudes of the resonantly interacting wave packets:

$$\frac{\partial C_1(X,T)}{\partial T} + v_1\frac{\partial C_1(X,T)}{\partial X} + i\mathcal{B}C_2(X,T)C_3^*(X,T) = 0,$$

$$\frac{\partial C_3(X,T)}{\partial T} + v_3\frac{\partial C_3(X,T)}{\partial X} + i\mathcal{B}C_1^*(X,T)C_2(X,T) = 0,$$

$$\left(\frac{\partial}{\partial T} + v_2\frac{\partial}{\partial X}\right)\left(\frac{\partial}{\partial T} + \hat{v}_2\frac{\partial}{\partial X}\right)C_2(X,T) - s^2C_2(X,T) + \mathcal{B}^2(|C_1|^2(X,T) + |C_3|^2(X,T))C_2(X,T) + i\mathcal{B}\left[(\hat{v}_2 - v_1)C_1(X,T)\frac{\partial C_3(X,T)}{\partial X} + (\hat{v}_2 - v_3)C_3(X,T)\frac{\partial C_1(X,T)}{\partial X}\right] = 0. \quad (10)$$

For three interacting harmonic waves and amplitudes C_j independent of X, Eqs. (10) reduce to the ordinary differential equations

$$\dot{C}_1 + i\mathcal{B}C_2C_3^* = 0,$$

$$\dot{C}_3 + i\mathcal{B}C_2C_1^* = 0,$$

$$\ddot{C}_2 - s^2C_2 + |\mathcal{B}|^2(|C_1|^2 + |C_3|^2)C_2 = 0.$$

A similar system of equations was obtained in [6] and analyzed analytically in [7] for the case of resonant interaction between Rossby baroclinic waves and a marginal mode. Analytical and numerical studies show that resonant interactions with neutral waves can stabilize a wave unstable in terms of linear theory.

The method used above is universal and independent of the physical nature of the weakly coupling waves under consideration. All characteristics of a particular physical problem appear only in the coefficients. Thus, the resulting equations describe the resonant interactions of arbitrary waves.

2. EVOLUTION EQUATIONS FOR THE RESONANT WAVE INTERACTION INVOLVING A WEAKLY UNSTABLE WAVE PACKET IN THE KELVIN–HELMHOLTZ MODEL

If instability takes place in a single mode, the evolution equations describing the resonant interaction involving a weakly nonlinear wave packet have a different form. As an example, we consider the Kelvin–Helmholtz model. In order to simplify the calculation of the interaction coefficients, we here solve the problem in the Boussinesq approximation, but the final conclusions are general. As is known, the equations describing disturbances in this model can be written out in the canonical form [8]:

$$\dot{\phi}(x,t) = -\frac{\delta H}{\delta\eta(x,t)}, \quad \dot{\eta}(x,t) = \frac{\delta H}{\delta\phi(x,t)}. \quad (11)$$

Here, $\eta(x, t)$ is the disturbance of the interface and $\phi(x, t)$ is the velocity potential difference at the interface. In terms of Fourier transforms, Eqs. (11) can be rewritten in the vector form

$$J\dot{\mathbf{d}}(k,t) = -\frac{\delta H}{\delta\mathbf{d}(-k,t)}. \quad (12)$$

Here,

$$\mathbf{d}(k,t) = (\phi(k,t), \eta(k,t))$$

is the vector of the dependent variables and the matrix J has the canonical form

$$J = \begin{pmatrix} 0 & -1 \\ 1 & 0 \end{pmatrix}.$$

The Hamiltonian H_2 is given by the quadratic form

$$H_2 = \frac{1}{2}\int(\mathbf{d}^*(k,t), h(k)\mathbf{d}(k,t))dk, \quad (13)$$

where

$$h(k) = \begin{pmatrix} A(k) & -ikV \\ ikV & C(k) \end{pmatrix}.$$

Here,

$$C(k) = \frac{g\Delta\rho}{\rho} + \frac{\sigma}{\rho k^2} - 2V^2|k|, \quad A(k) = \frac{|k|}{2},$$

where $\Delta\rho = \rho_1 - \rho_2$, $V = \frac{V_1 - V_2}{2}$, $\rho = \frac{\rho_1 + \rho_2}{2}$, and σ is the surface tension coefficient. The eigenfrequencies are equal to

$$\omega_{1,2} = kV \pm \operatorname{sgn}k\sqrt{g\frac{\Delta\rho}{2\rho}|k| + \frac{\sigma}{2\rho}|k|^3 - V^2k^2}. \quad (14)$$

The system becomes unstable when the frequencies corresponding to the upper and lower branches of the mode (i.e., to waves with energies of mutually opposite signs) coincide. In this case, the radicand in (14) is equal to zero at the point $k_0 = \sqrt{\frac{g\Delta\rho}{\sigma}}$. In the vicinity of this point, i.e., for $k = k_0 + \kappa$ and $\frac{\kappa}{k_0} \ll 1$, the frequencies are given by the expressions

$$\omega_{1,2} = \hat{\omega}_0 + V\kappa \pm \operatorname{sgn}k_0\delta,$$

where

$$\delta = \sqrt{A(k_0+\kappa)C(k_0+\kappa)} = V_0\sqrt{\kappa^2 - bk_0^2}.$$

Here, b is a small dimensionless parameter serving as a supercritical parameter of the problem. Positive b values correspond to the unstable case.

We change variables from $\mathbf{d}(k,t)$ to $a(k,t)$:

$$\mathbf{d}(k,t) = \mathscr{Z}(k)a(k,t) + \mathscr{Z}^*(-k)a^*(-k,t). \quad (15)$$

If k is inside the stability region, then $\mathscr{Z}$ is an eigenvector of the linear system and it follows from (15) that

$$\phi(k,t) = -i\sqrt{\frac{\delta}{2A}}(a(k,t) - a^*(-k,t)),$$

$$\eta(k,t) = \sqrt{\frac{A}{2\delta}}(a(k,t) + a^*(-k,t)).$$

In terms of the variables $a(k)$, the dynamic equation has the known form

$$a(k,t) = -i\frac{\delta H}{\delta a^*(k,t)}.$$

For small or zero values of δ, we take

$$\mathscr{Z} = \left(-\frac{i}{\sqrt{A}}\theta(-k), \sqrt{A}\theta(k)\right)$$

in Eq. (15), where $\theta(k)$ is the Heaviside step function. This vector can be rewritten in the different form

$$\mathscr{Z}(k) = \begin{cases} \mathscr{Z}_e, & k > 0 \\ \mathscr{Z}_a, & k < 0, \end{cases}$$

where

$$\mathscr{Z}_e = \frac{\mathbf{z}_1 + \mathbf{z}_2}{2}, \quad \mathscr{Z}_a = \frac{\mathbf{z}_1 - \mathbf{z}_2}{\omega_1 - \omega_2}.$$

Here, $\mathbf{z}_1$ and $\mathbf{z}_2$ are eigenvectors of the linear problem. For $\delta = 0$, vectors $\mathscr{Z}_e$ and $\mathscr{Z}_a$ become an eigenvector and an associated eigenvector, respectively.

In this case, transformation (15) yields the following canonical form of Eqs. (12) in terms of the variable $a(k,t)$ [5]:

$$\dot{a}(k,t) = i\operatorname{sgn}k\frac{\delta H}{\delta a(-k,t)}. \quad (16)$$

In the vicinity of the points k_0, and $-k_0$, the quadratic term in the Hamiltonian is

$$H_2 = \int\left(-\frac{\omega_0}{2}\operatorname{sgn}k\,a(k,t)a(-k,t) + \text{c.c.} + \tilde{\Omega}a(k,t)a^*(k,t)\right)dk, \quad (17)$$

where $\omega_0 = \frac{\omega_1 + \omega_2}{2}$ and

$$\tilde{\Omega}(k) = \begin{cases} 1, & k > 0 \\ \delta^2, & k < 0. \end{cases}$$

In this case, the quantities $a(k)$ and $a(-k)$ are a canonically conjugate pair.

If the resonant interaction under consideration is possible (this is the case in the Kelvin–Helmholtz model), the following two synchronism conditions must be satisfied:

$$k_{01} + k_{02} - k_{03} = 0, \quad \omega(k_{01}) + \omega(k_{02}) - \omega(k_{03}) = 0,$$

$$k_{01} - \hat{k}_{02} - k_{03} = 0, \quad \omega(k_{01}) - \omega(\hat{k}_{02}) - \omega(k_{03}) = 0,$$

$$k_{02} = k_0, \quad \hat{k}_{02} = -k_{02}.$$

We now consider the resonant interaction of two stable, spectrally narrow wave packets with the characteristic

wavenumbers k_{01} and k_{03} and one unstable wave packet with the characteristic wavenumbers k_{02} and $-k_{02}$. We represent $a(k)$ as a sum of finite functions defined near these wavenumbers:

$$a(k) = a(k_{01} + \kappa) + a(k_{02} + \kappa) + a(\hat{k}_{02} + \kappa) + a(k_{03} + \kappa). \quad (18)$$

Omitting immaterial terms and retaining the term of the leading order in the nonlinearity parameter, we obtain the cubic Hamiltonian in the form

$$H_3 = \frac{1}{\sqrt{2\pi}}\int [K(k_{01}, k_{02}, k_{03})a(k_{01} + \kappa_1) \times a(k_{02} + \kappa_2)a^*(k_{03} + \kappa_3) + \text{c.c.}] \times \delta(k_1 + k_2 - k_3)d\kappa_1 d\kappa_2 d\kappa_3. \quad (19)$$

In what follows, we also use the next expansion term H_4 describing the four-wave interactions of the unstable mode:

$$H_4 = \frac{W}{2\pi}\int a(k_{02} + \kappa_1)a(k_{02} + \kappa_2)a^*(k_{02} + \kappa_3) \times a^*(k_{02} + \kappa_4)\delta(\kappa_1 + \kappa_2 - \kappa_3 - \kappa_4)\Pi dk_j. \quad (20)$$

When deriving the evolution equations, we use Eq. (5) for the two stable wave packets with the characteristic wavenumbers k_{01} and k_{03} and Eq. (16) for the unstable wave packet with the characteristic wavenumbers k_{02} and $-k_{02}$. The Hamiltonian is given by the sum $H = H_2 + H_3 + H_4$, where H_2, H_3, and H_4 are determined by Eqs. (17), (19), and (20), respectively.

We now introduce slowly varying amplitudes Q_j:

$$a(k_{0j} + \kappa, t) = \exp(-i\omega(k_{0j})t)Q_j(\kappa, T), \quad j = 1, 2, 3,$$

$$a^*(-k_{02} - \kappa, t) = \exp(-i\omega_0(k_{02})t)Q_4(\kappa, T), \quad T = \varepsilon t.$$

The inverse Fourier transform of Q_j with respect to the variable κ has the form

$$\psi_j(X, T) = \frac{1}{\sqrt{2\pi}}\int Q_j(\kappa, T)\exp(i\kappa X)d\kappa,$$

where $X = \varepsilon x$. Hereinafter, we assume that the functions ψ_j are of the following orders in the small nonlinearity parameter ε:

$$\psi_1 \sim \psi_3 \sim \varepsilon^{3/2}, \quad \psi_2 \sim \varepsilon, \quad \psi_4 \sim \varepsilon^2.$$

Retaining only terms of leading order in ε, we arrive at

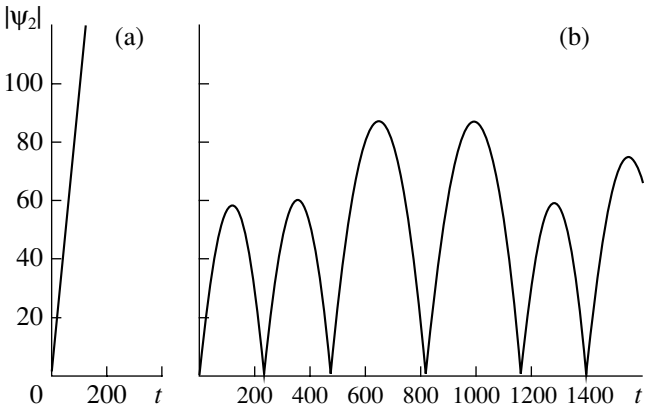

Fig. 1. Time dependence of $|\psi_2|$ found by numerically solving Eqs. (21), under the initial conditions $\psi_1(0) = \psi_3(0) = 0.1$, $\psi_2(0) = 1.0$, and $\dot{\psi}_2(0) = i$ for $\delta = 0$ and $W = 0$: (a) linear regimes with $K = 0$ and (b) nonlinear regime with $K = 1$.

the following system of equations:

$$\left(\frac{\partial}{\partial T} + v_{1gr}\frac{\partial}{\partial X}\right)\psi_1 + iK^*\psi_3\psi_2^* = 0,$$

$$\left(\frac{\partial}{\partial T} + v_{3gr}\frac{\partial}{\partial X}\right)\psi_3 + iK\psi_1\psi_2 = 0,$$

$$\left(\frac{\partial}{\partial T} + v_{2gr}\frac{\partial}{\partial X}\right)^2\psi_2 - V_0^2\left(\frac{\partial^2\psi_2}{\partial X^2} + bk_0^2\psi_2\right) + K^*\psi_1^*\psi_3 + 2W|\psi_2|^2\psi_2 = 0.$$

In the case of three harmonic waves, we obtain

$$\dot{\psi}_1 + iK^*\psi_3\psi_2^* = 0,$$

$$\dot{\psi}_3 + iK\psi_2\psi_1 = 0, \quad (21)$$

$$\ddot{\psi}_2 - r^2\psi_2 + K^*\psi_1^*\psi_3 + 2W|\psi_2|^2\psi_2 = 0,$$

where $r^2 = bk_0^2 V_0^2$.

This system of equations differs significantly from a similar system in the case of weak wave coupling and, in a sense, is more unstable. Indeed, if the resonant interaction with neutral waves is absent and the supercritical parameter b is equal to zero, the amplitude ψ_2 increases linearly with time; i.e., in this case the instability is algebraic. The cubic term serves as either a stabilizing or a destabilizing factor, depending on the sign of the four-wave interaction coefficient W. It is interesting to ascertain whether the interaction with neutral waves can stabilize the algebraic instability in the case of $W = 0$, i.e., for zero cubic nonlinearity. We solved this system of equations numerically for the case where the

initial amplitude of the unstable harmonic is significantly larger than the amplitude of the stable harmonics. As is shown in Fig. 1, the resonant interaction with the stable waves stabilizes the growth of the unstable wave. The solution has a quasiperiodic form, with a parabolic time dependence of the unstable-wave amplitude.

ACKNOWLEDGMENTS

This work was supported by the Russian Foundation for Basic Research, project nos. 01-05-64466 and 01-05-65140.

REFERENCES

1. V. P. Goncharov, Izv. Akad. Nauk SSSR, Fiz. Atm. Okeana **22** (4), 468 (1986).
2. V. E. Zakharov, Izv. Vyssh. Uchebn. Zaved., Radiofiz. **17** (4), 431 (1974).
3. V. E. Zakharov and E. A. Kuznetsov, Usp. Fiz. Nauk **167** (11), 1137 (1997) [Phys. Usp. **40**, 1087 (1997)].
4. V. P. Goncharov and V. I. Pavlov, *Problems of Hydrodynamics in Hamiltonian Description* (Mosk. Gos. Univ., Moscow, 1993).
5. N. N. Romanova, Nonlinear Processes Geophys. **5**, 241 (1999).
6. A. Z. Loesch, J. Atmos. Sci. **31**, 1137 (1974).
7. J. Pedlosky, J. Phys. Oceanogr. **5**, 608 (1975).
8. T. B. Benjamin and T. J. Bridges, J. Fluid Mech. **333**, 301 (1997).

Translated by V. Chechin

Doklady Physics, Vol. 48, No. 8, 2003, pp. 447–450. Translated from Doklady Akademii Nauk, Vol. 391, No. 5, 2003, pp. 634–637.

MECHANICS

Statically Definable Relationships in Ideal-Plasticity Theory

D. D. Ivlev and M. V. Mikhaĭlova

Presented by Academician A.Yu. Ishlinskiĭ August 12, 2002

Received August 27, 2002

The properties of statically definable relationships generalizing the ideal-plasticity condition in ideal-plasticity theory are considered.

1. Statically definable relationships exist in ideal-plasticity theory if, in addition to the equilibrium equations

$$\begin{aligned}\frac{\partial\sigma_x}{\partial x}+\frac{\partial\tau_{xy}}{\partial y}+\frac{\partial\tau_{xz}}{\partial z} &= 0,\\ \frac{\partial\tau_{xy}}{\partial x}+\frac{\partial\sigma_y}{\partial y}+\frac{\partial\tau_{yz}}{\partial z} &= 0,\\ \frac{\partial\tau_{xz}}{\partial x}+\frac{\partial\tau_{yz}}{\partial y}+\frac{\partial\sigma_z}{\partial z} &= 0\end{aligned} \tag{1.1}$$

three finite relationships are defined:

$$\begin{aligned}f_1(\sigma_x,\sigma_y,\sigma_z,\tau_{xy},\tau_{xz},\tau_{yz}) &= 0,\\ f_2(\sigma_x,\sigma_y,\sigma_z,\tau_{xy},\tau_{xz},\tau_{yz}) &= 0,\\ f_3(\sigma_x,\sigma_y,\sigma_z,\tau_{xy},\tau_{xz},\tau_{yz}) &= 0,\end{aligned} \tag{1.2}$$

where σ_{ij} are the stress components.

Relationships (1.2) can be written in the form

$$\begin{aligned}f_1(\sigma_1,\sigma_2,\sigma_3,l_i,m_i,n_i) &= 0,\\ f_2(\sigma_1,\sigma_2,\sigma_3,l_i,m_i,n_i) &= 0,\\ f_3(\sigma_1,\sigma_2,\sigma_3,l_i,m_i,n_i) &= 0,\end{aligned} \tag{1.3}$$

where σ_{ij} are the principal stresses and l_i, m_i, and n_i are the direction cosines specifying the orientation of the principal stresses in the *xyz* coordinate system.

For an isotropic body, relationships (1.3) are independent of the l_i, m_i, and n_i directions, and the conditions take the form

$$\begin{aligned}f_1(\sigma_1,\sigma_2,\sigma_3) = 0,\quad f_2(\sigma_1,\sigma_2,\sigma_3) &= 0,\\ f_3(\sigma_1,\sigma_2,\sigma_3) &= 0.\end{aligned} \tag{1.4}$$

Generally speaking, three finite relationships (1.4) determine a fixed stressed state. The statically definable stressed state of the isotropic body is possible under the ideal-plasticity condition. The volume stressed state of the isotropic ideal plastic body under the ideal-plasticity condition was considered in [1, 2].

Thus, statically definable relationships (1.2) and (1.3) describe the behavior of an anisotropic ideal plastic body under conditions different from the ideal-plasticity condition.

According to Eqs. (1.2), three of six stress components σ_{ij} are independent. We can put

$$\begin{aligned}\sigma_x = \sigma_x(\tau_{xy},\tau_{xz},\tau_{yz}),\quad \sigma_y &= \sigma_y(\tau_{xy},\tau_{xz},\tau_{yz}),\\ \sigma_z &= \sigma_z(\tau_{xy},\tau_{xz},\tau_{yz}).\end{aligned} \tag{1.5}$$

The following parametric notation can be used:

$$\sigma_{ij} = \sigma_{ij}(\xi,\eta,\varsigma), \tag{1.6}$$

where ξ, η, and ς are the independent variables.

Statically definable relationships in ideal-plasticity theory can be written in the form

$$\sigma_{ij} = \sigma_{ij}(\sigma, n_1, n_2, n_3),\quad \sigma = \frac{1}{3}(\sigma_x+\sigma_y+\sigma_z), \tag{1.7}$$

$$n_1^2+n_2^2+n_3^2 = 1. \tag{1.8}$$

When statically definable relationships (1.7) and (1.8) for the components of the stress deviator are valid, relation (1.7) can be represented as

$$\begin{aligned}\sigma_x &= \nu+f_1(n_1,n_2,n_3),\quad \tau_{xy} = f_4(n_1,n_2,n_3),\\ \sigma_y &= \nu+f_2(n_1,n_2,n_3),\quad \tau_{yz} = f_5(n_1,n_2,n_3),\\ \sigma_z &= \nu+f_3(n_1,n_2,n_3),\quad \tau_{xz} = f_6(n_1,n_2,n_3).\end{aligned} \tag{1.9}$$

It follows from Eqs. (1.9) that

$$\nu = \sigma-\frac{1}{3}(f_1+f_2+f_3). \tag{1.10}$$

Chuvash State University,
Moskovskiĭ pr. 15, Cheboksary, 428015 Russia

1028-3358/03/4808-0447$24.00

We also present statically definable relationships in the form

$$\sigma_x = \nu + \varphi_1(n_1, n_2, n_3)n_1^2, \quad \tau_{xy} = \varphi_4(n_1, n_2, n_3)n_1n_2,$$
$$\sigma_y = \nu + \varphi_2(n_1, n_2, n_3)n_2^2, \quad \tau_{yz} = \varphi_5(n_1, n_2, n_3)n_2n_3,$$
$$\sigma_z = \nu + \varphi_3(n_1, n_2, n_3)n_3^2, \quad (1.11)$$
$$\tau_{xz} = \varphi_6(n_1, n_2, n_3)n_1n_3;$$

$$\nu = \sigma - \frac{1}{3}(\varphi_1 n_1^2 + \varphi_2 n_2^2 + \varphi_3 n_3^2). \quad (1.12)$$

For ideal plasticity, all functions in relationships (1.11) and (1.12) are identical, i.e.,

$$\varphi_i(n_1, n_2, n_3) = \varphi(n_1, n_2, n_3). \quad (1.13)$$

2. We consider the functional

$$\Phi = \sigma_{ij}\varepsilon_{ij} - (A\varepsilon_x n_1^2 + B\varepsilon_y n_2^2 + C\varepsilon_z n_3^2 + 2F\varepsilon_{xy}n_1n_2 + 2H\varepsilon_{xz}n_1n_3 + 2G\varepsilon_{yz}n_3n_2) - \nu(\varepsilon_x + \varepsilon_y + \varepsilon_z) + \mu(n_1^2 + n_2^2 + n_3^2), \quad (2.1)$$

where A, B, C, F, G, and H are constants and ν and μ are the unknown Lagrange multipliers.

From the functional-extremum conditions

$$\frac{\partial\Phi}{\partial\varepsilon_{ij}} = 0 \quad (2.2)$$

we obtain

$$\sigma_x = \nu + An_1^2, \quad \tau_{xy} = Fn_1n_2,$$
$$\sigma_y = \nu + Bn_2^2, \quad \tau_{yz} = Gn_2n_3,$$
$$\sigma_z = \nu + An_3^2, \quad \tau_{xz} = Hn_1n_3, \quad (2.3)$$
$$\nu = \sigma - \frac{1}{3}(An_1^2 + Bn_2^2 + Cn_3^2).$$

Relationships (2.3) must be complemented by condition (1.8).

From Eqs. (2.3), it follows that

$$n_1^2 = \frac{G}{FH}\frac{\tau_{xy}\tau_{xz}}{\tau_{yz}}, \quad n_2^2 = \frac{H}{FG}\frac{\tau_{xy}\tau_{yz}}{\tau_{xz}}, \quad n_3^2 = \frac{F}{GH}\frac{\tau_{yz}\tau_{xz}}{\tau_{xy}}. \quad (2.4)$$

Equations (2.4) and (1.8) yield

$$\frac{G}{FH}\frac{\tau_{xy}\tau_{xz}}{\tau_{yz}} + \frac{H}{FG}\frac{\tau_{xy}\tau_{yz}}{\tau_{xz}} + \frac{F}{GH}\frac{\tau_{yz}\tau_{xz}}{\tau_{xy}} = 1. \quad (2.5)$$

According to Eqs. (1.8), (2.3), and (2.4), statically definable relationships in ideal-plasticity theory can be written in the form

$$3(\sigma_x - \sigma) = 2\frac{AG}{FH}\frac{\tau_{xy}\tau_{xz}}{\tau_{yz}} - \left(\frac{BH}{FG}\frac{\tau_{xy}\tau_{yz}}{\tau_{xz}} + \frac{CF}{GH}\frac{\tau_{yz}\tau_{xz}}{\tau_{xy}}\right),$$
$$3(\sigma_y - \sigma) = 2\frac{BH}{FG}\frac{\tau_{xy}\tau_{yz}}{\tau_{xz}} - \left(\frac{CF}{GH}\frac{\tau_{yz}\tau_{xz}}{\tau_{xy}} + \frac{AG}{FH}\frac{\tau_{xy}\tau_{xz}}{\tau_{yz}}\right), \quad (2.6)$$
$$3(\sigma_z - \sigma) = 2\frac{CF}{GH}\frac{\tau_{yz}\tau_{xz}}{\tau_{xy}} - \left(\frac{AG}{FH}\frac{\tau_{xy}\tau_{xz}}{\tau_{yz}} + \frac{BH}{FG}\frac{\tau_{xy}\tau_{yz}}{\tau_{xz}}\right),$$

or

$$\left[3(\sigma_x - \sigma) + \left(\frac{BH}{FG}\frac{\tau_{xy}\tau_{yz}}{\tau_{xz}} + \frac{CF}{GH}\frac{\tau_{yz}\tau_{xz}}{\tau_{xy}}\right)\right] = 2\frac{AG}{FH}\frac{\tau_{xy}\tau_{xz}}{\tau_{yz}},$$
$$\left[3(\sigma_y - \sigma) + \left(\frac{CF}{GH}\frac{\tau_{yz}\tau_{xz}}{\tau_{xy}} + \frac{AG}{FH}\frac{\tau_{xy}\tau_{xz}}{\tau_{yz}}\right)\right] = 2\frac{BH}{FG}\frac{\tau_{xy}\tau_{yz}}{\tau_{xz}}, \quad (2.7)$$
$$\left[3(\sigma_z - \sigma) + \left(\frac{AG}{FH}\frac{\tau_{xy}\tau_{xz}}{\tau_{yz}} + \frac{BH}{FG}\frac{\tau_{xy}\tau_{yz}}{\tau_{xz}}\right)\right] = 2\frac{CF}{GH}\frac{\tau_{yz}\tau_{xz}}{\tau_{xy}},$$

or

$$\left[3(\sigma_x - \sigma) + \left(\frac{BH}{FG}\frac{\tau_{xy}\tau_{yz}}{\tau_{xz}} + \frac{CF}{GH}\frac{\tau_{yz}\tau_{xz}}{\tau_{xy}}\right)\right] \times \left[3(\sigma_y - \sigma) + \left(\frac{CF}{GH}\frac{\tau_{yz}\tau_{xz}}{\tau_{xy}} + \frac{AG}{FH}\frac{\tau_{xy}\tau_{xz}}{\tau_{yz}}\right)\right] = 4\frac{AB}{F^2}\tau_{xy}^2,$$
$$\left[3(\sigma_y - \sigma) + \left(\frac{CF}{GH}\frac{\tau_{yz}\tau_{xz}}{\tau_{xy}} + \frac{AG}{FH}\frac{\tau_{xy}\tau_{xz}}{\tau_{yz}}\right)\right] \times \left[3(\sigma_z - \sigma) + \left(\frac{AG}{FH}\frac{\tau_{xy}\tau_{xz}}{\tau_{yz}} + \frac{BH}{FG}\frac{\tau_{xy}\tau_{yz}}{\tau_{xz}}\right)\right] = 4\frac{BC}{G^2}\tau_{yz}^2, \quad (2.8)$$
$$\left[3(\sigma_z - \sigma) + \left(\frac{AG}{FH}\frac{\tau_{xy}\tau_{xz}}{\tau_{yz}} + \frac{BH}{FG}\frac{\tau_{xy}\tau_{yz}}{\tau_{xz}}\right)\right] \times \left[3(\sigma_x - \sigma) + \left(\frac{BH}{FG}\frac{\tau_{xy}\tau_{yz}}{\tau_{xz}} + \frac{CF}{GH}\frac{\tau_{yz}\tau_{xz}}{\tau_{xy}}\right)\right] = 4\frac{AC}{H^2}\tau_{xz}^2,$$

or

$$\begin{aligned}
&\tau_{xy}[(2C+A)G^2\tau_{xz}^2+(2C+B)H^2\tau_{yz}^2]\\
&\quad=FGH(2C-3(\sigma_z-\sigma))\tau_{xz}\tau_{yz},\\
&\tau_{yz}[(2A+B)H^2\tau_{xy}^2+(2A+C)F^2\tau_{xz}^2]\\
&\quad=FGH(2A-3(\sigma_x-\sigma))\tau_{xy}\tau_{xz},\\
&\tau_{xz}[(2B+C)F^2\tau_{yz}^2+(2B+A)G^2\tau_{xy}^2]\\
&\quad=FGH(2B-3(\sigma_y-\sigma))\tau_{yz}\tau_{xy}.
\end{aligned}\tag{2.9}$$

From the extremum conditions for functional (2.1)

$$\frac{\partial\Phi}{\partial n_i}=0 \tag{2.10}$$

we obtain the following relationships for the associated flow rule:

$$\begin{aligned}
A\varepsilon_x n_1+F\varepsilon_{xy}n_2+H\varepsilon_{xz}n_3&=\mu n_1,\\
F\varepsilon_{xy}n_1+B\varepsilon_y n_2+G\varepsilon_{yz}n_3&=\mu n_2,\\
H\varepsilon_{xz}n_1+G\varepsilon_{yz}n_2+C\varepsilon_z n_3&=\mu n_3.
\end{aligned}\tag{2.11}$$

According to Eqs. (2.3), relationships (2.11) can be written as

$$\begin{aligned}
&A\varepsilon_x+\frac{FH}{G}\varepsilon_{xy}\frac{\tau_{yz}}{\tau_{xz}}+\frac{FH}{G}\varepsilon_{xz}\frac{\tau_{yz}}{\tau_{xy}}\\
&=\frac{FG}{H}\varepsilon_{xy}\frac{\tau_{xz}}{\tau_{yz}}+B\varepsilon_y+\frac{FG}{H}\varepsilon_{yz}\frac{\tau_{xz}}{\tau_{xy}}\\
&=\frac{HG}{F}\varepsilon_{xz}\frac{\tau_{xy}}{\tau_{yz}}+\frac{HG}{F}\varepsilon_{yz}\frac{\tau_{xy}}{\tau_{xz}}+C\varepsilon_z.
\end{aligned}\tag{2.12}$$

The two relationships (2.12) should be complemented by the incompressibility condition

$$\varepsilon_x+\varepsilon_y+\varepsilon_z=0. \tag{2.13}$$

3. We consider the statically definable set of relationships (2.3) in the cylindrical coordinate system $\rho\theta z$:

$$\begin{aligned}
\sigma_\rho&=\sigma+An_1^2-\frac{1}{3}(An_1^2+Bn_2^2+Cn_3^2),\quad \tau_{\rho\theta}=Fn_1n_2,\\
\sigma_\theta&=\sigma+Bn_2^2-\frac{1}{3}(An_1^2+Bn_2^2+Cn_3^2),\quad \tau_{\theta z}=Gn_2n_3,\\
\sigma_z&=\sigma+Cn_3^2-\frac{1}{3}(An_1^2+Bn_2^2+Cn_3^2),\quad \tau_{\rho z}=Hn_1n_3,\\
&n_1^2+n_2^2+n_3^2=1.
\end{aligned}\tag{3.1}$$

For an axisymmetric problem, we have

$$\sigma_{ij}=\sigma_{ij}(\rho,z),\quad \tau_{\rho\theta}=\tau_{\theta z}=0. \tag{3.2}$$

From Eqs. (3.1) and (3.2), we obtain

$$n_2=0,\quad n_1^2+n_3^2=1. \tag{3.3}$$

Condition (3.3) is satisfied by setting

$$n_1=\cos\alpha,\quad n_3=\sin\alpha. \tag{3.4}$$

According to Eqs. (3.1)–(3.4), we obtain

$$\begin{aligned}
\sigma_\rho&=\sigma+\frac{1}{6}((2A-C)+(2A+C)\cos2\alpha),\\
\sigma_\theta&=\sigma-\frac{1}{6}((A+C)+(A-C)\cos2\alpha),\\
\sigma_z&=\sigma+\frac{1}{6}((2C-A)-(2C+A)\cos2\alpha),\\
\tau_{\rho z}&=\frac{H}{2}\sin2\alpha.
\end{aligned}\tag{3.5}$$

From Eqs. (3.5), it follows that

$$\begin{aligned}
&H^2(2(\sigma_\rho-\sigma_z)-(A-C))^2+4(A+C)^2\tau_{\rho z}^2\\
&\quad=H^2(A+C)^2.
\end{aligned}\tag{3.6}$$

From the equilibrium equations

$$\begin{aligned}
\frac{\partial\sigma_\rho}{\partial\rho}+\frac{\partial\tau_{\rho z}}{\partial z}+\frac{\sigma_\rho-\sigma_\theta}{\rho}&=0,\\
\frac{\partial\sigma_z}{\partial z}+\frac{\partial\tau_{\rho z}}{\partial\rho}+\frac{\tau_{\rho z}}{\rho}&=0
\end{aligned}\tag{3.7}$$

and relationships (3.5), we obtain

$$\begin{aligned}
&\frac{\partial\sigma}{\partial\rho}-\frac{2A+C}{3}\sin2\alpha\frac{\partial\alpha}{\partial\rho}+H\cos2\alpha\frac{\partial\alpha}{\partial z}\\
&\quad=-\frac{A}{2\rho}(1+\cos2\alpha),\\
&\frac{\partial\sigma}{\partial z}+H\cos2\alpha\frac{\partial\alpha}{\partial\rho}+\frac{2C+A}{3}\sin2\alpha\frac{\partial\alpha}{\partial z}\\
&\quad=-\frac{H}{2\rho}\sin2\alpha.
\end{aligned}\tag{3.8}$$

Equations (3.8) are a hyperbolic system and have the orthogonal characteristics

$$\begin{aligned}
&\left(\frac{dz}{d\rho}\right)_{1,2}\\
&=\frac{(A+C)\tan2\alpha\pm\sqrt{(A+C)^2\tan^2 2\alpha+4H^2}}{2H}.
\end{aligned}\tag{3.9}$$

Relationships along characteristics (3.9) have the form

$$d\sigma\left(H\cos 2\alpha + \frac{2A + C}{3}\sin 2\alpha\frac{dz}{d\rho}\right)$$
$$+ d\alpha\frac{dz}{d\rho}\left(\frac{(2A + C)}{3}\frac{(2C + A)}{3}\sin^2 2\alpha + H^2\cos^2 2\alpha\right)$$
$$+ \frac{d\rho}{2\rho}\frac{dz}{d\rho}\left[A(1 + \cos 2\alpha)\right.$$
$$\left.\times\left(H\cos 2\alpha\frac{dz}{d\rho} - \frac{2C + A}{3}\sin 2\alpha\right)\right]$$
$$+ H\sin 2\alpha\left(H\cos 2\alpha + \sin 2\alpha\frac{dz}{d\rho}\right)\Bigg] = 0, \qquad (3.10)$$

where $\frac{dz}{d\rho}$ is determined from Eq. (3.9).

The strain-rate components can be determined from Eq. (3.6) according to the associated flow rule and the incompressibility condition

$$A\varepsilon_\rho - C\varepsilon_z - 2H\cot(2\alpha)\varepsilon_{\rho z} = 0,$$
$$\varepsilon_\rho + \varepsilon_\theta + \varepsilon_z = 0, \qquad (3.11)$$

where

$$\varepsilon_\rho = \frac{\partial u}{\partial\rho}, \quad \varepsilon_\theta = \frac{u}{\rho}, \quad \varepsilon_z = \frac{\partial w}{\partial z}, \quad \varepsilon_{\rho z} = \frac{1}{2}\left(\frac{\partial u}{\partial z} + \frac{\partial w}{\partial\rho}\right).$$

Equations (3.11) are hyperbolic, the characteristics coincide with the characteristics of the set of equations for stress components (3.9), and the following relationships are met along the characteristics:

$$du + dw\frac{dz}{d\rho} + u\,d(\ln\rho)\frac{dz}{d\rho}\left(\frac{dz}{d\rho} - \frac{C}{H}\tan(2\alpha)\right) = 0, \qquad (3.12)$$

where $\frac{dz}{d\rho}$ is determined from Eq. (3.9).

REFERENCES

1. A. Yu. Ishlinskiĭ, Uch. Zap., Mosk. Gos. Univ., Mekh., No. 117, 90 (1946).
2. D. D. Ivlev, Prikl. Mat. Mekh. **22** (1), 90 (1958).
3. A. Yu. Ishlinskiĭ, *Applied Problems of Mechanics* (Nauka, Moscow, 1986), Vol. 1, pp. 62–83.

Translated by V. Bukhanov

Doklady Physics, Vol. 48, No. 8, 2003, pp. 451–454. Translated from Doklady Akademii Nauk, Vol. 391, No. 6, 2003, pp. 759–763.

MECHANICS

Mass Transfer in a Stress Field Associated with Bending of a Bar

N. M. Vlasov and Corresponding Member of the RAS I. I. Fedik*

Received April 25, 2003

Construction elements of power plants operate at high temperatures inducing intense diffusion processes. These processes are sensitive to the intensity and distribution of stresses of various physical origins: temperature stresses, residual stresses, and stresses near structural defects. In the internal-stress field, a solid solution separates and regions of a new phase are formed. The formation of the inhomogeneous structure in the presence of residual stresses in a cylindrical shell was analyzed in [1, 2]. Stresses in construction elements also arise under mechanical loading such as bending, tension, compression, and shear. In particular, the concavities of tube guides or shells of fuel elements are bent under internal pressure. The section of a tube-guide wall or shell near a concavity is subjected to a bending moment. Pure bending of curved bars can be considered as an elastic model of such systems [3].

The diffusion of alloying elements depends on the first invariant of the stress tensor. This invariant can be easily determined, because the stress state for the accepted elastic model is known [3]. In this work, we analyze the kinetics of the formation of an inhomogeneous structure under bending of a curved bar. In the accepted model, the structure inhomogeneity is manifested as the separation of a solid solution or the formation of new-phase regions. The latter process occurs when the concentration of impurity atoms exceeds the solvability limit at a given temperature.

A constant-section curved bar is bent by moments in the curvature plane. The components of the stress tensor (plane stressed state) have the form [3]

$$\sigma_{rr} = -\frac{4M}{N}\left(\frac{a^2b^2}{r^2}\ln\frac{b}{a} + b^2\ln\frac{r}{b} + a^2\ln\frac{a}{r}\right),$$

$$\sigma_{\theta\theta} = -\frac{4M}{N}\left(-\frac{a^2b^2}{r^2}\ln\frac{b}{a} + b^2\ln\frac{r}{b} + a^2\ln\frac{a}{r} + b^2 - a^2\right), \quad (1)$$

$$\sigma_{r\theta} = 0.$$

Here, a and b are the inner and outer radii of the bar, respectively; M is the bending moment; and

$$N = (b^2 - a^2)^2 - 4a^2b^2\left(\ln\frac{b}{a}\right)^2.$$

The first invariant of the stress tensor depends logarithmically on the radial coordinate:

$$\sigma_{ll} = \sigma_{rr} + \sigma_{\theta\theta}$$

$$= -\frac{4M}{N}\left(b^2 - a^2 + 2b^2\ln\frac{r}{b} - 2a^2\ln\frac{r}{a}\right). \quad (2)$$

This dependence allows the exact analytical solution of the diffusion equation in the force field. Relation (2) shows that the outer and inner regions of the curved bar under bending are in the compressed and extended states, respectively. The nonuniform stress field induces the diffusion migration of impurity atoms of various kinds (Gorsky effect). Substitutional impurities of large and small atomic radii (compared to the basic metal) migrate to the tension and compression regions, respectively. The inhomogeneous structure thereby forms through the separation of the solid solution of alloying elements of different kinds. With an increase in the concentration of impurity atoms, new-phase regions are formed. This is a qualitative pattern of the formation of the inhomogeneous structure when the bar is bent. A mathematical model of this process will be developed below.

The interaction of an impurity atom with a stress field associated with bending of a bar is described by the potential

$$V = -\frac{\sigma_{ll}}{3}\delta v, \quad (3)$$

where δv is the variation in the crystal volume when introducing an impurity atom. If the alloying impurity increases (decreases) the crystal-lattice constant, δv is positive (negative). For positive (tensile stress) and negative σ_{ll} values and $\delta v > 0$, the potential V is negative and positive, respectively. Alloying elements of a large atomic radius are attracted to the tension region. Impurities of a small atomic radius are attracted to the com-

NPO Luch Research Institute,
ul. Zheleznodorozhnaya 24, Podol'sk,
Moscow oblast, 142100 Russia
** e-mail: iifedik@podolsk.ru*

1028-3358/03/4808-0451$24.00

pression region and are displaced from the tension region. This process finally results in the separation of the solid solution of alloying elements of different kinds.

The diffusion migration of impurity atoms under bending of the bar is described by the time-dependent diffusion equation in the potential V with the corresponding initial and boundary conditions (in the polar coordinate system)

$$\frac{1}{D}\frac{\partial C}{\partial t} = \Delta C + \frac{\nabla(C\nabla V)}{kT}, \quad a < r < b,$$
$$C(r, 0) = C_0, \quad C(a, t) = C_p^1, \quad C(b, t) = C_p^2. \tag{4}$$

Here, D is the diffusion coefficient of impurity atoms, C_0 is the average concentration of impurity atoms, k is the Boltzmann constant, T is the absolute temperature, and C_p^1 and C_p^2 are the equilibrium concentration of impurity atoms at the region's boundary. The physical meaning of the initial and boundary conditions for problem (4) is obvious. At the initial time, the concentration of impurity atoms is constant over the entire region and is equal to the average concentration. The boundary conditions mean that the equilibrium concentration of impurity atoms is instantaneously established at the boundary and further remains constant in the diffusion process.

Diffusion equation (4) shows that the migration of impurity atoms is proportional to the gradient of the potential V. This means that the constants in the relation for σ_{ll} do not affect the diffusion process. The equilibrium concentrations of impurity atoms at the boundaries depend on the constants entering into relation (2). Simple transformations with the use of the expression for σ_{ll} lead to the following simpler variant of problem (4):

$$\frac{1}{D}\frac{\partial C}{\partial t} = \frac{\partial^2 C}{\partial r^2} + \frac{1+\alpha}{r}\frac{\partial C}{\partial r}, \quad a < r < b,$$
$$C(r, 0) = C_0, \quad C(a, t) = C_p^1, \quad C(b, t) = C_p^2. \tag{5}$$

The dimensionless parameter α of the problem determines the ratio of the binding energy of an impurity atom in the stress field of the crystal to the thermal-motion energy:

$$\alpha = -\frac{8}{3}\frac{M(b^2 - a^2)\delta v}{NkT}. \tag{6}$$

The notation corresponds to the notation introduced above. When deriving Eqs. (4), we took into account that $\Delta\sigma_{ll} = 0$, because σ_{ll} is a harmonic function. The parameter α is dimensionless, because the moment per unit length is considered in the accepted elastic model; i.e., $[M]$ = N the applied moment per unit bar length is measured in units of force. This note also applies to the dimension of the components of the stress tensor.

The parameter α determines the contribution of the stress field to the development of the diffusion process. If $|\alpha| \ll 1$, the stress field in the accepted elastic model is a weak perturbation of the diffusion flux of impurity atoms. For $|\alpha| \gg 1$, the stress field associated with bending of the crystal makes the basic contribution to the diffusion process. For $|\alpha| \approx 1$, the diffusion fluxes of impurity atoms due to gradients of the concentration and potential V are comparable with each other. Let us estimate the parameter α for the Zr–Sn alloy. Zirconium alloys are used as materials for the shells of fuel elements in nuclear reactors because of the successful combination of physico-mechanical properties and small cross section for the absorption of thermal neutrons. In the process of operation, the solid solution can separate, which is accompanied by a change in the properties of the material. For $a = 1$ cm, $b = 1.5$ cm, $M = 0.5 \times 10^{-3}$ N, $N = 0.57$ cm^4, $\delta v = 5.57 \times 10^{-24}$ cm^3, and $kT = 1.38 \times 10^{-20}$ J, we have $\alpha = -1.16$. These characteristics are of course conditional. They are used to illustrate the effect of the stress field associated with bending of the bar on the kinetics of the separation of the solid solution. The value $M = 0.5 \times 10^3$ N for the taken geometry of the bar provides the stress $\sigma_{\theta\theta} = 20$ MPa for $r = a$, i.e., at the inner boundary. This value is quite reasonable.

In what follows, we take the dimensionless parameter $\alpha = -1$, for which problem (5) reduces to the more simple form

$$\frac{1}{D}\frac{\partial C}{\partial t} = \frac{\partial^2 C}{\partial r^2}, \quad a < r < b,$$
$$C(r, 0) = C_0, \quad C(a, t) = C_p^1, \quad C(b, t) = C_p^2. \tag{7}$$

The stress field for the accepted dimensionless parameter changes the symmetry of the diffusion equation. The diffusion process in the curved bar (polar coordinate system) is plane symmetric. The transformation of the coordinate dependence increases the rate of variation in the concentration of impurity atoms. This conclusion follows mathematically from the form of the diffusion equation. Indeed, for $\frac{\partial C}{\partial r} < 0$, the rate of variation in the impurity concentration $\frac{\partial C}{\partial t}$ in Eq. (7) is higher than that in Eq. (5). The process is accelerated due to stresses associated with bending of the bar. In this case, tensile stresses displace impurities of a large atomic radius, and compressive stresses accelerate their migration to the boundary of their maximum value. For the accepted elastic model, this process finally results in the establishment of the equilibrium concentration of alloying elements over the bar radius. The time depen-

dence of the concentration field is found by solving problem (7) and has the form

$$C - C_0 = \frac{b(C_p^{1'} - C_0) - a(C_p^2 - C_0) + r(C_p^2 - C_p^1)}{b - a} + \frac{2}{\pi}\sum_{n=1}^{\infty}\frac{1}{n}[(-1)^n(C_p^2 - C_0) - (C_p^1 - C_0)] \times \sin\frac{\pi n(r-a)}{b-a}\exp\left(-\frac{\pi^2 n^2 Dt}{(b-a)^2}\right). \quad (8)$$

This relation involves the equilibrium concentrations at the inner and outer boundaries of the curved bar. Their values are usually determined by the relation

$$C = C_0\exp\left(-\frac{\sigma_{ll}}{3}\delta v\right), \quad (9)$$

where σ_{ll} takes the value

$$\sigma_{ll}\big|_{r=a} = -\frac{4M}{N}\left(b^2 - a^2 + 2b^2\ln\frac{a}{b}\right), \quad \sigma_{ll}\big|_{r=b} - \frac{4M}{N}\left(b^2 - a^2 + 2a^2\ln\frac{a}{b}\right) \quad (10)$$

at the respective region boundaries. As is seen, the equilibrium concentration of impurity atoms at the inner boundary of the bar exceeds the average concentration of impurity atoms due to tensile stresses. The equilibrium concentration of impurity atoms at the outer boundary of the bar is lower than the average concentration of impurity atoms due to compressive stresses.

Thus, relation (8) describes the separation of a solid solution of substitutional impurities of a large atomic radius. For such impurities of a small atomic radius, the mathematical formulation of the diffusion problem is the same. The difference is that these impurities diffuse in the opposite direction, i.e., from the tensile region to the compressive region. When the solid solution separates, the total concentration of impurity atoms is conserved; i.e., they are only redistributed. If the concentration of impurity atoms exceeds the solubility limit at a given temperature, regions of a new phase are formed. Some impurity atoms leave the solution. In this case, the solid solution is depleted. The concentration of impurity atoms is maximal at the boundaries of the region under consideration. Therefore, regions of the new phase are also formed near the boundaries of the material.

The characteristic size of a new-phase nucleus is usually much smaller than the radial dimension of the bar. For this reason, the diffusion processes are described in the unbounded matrix when describing the growth kinetics of the new phase. At the moving interface of the new-phase region, the concentrations of impurity atoms change stepwise: $C = C_1$ for the new phase and $C = C_2$ in the surrounding matrix. In this case, the inequalities $C_1 > C_2$ and $C_2 < C_0$, where C_0 is the average concentration of impurity atoms, are valid. The stepwise change in the impurity concentration at the interface means that this interface instantaneously captures impurities from the solid solution and supplies them to the new phase with higher concentration. In the accepted model, the new phase is formed on the inner surface of the bar. This is caused by tensile stresses and impurities of a large atomic radius. As an example, it is sufficient to mention the formation of hydride phases in zirconium alloys. Hydrogen is formed in the parazirconium reaction and migrates rapidly to the shell of a fuel element. At temperatures below 350°C, hydrogen is in the solid-solution form. When temperature decreases, hydride nuclei are formed. Their further growth occurs due to the diffusion of hydrogen atoms. Hydrogen is an interstitial impurity; i.e., it increases the lattice parameter.

The kinetics of the diffusion growth of the new phase (after the formation of a nucleus) near the inner surface of the bar is mathematically formulated as

$$\frac{1}{D}\frac{\partial C}{\partial t} = \frac{\partial^2 C}{\partial r^2} + \frac{1+\alpha}{r}\frac{\partial C}{\partial r}, \quad C(R,t) = C_2, \quad C(r,0) = C_0, \quad r \ge R_0; \quad C(\infty,t) = C_0, \quad (C_1 - C_2)\frac{dR}{dt} = D\left(\left|\frac{\partial C}{\partial r}\right| + \left|\frac{C\alpha}{r}\right|\right)_{r=R}, \quad (11)$$

where $R_0 > a$ is the radius of the new-phase nucleus and R is the current radius of the new phase. For the $\alpha = -1$ case under consideration, problem (11) takes the more simple form

$$\frac{1}{D}\frac{\partial C}{\partial t} = \frac{\partial^2 C}{\partial r^2}, \quad C(R,t) = C_2, \quad C(r,0) = C_0, \quad r \ge R_0; \quad C(\infty,t) = C_0, \quad (C_1 - C_2)\frac{dR}{dt} = D\left(\frac{\partial C}{\partial r} + \frac{C}{r}\right)_{r=R}. \quad (12)$$

Further, we consider the case where the growth of the new phase is limited by the diffusion supply of impurity atoms. The radius of the new-phase region varies as $R(t) = \beta\sqrt{Dt}$, where β is the dimensionless parameter of the problem and is determined from the mass-balance equation at the interface. For clarity, we

use the fixed-interface approximation. We obtain the quadratic equation

$$\beta^2 - \frac{2\beta}{\sqrt{\pi}}\left|\frac{C_2 - C_0}{C_1 - C_0}\right| - \left|\frac{2C_2}{C_1 - C_2}\right| = 0 \qquad (13)$$

for the calculation of the parameter β.

For $\alpha = 0$, problem (11) takes the form

$$\begin{gathered}\frac{1}{D}\frac{\partial C}{\partial t} = \frac{\partial^2 C}{\partial r^2} + \frac{1}{r}\frac{\partial C}{\partial r},\\ C(R, t) = C_2, \quad C(r, 0) = C_0, \quad r \geq R_0;\\ C(\infty, t) = C_0,\\ (C_1 - C_2)\frac{dR}{dt} = D\left(\frac{\partial C}{\partial r}\right)_{r = R}.\end{gathered} \qquad (14)$$

The stress field of the bar is disregarded in this formulation of the problem. Writing the time dependence of the radius of the new-phase region in the form $R = \beta_1\sqrt{Dt}$, we arrive at the following transcendental equation for the dimensionless parameter β_1 [1]:

$$\beta_1 = \frac{2}{\sqrt{\pi}}\left|\frac{C_2 - C_0}{C_1 - C_0}\right|\frac{K_1\left(\beta_1\frac{\sqrt{\pi}}{2}\right)}{K_0\left(\beta_1\frac{\sqrt{\pi}}{2}\right)}, \qquad (15)$$

where $K_0(x)$ and $K_1(x)$ are the modified Bessel functions of the second kind of the zeroth and first orders, respectively. The solution of Eqs. (13) and (15) for arbitrary concentrations reveals the contribution of stresses under bending of the bar to the kinetics of the growth of the new phase.

Without loss in generality, we set $C_0 = 2 \times 10^{-4}$ atom, $C_2 = 10^{-4}$ atom, and $C_1 = 3 \times 10^{-4}$ atom and, for these concentrations, we obtain [1]

$$\beta^2 - \frac{\beta}{\sqrt{\pi}} - 1 = 0, \quad \beta_1 = \frac{1}{\sqrt{\pi}}\frac{K_1\left(\beta_1\frac{\sqrt{\pi}}{2}\right)}{K_0\left(\beta_1\frac{\sqrt{\pi}}{2}\right)}. \qquad (16)$$

Numerically solving Eqs. (16), we obtain $\beta = 1.3$ and $\beta_1 = 0.8$. Therefore, the stress field associated with bending of the bar accelerates the growth of a nucleus of the new phase. The use of different concentrations only changes the values of the parameters β and β_1. With an increase in the characteristic size of the new phase, the solid solution is depleted. The growth of the new-phase region decelerates. Moreover, variations in the new-phase volume are accompanied by the appearance of stresses at the interface. These stresses change the kinetics of the diffusion process. However, this effect can be disregarded for small volume variations in the new phase and at early stages of the process.

Thus, bending of the curved bar induces stresses. The self-equilibrium system of stresses gives rise to the separation of the solid solution. Alloying elements of large and small atomic radii (compared to the basic metal) migrate to the tension and compression regions, respectively. In other words, impurity atoms are redistributed, while their total concentration is conserved. If the concentration of impurity atoms near the bar boundary reaches the solubility limit at a given temperature, nuclei of the new phase are formed. Their diffusion growth is accompanied by the depletion of the solid solution.

REFERENCES

1. N. M. Vlasov and I. I. Fedik, Dokl. Akad. Nauk **383**, 186 (2002) [Dokl. Phys. **47**, 47 (2002)].
2. N. M. Vlasov and I. I. Fedik, Dokl. Akad. Nauk **384**, 324 (2002) [Dokl. Phys. **47**, 337 (2002)].
3. S. P. Timoshenko and J. N. Goodier, *Theory of Elasticity* (McGraw-Hill, New York, 1970; Nauka, Moscow, 1979).

Translated by R. Tyapaev

Doklady Physics, Vol. 48, No. 8, 2003, pp. 455–458. Translated from Doklady Akademii Nauk, Vol. 391, No. 6, 2003, pp. 764–768.

MECHANICS

Inclusion of the Moment Interaction in the Calculation of the Flexural Rigidity of Nanostructures

E. A. Ivanova*, A. M. Krivtsov*,
Academician N. F. Morozov, and A. D. Firsova*****

Received April 25, 2003

In recent years, in addition to the investigation of the electronic and optical properties of nanostructures [1], the study of their mechanical properties has become particularly important. Many works have been devoted to the production of nanotubes and investigation of their properties [2–8]. According to the data obtained in [4], nanotubes can retain their elastic properties under significant strains. The stress–strain state of nanotubes is usually calculated in the theory of elastic shells [9]. In this case, the elastic moduli are determined in discrete models, where only the force interaction between atoms forming a nanotube is taken into account. However, the existence of monolayer nanotubes [5–8] makes it necessary to consider also the moment interaction between atoms. Otherwise, the atomic layer forming the nanotube would have zero flexural rigidity, so that such a nanotube would be unstable.

The aim of this study is the development of a method of determining the flexural rigidity of nanostructures with allowance for the moment interaction on the nanolevel. First, we obtain general formulas for the moment interaction between atoms or molecules. Then, we apply these formulas to the discrete model [10, 11] to obtain the corrections associated with the moment interaction. These corrections make it possible to describe the mechanical properties of monolayer nanostructures.

* *Faculty of Physics and Mechanics, St. Petersburg State Technical University, ul. Politekhnicheskaya 29, St.-Petersburg, 195251 Russia*
e-mails: ivanova@EI5063.spb.edu; krivtsov@AK5744.spb.edu

** *Faculty of Mathematics and Mechanics, St. Petersburg State University, Staryĭ Petergof, Bibliotechnaya pl. 2, St. Petersburg, 198904 Russia*
e-mail: morozov@NM1016.spb.edu

*** *Institute of Problems of Mechanical Engineering, Russian Academy of Sciences, Vasil'evskiĭ Ostrov, Bol'shoĭ pr. 61, St. Petersburg, 199178 Russia*
e-mail: schnecke@mail.wplus.net

We consider a crystal consisting of particles (atoms or molecules) whose interaction depends not only on their mutual arrangement in space but also on their mutual orientation. This interaction is characterized by the force vector and moment vector. The force and moment of the interaction between crystal particles are defined according to the theory of shells and rods [12, 13]. We consider two interacting particles (Fig. 1). In the actual configuration, the positions and orientations of the particles are specified by the radius-vectors $\mathbf{r}_1$ and $\mathbf{r}_2$ and rotation vectors $\boldsymbol{\varphi}_1$ and $\boldsymbol{\varphi}_2$, respectively. In the equilibrium position, $\mathbf{r}_2 - \mathbf{r}_1 = \mathbf{r}_0$, $\boldsymbol{\varphi}_1 = 0$, and $\boldsymbol{\varphi}_2 = 0$. Let us introduce the following notation: $\mathbf{F}_1$ and $\mathbf{M}_1$ are the force and moment, respectively, acting on particle 1 by particle 2; $\mathbf{F}_2$ and $\mathbf{M}_2$ are the force and moment, respectively, acting on particle 2 by particle 1; and $\mathbf{F}_i^{\mathrm{e}}$ and $\mathbf{M}_i^{\mathrm{e}}$ are the external forces and moments, respectively, acting on the ith particle. The moments $\mathbf{M}_i$ and $\mathbf{M}_i^{\mathrm{e}}$ are calculated with respect to the ith particle. Following the moment theory of elasticity [14], we write the equations of motion for particle 1, particle 2, and the system including both particles in the form

$$\begin{aligned}
m_1\dot{\mathbf{v}}_1 &= \mathbf{F}_1 + \mathbf{F}_1^{\mathrm{e}}, \quad (\theta_1 \cdot \boldsymbol{\omega}_1)^{\cdot} = \mathbf{M}_1 + \mathbf{M}_1^{\mathrm{e}},\\
m_2\dot{\mathbf{v}}_2 &= \mathbf{F}_2 + \mathbf{F}_2^{\mathrm{e}}, \quad (\theta_2 \cdot \boldsymbol{\omega}_2)^{\cdot} = \mathbf{M}_2 + \mathbf{M}_2^{\mathrm{e}},\\
(m_1\mathbf{v}_1 + m_2\mathbf{v}_2)^{\cdot} &= \mathbf{F}_1^{\mathrm{e}} + \mathbf{F}_2^{\mathrm{e}},\\
(\mathbf{r}_1 \times m_1\mathbf{v}_1 + \theta_1 \cdot \boldsymbol{\omega}_1 + \mathbf{r}_2 \times m_2\mathbf{v}_2 + \theta_2 \cdot \boldsymbol{\omega}_2)^{\cdot}&\\
= \mathbf{r}_1 \times \mathbf{F}_1^{\mathrm{e}} + \mathbf{M}_1^{\mathrm{e}} + \mathbf{r}_2 \times \mathbf{F}_2^{\mathrm{e}} + \mathbf{M}_2^{\mathrm{e}}.&
\end{aligned} \tag{1}$$

Here, m_1 and m_2 are the masses of the particles, θ_1 and θ_2 are their inertia tensors, $\mathbf{v}_1$ and $\mathbf{v}_2$ are the velocities of the particles, and $\boldsymbol{\omega}_1$ and $\boldsymbol{\omega}_2$ are their angular velocities. We emphasize that the moment balance equation in a system of bodies, in contrast to a system of material points, does not result from the force balance equation. These equations are independent laws. Newton's third

1028-3358/03/4808-0455$24.00

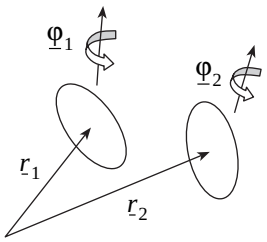

Fig. 1. Moment interaction between two particles.

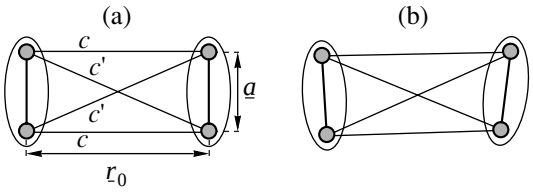

Fig. 2. Two interacting particles: (a) reference (equilibrium) position and (b) actual position.

law for forces and its analogue for moments follow from Eqs. (1):

$$\mathbf{F}_1 + \mathbf{F}_2 = 0, \quad \mathbf{r}_1 \times \mathbf{F}_1 + \mathbf{M}_1 + \mathbf{r}_2 \times \mathbf{F}_2 + \mathbf{M}_2 = 0. \quad (2)$$

The energy balance equation for the two-particle system is written in the form

$$\left(\frac{1}{2}[m_1\mathbf{v}_1 \cdot \mathbf{v}_1 + \boldsymbol{\omega}_1 \cdot \theta_1 \cdot \boldsymbol{\omega}_1 + m_2\mathbf{v}_2 \cdot \mathbf{v}_2 + \boldsymbol{\omega}_2 \cdot \theta_2 \cdot \boldsymbol{\omega}_2] + U\right)^{\cdot} = \mathbf{F}_1^e \cdot \mathbf{v}_1 + \mathbf{M}_1^e \cdot \boldsymbol{\omega}_1 + \mathbf{F}_2^e \cdot \mathbf{v}_2 + \mathbf{M}_2^e \cdot \boldsymbol{\omega}_2, \quad (3)$$

where U is the internal energy of the system (the energy of interaction between particles 1 and 2). For small displacements from the equilibrium position in view of Eqs. (1) and (2), energy balance equation (3) reduces to the form

$$\begin{aligned} \dot{U} &= \mathbf{F} \cdot \dot{\boldsymbol{\varepsilon}} + \mathbf{M} \cdot \dot{\boldsymbol{\kappa}}, \quad \mathbf{F} = \mathbf{F}_1 = -\mathbf{F}_2, \\ \mathbf{M} &= \mathbf{M}_1 + \frac{1}{2}(\mathbf{r}_1 - \mathbf{r}_2) \times \mathbf{F}_1 \\ &= -\mathbf{M}_2 - \frac{1}{2}(\mathbf{r}_2 - \mathbf{r}_1) \times \mathbf{F}_2, \\ \boldsymbol{\varepsilon} &= \mathbf{r} - \mathbf{r}_0 + \frac{1}{2}\mathbf{r}_0 \times (\boldsymbol{\varphi}_1 + \boldsymbol{\varphi}_2), \\ \boldsymbol{\kappa} &= \boldsymbol{\varphi}_2 - \boldsymbol{\varphi}_1, \quad \mathbf{r} = \mathbf{r}_2 - \mathbf{r}_1. \end{aligned} \quad (4)$$

Here, $\mathbf{M}$ is the moment acting on particle 1 by particle 2 about the middle of the segment connecting these particles. The vectors $\boldsymbol{\varepsilon}$ and $\boldsymbol{\kappa}$ on which the force and moment, respectively, do work [see formulas (4)] are referred to as deformation vectors. In what follows, we discuss the elastic deformation of the system. We assume that the internal energy, force, and moment depend only on the deformation vectors and are independent of the velocities. Then,

$$\mathbf{F} = \frac{\partial U}{\partial \boldsymbol{\varepsilon}}, \quad \mathbf{M} = \frac{\partial U}{\partial \boldsymbol{\kappa}}. \quad (5)$$

We assume that the internal energy is a quadratic form of the deformation vectors

$$U = \frac{1}{2}\boldsymbol{\varepsilon} \cdot A \cdot \boldsymbol{\varepsilon} + \boldsymbol{\varepsilon} \cdot B \cdot \boldsymbol{\kappa} + \frac{1}{2}\boldsymbol{\kappa} \cdot C \cdot \boldsymbol{\kappa}. \quad (6)$$

The coefficients of quadratic form (6) are called the elasticity tensors. In the linear theory of elasticity, the elasticity tensors are constants such that the tensors A and C are symmetric, while the tensor B is arbitrary. According to formulas (5) and (6), the force and moment have the form

$$\mathbf{F} = A \cdot \boldsymbol{\varepsilon} + B \cdot \boldsymbol{\kappa}, \quad \mathbf{M} = \boldsymbol{\varepsilon} \cdot B + C \cdot \boldsymbol{\kappa}. \quad (7)$$

For illustration, we consider the simplest model of the moment interaction, where any particle is simulated by two rigidly bound material points (Fig. 2). The following notation is used: $\mathbf{a}$ is the vector connecting two material points within one particle and $\mathbf{r}_0$ is the vector specifying the equilibrium distance between different particles. Both vectors correspond to the reference (equilibrium) configuration for the two-particle system (Fig. 2a). The actual configuration of the system is shown in Fig. 2b. The interaction between material points belonging to different particles is described by the pure force interaction (the rigidities of the corresponding bonds are denoted as c and c'). However, the total interaction between particles has both force and moment components. In Fig. 2, the quantity a characterizes the arm of the moment interaction. When $a \longrightarrow 0$, the moment interaction transforms to the pure force interaction. Calculation of the force and moment acting on particle 1 by particle 2 showed that these quantities have form (7), where

$$\begin{aligned} A &= C_1\mathbf{ii} + C_1^*\mathbf{jj}, \quad B = 0, \quad C = C_2\mathbf{kk}, \\ \mathbf{i} &= \frac{\mathbf{r}_0}{|\mathbf{r}_0|}, \quad \mathbf{j} = \frac{\mathbf{a}}{a}, \quad \mathbf{k} = \mathbf{i} \times \mathbf{j}, \\ C_1 &= 2(c + c'\cos^2\alpha), \\ C_1^* &= 2c'\sin^2\alpha, \quad C_2 = \frac{ca^2}{2}, \quad \tan\alpha = \frac{\alpha}{r_0}. \end{aligned} \quad (8)$$

As a rule, atoms in a nanocrystal are simulated by material points. The simulation of nanocrystal atoms by particles with rotational degrees of freedom complicates the theory of the interaction between particles. However, this complication is justified, because it enables one to describe a number of physical effects that can be described only by multiparticle interaction

potentials in a system of material points [8, 15]. In particular, the class of stable crystal lattices is extended. At the same time, formulations of problems in the theory of moment interactions are much simpler than those in the approach using multiparticle potentials. As is shown below, the inclusion of the moment interactions makes it possible to find an analytical expression for the flexural rigidity of a nanocrystal that does not vanish when the crystal consists of a single atomic layer.

As an example, we apply moment theory to the model problem of the bending of a nanocrystalline strip [10, 11]. We consider a two-dimensional single crystal composed of N and K layers in the y and x directions, respectively, so that $K \gg N$ (Fig. 3). For the force and moment characterizing the interaction between particles, we will use expressions (7), where the elasticity tensors are represented in the form

$$A = C_1\frac{\mathbf{r}_0\mathbf{r}_0}{|\mathbf{r}_0|^2} + C_1^*\frac{\mathbf{k}\times\mathbf{r}_0\mathbf{k}\times\mathbf{r}_0}{|\mathbf{r}_0|^2}, \quad B = 0, \quad C = C_2\mathbf{k}\mathbf{k}. \tag{9}$$

Here, $\mathbf{k}$ is the unit vector perpendicular to the strip plane. The coefficients C_1, C_1^*, and C_2 depend on the structure and sizes of interacting particles. Formulas (9) present the general form of the tensors A, B, and C in the plane problem provided that the system consisting of two interacting particles has two mutually perpendicular symmetry axes. This conclusion can be easily proved by using the symmetry theory of tensors [12].

In this study, we consider only a triangular crystal lattice. The particles that are described by relationships (9) and satisfy the symmetry of a triangular lattice can be simulated by a set of six material points situated at the vertices of a regular hexagon. However, below, we will use general relationship (9) disregarding the internal structure of a particle. For clarity, particles will be represented as ovals, which makes it possible to show their relative rotations (Fig. 3).

The particles located at crystal sides are subjected to the forces Q_j (Fig. 3) varying linearly when going from one layer to another such that the total load is purely moment:

$$\sum_{j=1}^{N} Q_j = 0, \quad \sum_{j=1}^{N} R_j Q_j = M_\Sigma. \tag{10}$$

It is assumed that particles on the crystal sides cannot rotate about each other; i.e., the crystal sides rotate as a rigid body. Only interactions between an atom and its nearest neighbors in the crystal lattice are taken into account (Fig. 3). The strain state of the crystal is determined by the distances $a_{i,j}$ between neighboring atoms in each layer, the distances $b_{i,j}$ between the nearest atoms in the neighboring layers, and the rotation angles $\varphi_{i,j}$ of the atoms. The indices i and j correspond to the numbers of layers in the x and y directions, respectively

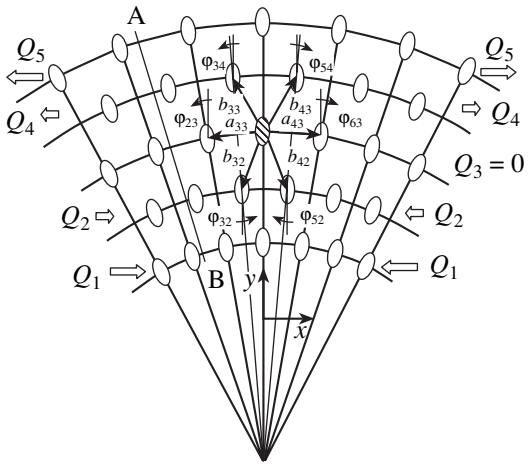

Fig. 3. Bending of the nanocrystalline strip.

(Fig. 3). The distances between the neighboring layers are determined from the relationship $h_{i,j}^2 = b_{i,j}^2 - \frac{a_{i,j}^2}{4}$. In the undeformed state, the crystal lattice consists of equilateral triangles with the side $a = b = a_0$; the rotation angles $\varphi_{i,j}$ of the atoms are assumed to be equal to zero. It is easy to check that, in the undeformed state, the relationships $h_0 = \frac{\sqrt{3}a_0}{2}$, and $R_j = (j-1)h_0$, where R_j is the distance between the jth and first atomic layers, are valid. Writing the equilibrium equations for the atoms, we arrive at the system of equations whose solution has the form

$$\Delta b_{i,j} = 0, \quad \Delta a_{i,j} = \frac{4\sqrt{3}M_\Sigma(2j-N-1)}{C_1 a_0(N-1)N(N+1)}, \quad \varphi_{i,j} = (i-1)\alpha, \quad \alpha = \frac{\frac{\Delta a_{i,N}}{2} - \frac{\Delta a_{i,1}}{2}}{h_0(N-1)}. \tag{11}$$

It is seen from relationships (11) that, under the deformation of the crystal, the layers of atoms in the y direction remain rectilinear, the angles between any neighboring atomic layers are identical, and the rotation angles of the atoms coincide with those of the corresponding layers. Since the problem of pure bending is considered, the shear strain is equal to zero. Thus, the coefficient C_1^* characterizing the shear rigidity is absent in the solution of the problem and cannot therefore affect the flexural rigidity.

To determine the flexural rigidity of a single crystal strip, we mentally cut the crystal by a vertical straight line AB (Fig. 3). According to formulas (11), the total normal force acting from one part of the crystal to

another is equal to zero, and the total bending moment M^* has the form

$$M^* = M_\Sigma + C_2\alpha(3N-1). \quad (12)$$

The flexural rigidity is defined as the ratio of the moment M^* to the curvature β:

$$D \stackrel{\text{def}}{=} \frac{M^*}{\beta}, \quad \beta = \frac{2\alpha}{a_0}. \quad (13)$$

The substitution of formulas (11) and (12) into Eq. (13) gives

$$D = \frac{C_1 a_0^3}{16}(N-1)N(N+1) + \frac{C_2 a_0}{2}(3N-1). \quad (14)$$

The first term in (14) coincides with the formula for the flexural rigidity obtained in [11], where a similar problem was considered disregarding moment interactions between crystal particles. The second term is the correction caused by the moment interaction between the particles. The first term in formula (14) for $N = 1$ vanishes so that the flexural rigidity is completely determined by the quantity C_2 characterizing the moment interactions between crystal atoms

$$N = 1: \quad D = C_2 a_0. \quad (15)$$

When $N \longrightarrow \infty$, the second term in Eq. (14) becomes negligibly small compared to the first term, and the first term tends to the value taken in the macroscopic theory of plates

$$N \to \infty: \quad D \to D_\infty = \frac{E_\infty H^3}{12}, \quad E_\infty = \frac{2C_1}{\sqrt{3}}, \quad (16)$$

where E_∞ is the Young modulus of the infinite crystal and $H \stackrel{\text{def}}{=} Nh_0$ is the macroscopic thickness of the strip.

Thus, in this study, we found the general formulas describing the moment interaction between atoms or molecules under linear elastic deformation. These formulas are illustrated in application to the simplified problem of the bending of a two-dimensional nanocrystalline strip. However, these formulas can be similarly used in the general three-dimensional formulation. In addition, it is shown that, by including the moment interaction on the nanolevel, the elastic deformation of mono- and multilayer nanostructures can be commonly described, and the correction to the flexural rigidity that is nonzero for monolayer nanoobjects can be calculated.

ACKNOWLEDGMENTS

We are grateful to I.I. Blekhman for discussions of the results. This work was supported by the Russian Foundation for Basic Research, project no. 02-01-00514.

REFERENCES

1. N. N. Ledentsov, V. M. Ustinov, V. A. Shchukin, *et al.*, Fiz. Tekh. Poluprovodn. (St. Petersburg) **32** (4), 385 (1998) [Semiconductors **32**, 343 (1998)].
2. V. Ya. Prinz, A. V. Chekhovskiy, V. V. Preobrazhenskiĭ, *et al.*, Nanotechnology **21** (2), 231 (2002).
3. A. V. Maslov, É. N. Korytkova, and V. V. Gusarov, in *Proceedings of 4th International Symposium on Mineralogical Museum, St. Petersburg, 2002*, p. 286.
4. T. Kizuka, Phys. Rev. B: Condens. Matter **59**, 4646 (1999).
5. L.-M. Peng, Z. L. Zhang, Z. Q. Xue, *et al.*, Phys. Rev. Lett. **85**, 3249 (2000).
6. J.-P. Salvetat, G. A. D. Briggs, J.-M. Bonard, *et al.*, Phys. Rev. Lett. **82**, 944 (1999).
7. Y. H. Lee, S. G. Kim, and D. Tomanek, Phys. Rev. Lett. **78**, 2393 (1997).
8. P. Zhang, Y. Huang, H. Gao, and K. C. Hwang, ASME Trans. J. Appl. Mech. **69**, 454 (2002).
9. C. Q. Ru, Phys. Rev. B: Condens. Matter **62**, 9973 (2000).
10. A. M. Krivtsov and N. F. Morozov, Dokl. Akad. Nauk **381**, 345 (2001) [Dokl. Phys. **46**, 825 (2001)].
11. E. A. Ivanova, A. M. Krivtsov, and N. F. Morozov, Dokl. Akad. Nauk **385**, 494 (2002) [Dokl. Phys. **47**, 620 (2002)].
12. P. A. Zhilin, Tr. Leningr. Politekh. Inst. im. M. I. Kalinina **386**, 29 (1982).
13. P. A. Zhilin, A. D. Sergeeva, and T. P. Tovstik, in *Proceedings of 24th All-Russia School-Seminar on Analysis and Synthesis of Nonlinear Mechanical Oscillatory Systems, St. Petersburg, 1996* (1997), p. 313.
14. W. Nowacki, *Theory of Elasticity* (PWN, Warszawa, 1970; Mir, Moscow, 1975).
15. J. Tersoff, Phys. Rev. B: Condens. Matter **37**, 6991 (1988).

Translated by Yu. Vishnyakov

Doklady Physics, Vol. 48, No. 8, 2003, pp. 459–461. Translated from Doklady Akademii Nauk, Vol. 391, No. 6, 2003, pp. 769–771.

MECHANICS

On Linearized Equations of Statically Definable Relationships in Ideal-Plasticity Theory

D. D. Ivlev and M. V. Mikhaĭlova

Presented by Academician A.Yu. Ishlinskiĭ August 13, 2002

Received August 27, 2002

Linearized equations were considered in [1, 2, 5] for the 2D ideal-plasticity problem and in [3, 4] for the 3D problem under the full-plasticity condition. Below, we consider linearized equations of ideal-plasticity theory with statically definable relationships different from the full-plasticity conditions. The linearized equations with statically definable relationships are shown to be of the hyperbolic type.

1. Let statically definable relationships in ideal-plasticity theory be written as

$$\begin{aligned}\sigma_x &= \nu + f_1(n_1, n_2, n_3)n_1^2, \quad \tau_{xy} = f_4(n_1, n_2, n_3)n_1n_2,\\ \sigma_y &= \nu + f_2(n_1, n_2, n_3)n_2^2, \quad \tau_{yz} = f_5(n_1, n_2, n_3)n_2n_3,\\ \sigma_z &= \nu + f_3(n_1, n_2, n_3)n_3^2, \quad \tau_{xz} = f_6(n_1, n_2, n_3)n_1n_3.\end{aligned} \tag{1.1}$$

$$\begin{aligned}\nu &= \sigma - \frac{1}{3}(f_1n_1^2 + f_2n_2^2 + f_3n_3^2),\\ \sigma &= \frac{1}{3}(\sigma_x + \sigma_y + \sigma_z),\\ n_1^2 + n_2^2 + n_3^2 &= 1.\end{aligned} \tag{1.2}$$

The full-plasticity condition [3] follows from Eqs. (1.1) for

$$f_i = f. \tag{1.3}$$

The initial-state values are denoted by the superscript 0, and primed quantities refer to the excited-state components. Let us set

$$\sigma_{ij} = \sigma_{ij}^0 + \sigma_{ij}'. \tag{1.4}$$

It is assumed that

$$n_1^0 = n_2^2 = 0, \quad n_3^0 = 1. \tag{1.5}$$

According to Eqs. (1.1) and (1.5), we have

$$\sigma_x^0 = \sigma_y^0 = \nu^0, \quad \sigma_z^0 = \nu^0 + f_3^0, \quad \tau_{ij}^0 = 0. \tag{1.6}$$

From Eqs. (1.2) and (1.4), it follows that

$$n_3' = 0. \tag{1.7}$$

According to Eqs. (1.1) and (1.4)–(1.7), we obtain

$$\sigma_x' = \nu', \quad \sigma_y' = \nu', \quad \sigma_z' = \frac{\partial f_3^0}{\partial n_1}n_1' + \frac{\partial f_3^0}{\partial n_2}n_2', \tag{1.8}$$

$$\tau_{xy}' = 0, \quad \tau_{yz}' = f_6^0n_2', \quad \tau_{xz}' = f_5^0n_1', \tag{1.9}$$

where derivatives and functions (1.8) and (1.9) with the superscript zero are taken for values (1.5).

From Eqs. (1.8) and (1.9), it follows that

$$\sigma_z' = A\tau_{xz}' + B\tau_{yz}', \quad A = \frac{\partial f_3^0}{\partial n_1}\Big/f_5^0, \quad B = \frac{\partial f_3^0}{\partial n_2}\Big/f_6^0. \tag{1.10}$$

From the equilibrium equations

$$\begin{aligned}\frac{\partial \sigma_x}{\partial x} + \frac{\partial \tau_{xy}}{\partial y} + \frac{\partial \tau_{xz}}{\partial z} &= 0,\\ \frac{\partial \tau_{xy}}{\partial x} + \frac{\partial \sigma_y}{\partial y} + \frac{\partial \tau_{yz}}{\partial z} &= 0,\\ \frac{\partial \tau_{xz}}{\partial x} + \frac{\partial \tau_{yz}}{\partial y} + \frac{\partial \sigma_z}{\partial z} &= 0,\end{aligned} \tag{1.11}$$

and relationships (1.8)–(1.10), we obtain

$$\begin{aligned}\frac{\partial \nu'}{\partial x} + \frac{\partial \tau_{xz}'}{\partial z} &= 0,\\ \frac{\partial \nu'}{\partial y} + \frac{\partial \tau_{yz}'}{\partial z} &= 0,\\ \frac{\partial \tau_{xz}'}{\partial x} + \frac{\partial \tau_{yz}'}{\partial y} + \frac{\partial \nu'}{\partial z} + A\frac{\partial \tau_{xz}'}{\partial z} + B\frac{\partial \tau_{yz}'}{\partial z} &= 0.\end{aligned} \tag{1.12}$$

Chuvash State University,
Moskovskiĭ pr. 15, Cheboksary,
428015 Russia

1028-3358/03/4808-0459$24.00

Introducing the function W such that

$$\tau'_{xz} = \frac{\partial W}{\partial x}, \quad \tau'_{yz} = \frac{\partial W}{\partial y}, \quad \nu' = -\frac{\partial W}{\partial z} \tag{1.13}$$

and using Eqs. (1.12) and (1.13), we arrive at the wave equation

$$\frac{\partial^2 W}{\partial x^2} + \frac{\partial^2 W}{\partial y^2} - \frac{\partial^2 W}{\partial z^2} + A\frac{\partial^2 W}{\partial x \partial y} + B\frac{\partial^2 W}{y \partial z} = 0. \tag{1.14}$$

It is evident that, for

$$n_1^0 = 1, \quad n_3^0 = n_2^0 = 0; \quad n_2^0 = 1, \quad n_1^0 = n_3^0 = 0 \tag{1.15}$$

we obtain wave equations that can be derived according to Eqs. (1.5)–(1.15) by the corresponding permutation of subscripts.

2. To define the relationships for the associated flow rule, we compose the functional

$$\begin{aligned}\Phi &= \sigma_{ij}\varepsilon_{ij} - (\varepsilon_x f_1 n_1^2 + \varepsilon_y f_2 n_2^2 + \varepsilon_z f_3 n_3^2 \\ &+ 2\varepsilon_{xy} f_4 n_1 n_2 + 2\varepsilon_{xz} f_5 n_1 n_3 + 2\varepsilon_{yz} f_6 n_3 n_2) \\ &- \nu(\varepsilon_x + \varepsilon_y + \varepsilon_z) + \mu(n_1^2 + n_2^2 + n_3^2), \\ f_i &= f_i(n_1, n_2, n_3),\end{aligned} \tag{2.1}$$

where ε_{ij} are the components of the plastic-strain rate. Relationships (1.1) follow from the extremum conditions

$$\frac{\partial \Phi}{\partial \varepsilon_{ij}} = 0 \tag{2.2}$$

for functional (2.1).

The extremum conditions

$$\frac{\partial \Phi}{\partial n_i} = 0 \tag{2.3}$$

for functional (2.1) provide the following relationships of the associated plastic-flow rule:

$$\begin{aligned}&\varepsilon_x \frac{\partial (f_1 n_1^2)}{\partial n_1} + \varepsilon_y \frac{\partial f_2}{\partial n_1} n_2^2 + \varepsilon_z \frac{\partial f_3}{\partial n_1} n_3^2 + 2\varepsilon_{xy} \frac{\partial (f_4 n_1)}{\partial n_1} n_2 \\ &+ 2\varepsilon_{xz} \frac{\partial (f_5 n_1)}{\partial n_1} n_3 + 2\varepsilon_{yz} \frac{\partial f_6}{\partial n_1} n_2 n_3 = 2\mu n_1, \\ &\varepsilon_x \frac{\partial f_1}{\partial n_2} n_1^2 + \varepsilon_y \frac{\partial (f_2 n_2^2)}{\partial n_2} + \varepsilon_z \frac{\partial f_3}{\partial n_2} n_3^2 + 2\varepsilon_{xy} \frac{\partial (f_4 n_2)}{\partial n_2} n_1 \\ &+ 2\varepsilon_{xz} \frac{\partial f_5}{\partial n_2} n_1 n_3 + 2\varepsilon_{yz} \frac{\partial (f_6 n_2)}{\partial n_2} n_3 = 2\mu n_2, \\ &\varepsilon_x \frac{\partial f_1}{\partial n_2} n_1^2 + \varepsilon_y \frac{\partial f_2}{\partial n_3} n_2^2 + \varepsilon_z \frac{\partial (f_3 n_3^2)}{\partial n_3} + 2\varepsilon_{xy} \frac{\partial f_4}{\partial n_3} n_1 n_2 \\ &+ 2\varepsilon_{xz} \frac{\partial (f_5 n_3)}{\partial n_3} n_1 + 2\varepsilon_{yz} \frac{\partial (f_6 n_3)}{\partial n_3} n_2 = 2\mu n_3.\end{aligned} \tag{2.4}$$

Relationships (2.4) must be complemented by the incompressibility condition

$$\varepsilon_x + \varepsilon_y + \varepsilon_z = 0. \tag{2.5}$$

Setting

$$\varepsilon_{ij} = \varepsilon_{ij}^0 + \varepsilon'_{ij} \tag{2.6}$$

and using relationships (1.5) and (1.7), we reduce Eqs. (2.4) for the initial state to the form

$$\begin{aligned}&\varepsilon_z^0 \frac{\partial f_3^0}{\partial n_1} + \varepsilon_{xz}^0 \frac{\partial f_5^0}{\partial n_1} = 0, \\ &\varepsilon_z^0 \frac{\partial f_3^0}{\partial n_2} + \varepsilon_{yz}^0 \frac{\partial f_6^0}{\partial n_2} = 0, \\ &\varepsilon_z^0 \left(\frac{\partial f_3^0}{\partial n_3} + 2 f_3^0\right) = 2\mu^0.\end{aligned} \tag{2.7}$$

According to Eqs. (1.5), (1.7), and (2.4)–(2.6), the perturbation components satisfy the relations

$$\begin{aligned}&\varepsilon'_z \frac{\partial f_3^0}{\partial n_1} + \varepsilon_z^0 \left(\frac{\partial^2 f_3^0}{\partial n_1^2} n'_1 + \frac{\partial^2 f_3^0}{\partial n_1 \partial n_2} n'_2\right) + 2\varepsilon'_{xz} f_5^0 = 2\mu^0 n'_1, \\ &\varepsilon'_z \frac{\partial f_3^0}{\partial n_2} + \varepsilon_z^0 \left(\frac{\partial^2 f_3^0}{\partial n_1 \partial n_2} n'_1 + \frac{\partial^2 f_3^0}{\partial n_2^2} n'_2\right) + 2\varepsilon'_{yz} f_6^0 = 2\mu^0 n'_2, \\ &\varepsilon'_z \left(\frac{\partial f_3^0}{\partial n_3} + 2 f_3^0\right) + \varepsilon_z^0 \left(\frac{\partial^2 f_3^0}{\partial n_1 \partial n_3} n'_1 + \frac{\partial^2 f_3^0}{\partial n_2 \partial n_3} n'_2\right) = 2\mu',\end{aligned} \tag{2.8}$$

$$\varepsilon'_x + \varepsilon'_y + \varepsilon'_z = 0. \tag{2.9}$$

Passing to the velocity components

$$\begin{aligned}&\varepsilon_x = \frac{\partial u}{\partial x}, \quad \varepsilon_y = \frac{\partial v}{\partial y}, \quad \varepsilon_z = \frac{\partial w}{\partial z}, \\ &\varepsilon_{xz} = \frac{1}{2}\left(\frac{\partial u}{\partial z} + \frac{\partial w}{\partial x}\right), \quad \varepsilon_{yz} = \frac{1}{2}\left(\frac{\partial v}{\partial z} + \frac{\partial w}{\partial t}\right)\end{aligned} \tag{2.10}$$

and setting

$$u = u^0 + u', \quad v = v^0 + v', \quad w = w^0 + w' \tag{2.11}$$

in Eqs. (2.8)–(2.10), we obtain

$$\begin{aligned}&\frac{\partial u'}{\partial z} + \frac{\partial w'}{\partial x} + A\frac{\partial w'}{\partial z} - 2\mu^0 \frac{\partial W}{\partial x} + F = 0, \\ &\frac{\partial v'}{\partial z} + \frac{\partial w'}{\partial y} + B\frac{\partial w'}{\partial z} - 2\mu^0 \frac{\partial W}{\partial y} + H = 0,\end{aligned} \tag{2.12}$$

where

$$F = \varepsilon_z^0\left(\frac{\partial^2 f_3^0}{\partial n_1^2}\frac{\partial W}{\partial x} + \frac{\partial^2 f_3^0}{\partial n_1 \partial n_2}\frac{\partial W}{\partial y}\right),$$

$$H = \varepsilon_z^0\left(\frac{\partial^2 f_3^0}{\partial n_1 \partial n_2}\frac{\partial W}{\partial x} + \frac{\partial^2 f_3^0}{\partial n_2^2}\frac{\partial W}{\partial y}\right).$$

From Eqs. (2.9) and (2.12), we find

$$\frac{\partial^2 w'}{\partial x^2} + \frac{\partial^2 w'}{\partial y^2} - \frac{\partial^2 w'}{\partial z^2} + A\frac{\partial^2 w'}{\partial x \partial z} + B\frac{\partial^2 w'}{\partial y \partial z}$$

$$- 2\mu^0\left(\frac{\partial^2 W}{\partial x^2} + \frac{\partial^2 W}{\partial y^2}\right) \qquad (2.13)$$

$$- \varepsilon_z^0\left(\frac{\partial^2 f_3^0}{\partial n_1^2}\frac{\partial^2 W}{\partial x^2} + 2\frac{\partial^2 f_3^0}{\partial n_1 \partial n_2}\frac{\partial^2 W}{\partial x \partial y} + \frac{\partial^2 f_3^0}{\partial n_2^2}\frac{\partial^2 W}{\partial y^2}\right) = 0,$$

where μ^0 is defined according to Eqs. (2.7).

The equations for perturbed stress components (1.14) and those for the velocity w' have coinciding characteristics.

REFERENCES

1. E. Onat and V. Prager, in *Mechanics* (Inostrannaya Literatura, Moscow, 1955), No. 4, pp. 93–97.
2. A. Yu. Ishlinskiĭ, Dokl. Akad. Nauk Ukr. SSR, No. 1, 12 (1958).
3. D. D. Ivlev, Dokl. Akad. Nauk **130**, 1232 (1960).
4. L. A. Maksimova, Dokl. Akad. Nauk **358**, 772 (1998) [Dokl. Phys. **43**, 131 (1998)].
5. A. Yu. Ishlinskiĭ, *Applied Problems of Mechanics* (Nauka, Moscow, 1986), Vol. 1, pp. 43–48.

Translated by V. Bukhanov